2014

# Relationship Between Membrane Efficiency and Solute Diffusion Through a Dense, Prehydrated Geosynthetic Clay Liner

Akmal Shukhratovich Daniyarov
ASD007@bucknell.edu

I, Akmal Daniyarov, do grant permission for my thesis to be copied.

# RELATIONSHIP BETWEEN MEMBRANE EFFICIENCY AND SOLUTE DIFFUSION THROUGH A DENSE, PREHYDRATED GEOSYNTHETIC CLAY LINER

by

Akmal Daniyarov

Master's Thesis

Presented to the Faculty of
Bucknell University
In Partial Fulfillment of the Requirements for the Degree of
Master of Science in Civil Engineering

Approved:

Adviser: Michael Malusis

Department Chairperson: Thomas DiStefano

Engineering Thesis Committee Member: Jeffrey Evans

EngineeringThesis Committee Member: Rob Jacob

July 2014

(Date: month and year)

## ACKNOWLEDGMENTS

I would like to thank my adviser, Michael A. Malusis, for his counsel and support that motivated me throughout this endeavor. It was a great privilege to work with such an enthusiastic and dedicated scholar. I would also like to thank Jeffrey C. Evans for encouraging me to attend graduate school at Bucknell Unviersity and for many other great advices. I am grateful for the time and effort put into this thesis by another committee member, Rob Jacob.

The support for this thesis was provided by the Department of Civil and Environmental Engineering, McKenna Grant and Rawell Environmental Ltd. This thesis would not be possible without the assistance of the following individuals: Huan Luong, Steven Beightol, James Gutelius, Melissa Replogle, and Minwoo Cho.

Finally, I would like to thank my family who supported my decision to pursue Master's Degree and my girlfriend, Gaby, for her love and inspiration.

# TABLE OF CONTENTS

## LIST OF TABLES

## LIST OF FIGURES

## ABSTRACT

Geosynthetic Clay Liners (GCLs) are manufactured flat sheets composed of a layer of bentonite sandwiched between two geotextiles. GCLs are used as containment material in environmental and hydraulic applications (Koerner 1998). Previous studies have shown that hydraulic conductivity and diffusion coefficient of bentonite tend to increase when in contact with chemical solutions, making this material less efficient.

The purpose of this study was to investigate the relationship between the membrane efficiency coefficient and effective salt-diffusion coefficient of a dense, prehydrated geosynthetic clay liner (DPH-GCL) in the presence of monovalent salt (KCl) solutions. It was also aimed to compare the DPH-GCLs to conventional GCLs based on the abovementioned properties. The $D_s^*$ - ω relationship determined for DPH-GCLs was found to be accurately approximated by linear fit as in the case of conventional GCLs tested in previous studies.

The membrane efficiency coefficients, ω, and effective salt-diffusion coefficients, $D_s^*$, were determined for 5-mm-thick DPH-GCL specimens subjected to five different KCl solutions (source concentration, $C_{ot}$ = 8.7, 20, 47, 80 and 160 mM) in rigid-wall diffusion cells under no-flow conditions. The source KCl solutions and de-ionized water (DIW) were circulated across the top and bottom specimen boundaries, respectively, in a closed system and values of ω were determined based on the differential pressure induced across the specimens due to prevention of chemico-osmotic liquid flux. The $D_s^*$ values were

calculated using the measured concentrations and electrical conductivities of the solutions exiting top and bottom boundaries. The DPH-GCL specimens exhibited the same trends of decreasing ω with increasing $D_s^*$ as conventional (non-prehydrated) granular GCL specimens tested in previous studies. However, the DPH-GCL specimens exhibited higher ω and lower $D_s^*$ values per given source concentrations relative to conventional GCL specimens tested at the same source concentrations. These findings are consistent with the lower hydraulic conductivities, *k*, measured for the DPH-GCL specimens and are attributed primarily to the higher dry density of the DPH-GCL specimens (~1.2 $Mg/m^3$) relative to the conventional GCL specimens (~0.4 $Mg/m^3$), although differences in bentonite texture (i.e., powdered bentonite in the DPH-GCL versus granular bentonite in the conventional GCL) and polymer treatment of the bentonite in the DPH-GCL (via the prehydration solution) also may have contributed to higher ω and lower $D_s^*$ for the DPH-GCL.

# 1. INTRODUCTION

Geosynthetic Clay Liners (GCLs) are factory-manufactured sheets that are widely used in liners and covers for landfills. GCLs are also used as liners for canals and as secondary liners for underground storage tanks (Koerner 1998).

The most commonly used GCLs are composed of a thin layer of granular sodium bentonite (Na bentonite) held between two geotextiles by needle-punching or stitching. These conventional GCLs have a lower hydraulic conductivity to water and a lower thickness when compared to compacted clay liners (CCLs). For example, conventional GCLs are typically ~10 mm thick and exhibit a hydraulic conductivity to water of $1x10^{-9}$ to $5x10^{-9}$ cm/s, whereas CCLs are typically 600-1500 mm thick and exhibit a hydraulic conductivity to water between $1x10^{-6}$ and $5x10^{-8}$ cm/s (Koerner 1998). The lower thickness of a GCL contributes to easy installation, reduced cost, and greater airspace for waste disposal (Di Emidio 2010). Another major advantage of GCLs over CCLs is significantly greater ability to exhibit membrane behavior, which can be described as the ability to restrict the passage of miscible contaminants (solutes) while allowing for relatively unrestricted passage of the solvent (water) (Malusis and Shackelford 2002a). This behavior reduces the flux of solutes through the GCL, thereby enhancing the containment performance.

Despite the numerous advantages over CCLs, GCLs also have some drawbacks. The high swelling potential of the bentonite ensures that a GCL will have a low hydraulic conductivity to water. On the other hand, exposure of the bentonite to chemical solutions

causes a decrease in swelling and a corresponding increase in GCL hydraulic conductivity. The ability of certain solutions to decrease the swell potential and increase hydraulic conductivity of Na bentonite is well documented (e.g., Shackelford 1994; Petrov and Rowe 1997; Lee and Shackelford 2005; Katsumi et al. 2008; Di Emidio et al. 2008). Increases in GCL hydraulic conductivity upon exposure to chemical solutions can be reduced if the GCL is first hydrated with water to reach maximum swell potential. A GCL that was prehydrated at first and then exposed to a chemical solution will still experience an increase in hydraulic conductivity; nevertheless, this final hydraulic conductivity will be significantly less than that of the same GCL that was not prehydrated and undergoing the exact same process under the same conditions. Thus, prehydration is desired for a better hydraulic performance of a GCL. The phenomenon that describes the benefits of prehydration is termed the "first exposure effect" and has been discussed in several studies (e.g., Shackelford 1994; Shackelford and Lee 2003).

### 1.1 Dense, Prehydrated GCLs

A new GCL product known as a dense prehydrated GCL (DPH-GCL) has emerged recently and is being considered as an alternative to conventional GCLs. Whereas conventional GCLs typically are ~10 mm thick and contain dry (non-prehydrated), granular bentonite, DPH-GCLs are ~5 mm thick and contain a calendered layer of powdered, prehydrated bentonite. Also, DPH-GCLs contain more bentonite mass per unit area than a conventional GCL (6 kg/m$^2$ versus 4.3 kg/m$^2$; see Kolstad et al. 2004). As a result, DPH-GCLs are about three times less permeable to water (Kolstad et al. 2004).

Additionally, the prehydration causes DPH-GCLs to have greater resilience in the presence of chemical solutions (Di Emidio 2010). Findings by Kolstad et al. (2004) indicate that DPH-GCLs are significantly more resistant to highly concentrated salts, bases and acids. Kolstad et al. (2004) demonstrated that the DPH-GCLs perform almost identically under permeation to deionized water (DIW) and to aggressive chemical solutions.

## 1.2 Research Objectives

DPH-GCLs are a relatively new technology that has to be further studied. For example, while some research has been done to evaluate permeability and chemical compatibility of DPH-GCLs (Katsumi et al. 2008, Di Emidio et al. 2008), there has been little research to date on the rate of diffusion of inorganic solutes through DPH-GCLs and the influence of semipermeable membrane behavior on the diffusion rate (Di Emidio 2010). Previous studies have shown that conventional GCLs can exhibit significant membrane behavior in the presence of monovalent salt solutions (e.g., KCl; see Malusis and Shackelford 2002a, Malusis et al. 2003), and that an increase in the membrane efficiency causes a decrease in the rate of salt-diffusion through these GCLs (Malusis and Shackelford 2002b, Malusis et al. 2013). Even higher membrane efficiencies and, thus, even lower diffusion rates may be expected for DPH-GCLs relative to conventional GCLs, given the greater bentonite density in the DPH-GCLs. However, no systematic study has yet been performed to compare the membrane efficiency of DPH-GCLs and conventional GCLs or to

investigate the relationship between membrane efficiency and solute diffusion for DPH-GCLs.

Therefore, the primary objectives of this research are (1) to evaluate membrane efficiencies for DPH-GCL specimens as a function of solute concentration, such that the results can be compared directly against those reported in the literature for conventional GCLs, and (2) to determine the relationship between membrane efficiency and the effective salt-diffusion coefficient for DPH-GCLs. Determining these relationships will be of great value for understanding the potential influence of membrane behavior on the performance of DPH-GCLs used in waste containment applications.

The relationship between membrane efficiency and the effective salt-diffusion coefficient for DPH-GCLs is determined herein based on the results of membrane/diffusion tests in which DPH-GCL specimens were subjected to a solution containing a different concentration of a monovalent salt (KCl). Membrane efficiencies were determined by measuring the differential pressure induced during the tests, and the diffusion coefficients were determined by analyzing ion ($K^+$ and $Cl^-$) concentrations at the boundaries of the specimens over time. This thesis contains (1) a review of the relevant literature pertaining to membrane behavior and solute diffusion in GCLs, (2) a description of the materials and methods that were employed in this study, (3) presentation, analysis, and discussion of the test results, (4) a conclusions section that summarizes the major findings of this research and (5) provides recommendations for future work.

# 2. LITERATURE REVIEW

This section presents an overview of conventional GCLs and DPH-GCLs and summarizes the findings from previous studies in which conventional GCLs (or Na bentonite specimens representative of conventional GCLs) and/or DPH-GCLs were evaluated for hydraulic and waste containment applications. Mechanisms known to influence the contaminant transport properties (including membrane efficiency) of GCLs also are described herein. Currently, our ability to quantitatively assess the role of membrane efficiency on solute transport through DPH-GCLs based on the literature is limited due to the lack of existing research, particularly when compared to conventional GCLs. Therefore, much of the data presented in this literature review is for conventional GCLs. However, the vast amount of literature on conventional GCLs provides insights into how DPH-GCLs may behave when tested in a similar fashion and subjected to similar conditions.

## 2.1 Overview of Conventional GCLs

Traditional Geosynthetic Clay Liners (GCLs) are thin (~10-mm thick), manufactured layers of sodium bentonite clay sandwiched between two geotextiles or bonded to a geomembrane. The components of a GCL are held together by needle punching, stitching, or physical bonding. The GCLs are used as containment material in transportation, geotechnical and hydraulic applications (Koerner 1998).

### *2.1.1 Fabrication and Composition*

There are several types of GCLs available on the market. For example, the most commonly used types of GCLs are the Bentomat® line of products (CETCO, Hoffman Estates, IL), which are GCLs containing a layer of granular Na bentonite between two geotextiles (either two nonwoven geotextiles or one woven and one nonwoven geotextile). Similar products are available containing either powdered or granular bentonite, including Bentofix® (NAUE GmbH & Co., Germany) NaBento® (Heusker Synthetic GmbH, Germany) and BentoLiner® (GSE Environmental, Houston, TX). These GCLs may be reinforced with stitching or needle-punched fibers, and the outer geotextiles may be surface coated to improve the friction against adjacent materials. There are also geomembrane-supported GCLs, such as Gundseal® (GSE Environmental, Houston, TX), which consist of powdered bentonite bonded onto a geomembrane. The performance of the fabric (geotextile) encased GCLs is governed by the bentonite, whereas the performance of geomembrane-supported GCLs is governed largely by the geomembrane. Therefore, the focus of this literature review is on the fabric-encased types of GCLs, which have been studied intensively in previous research (Malusis and Shackelford 2002a and b; Kolstad et al. 2004; Lee and Shackelford 2003; Di Emidio 2010; Kang and Shackelford 2011; Malusis et al. 2013).

### *2.1.2 Advantages and Limitations of Conventional GCLs for Waste Containment*

The conventional GCLs described above have been used widely in liners and cover systems for landfills and other types of containment facilities, often as an alternative to

compacted clay liners (CCLs). One of the reasons why GCLs are considered for use in lieu of CCLs is cost savings associated with the GCLs and the reduced thickness (10 mm for a GCL versus 300-900 mm for a CCL), which makes more space available for waste storage. Additionally, GCLs have a lower hydraulic conductivity to water than CCLs. Conventional GCLs typically exhibit a hydraulic conductivity to water of $<5x10^{-9}$ cm/s, whereas CCLs exhibit a hydraulic conductivity to water between $10^{-7}$ and $10^{-8}$ cm/s (Koerner 1998). Finally, GCLs can, in some situations, exhibit self-healing capability (because of the high swelling capacity of the bentonite), and generally have a greater ability to withstand differential settlements when compared to CCLs. Self-healing capability can assist GCLs in recovering from puncture holes up to 75 mm upon hydration (EPA 2001).

Even though GCLs are superior to CCLs in some aspects, GCLs also have some important disadvantages. As was mentioned in the introduction, the swell potential can be severely diminished when GCLs are exposed to chemical solutions (e.g., Shackelford 1994; Shackelford and Lee 2003; Rowe 2007; Katsumi et al. 2008; Di Emidio et al. 2008). The impacts of the chemical solutions can be mitigated, in part, by prehydrating the GCL with water so that the bentonite can undergo extensive swelling before exposure to the chemical solution. When unhydrated bentonite is exposed to aggressive chemical solutions, the bentonite will exhibit limited swell and, thus, substantially higher hydraulic conductivity than prehydrated specimens subjected to the same solutions. This phenomenon has been referred to as the “first exposure effect” (see Chapter 1 for definition). Shackelford (1994) demonstrated that the first exposure effect can be

responsible for an increase in hydraulic conductivity by more than two orders of magnitude by testing specimens containing 16% bentonite subjected to calcium solutions. However, the first exposure effect, does not always affect hydraulic conductivity results. Lee and Shackelford (2005) performed long term hydraulic conductivity tests indicating that conventional GCLs permeated with $CaCl_2$ solutions of concentrations $\leq$ 50 mM are not impacted by first exposure effect, because this range of concentrations is not high enough to inhibit swelling of the bentonite.

Another drawback of a GCL is that it experiences an increase in permeability following desiccation, a series of material drying-wetting events. Egloffstein (2001) showed that both cation exchange and desiccation (happening in tandem) can be responsible for dramatic permeability increases within GCLs, with desiccation being a controlling factor. Desiccation develops cracks within the bentonite of GCLs which are a primary reason for increased permeability. These cracks can be sealed due to the self-healing capabilities of bentonite. Egloffstein (2001) concluded that small numerous cracks observed in needle punched GCLs are more likely to self-heal as opposed to fewer and larger cracks typically developed within stitched GCLs.

## 2.2 Dense, Prehydrated GCLs (DPH-GCLs)

DPH-GCLs have been designed to overcome the limitations of conventional GCLs described above. Specifically, DPH-GCLs are manufactured with a greater dry density of bentonite (and therefore a lower porosity) and contain Na bentonite that has been prehydrated during the manufacturing process with an engineered chemical solution

designed to improve the workability and resilience to chemicals of the bentonite. This section provides an overview of the fabrication process and the physical and chemical properties of the DPH-GCL tested in this study.

### *2.2.1 Fabrication and Composition*

The DPH-GCL considered in this study consists of a high strength woven polypropylene geotextile on one side and a perforated polyester scrim (non-woven geotextile) on the other (see Figure 2.1, labels 3 and 4 respectively). The two materials sandwich a prehydrated and densified bentonite sheet. This bentonite sheet is composed of Na bentonite that has been mixed in a high speed, high shear mixer (Figure 2.1, label 1) with a dilute polymer solution composed of carboxymethyl cellulose (CMC), sodium polyacrylate (Na-PAAS or SPA) and methanol (Note: tested product did not contain methanol). All of the solutions are introduced through the funnels placed above the mixer. The prehydrated bentonite is then calendered under vacuum to reduce the size and the number of voids (see Figure 2.1, label 2; Figure 2.1A) (Flynn and Carter 1998).

The exact quantities of the components in the DPH-GCL are proprietary; however, the patent describing the manufacturing process gives percentage ranges by weight for each component (see Table 2.1). The purpose of the CMC is to grant the DPH-GCL ductility, workability, fungicidal and lubricant properties. Sodium polyacrylate coats clay particles and provides additional exchangeable sodium cations which further increases the resilience of the DPH-GCL to chemical solutions. Sodium hexametaphosphate is used as

a deflocculating agent to promote impermeability whereas methanol's objective (similar to CMC) is to further increase the workability of the material (Flynn and Carter 1998).

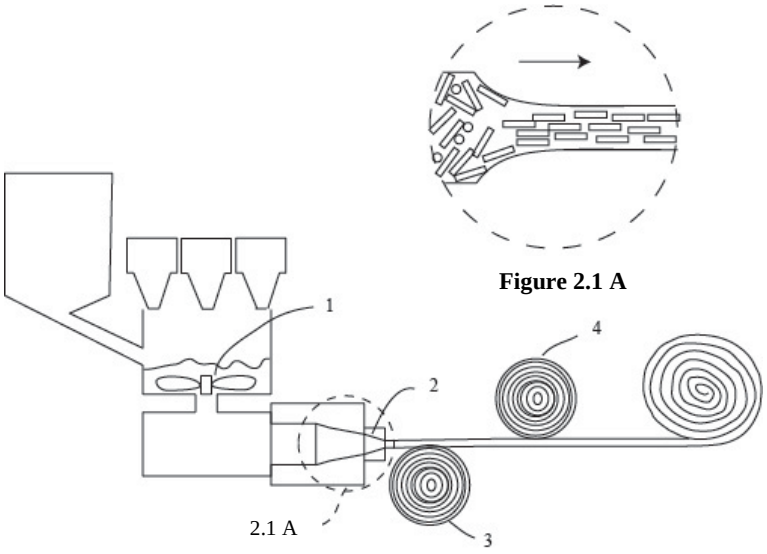


**Figure 2.1 DPH-GCL manufacturing process (redrawn after Flynn and Carter 1998).**

**Table 2.1 DPH-GCL constituent content (data from Flynn and Carter 1998).**

| Component | Percentage range (by weight) |
|---|---|
| Water | 15-25 |
| Sodium Polyacrylate | 8-16 |
| Methanol | 0-5 (0 for the tested product) |
| Wyoming Bentonite | 50-75 |
| Carboxy Methyl Cellulose (CMC) | 0-3 |
| Sodium Hexametaphosphate | 0-0.5 |

### *2.2.2 Hydraulic Performance of DPH-GCLs*

As mentioned in the introduction, DPH-GCLs have been shown to be less permeable to water and chemical solutions than conventional GCLs as a result of the increased bentonite content per unit area (6.0 kg/m$^2$ as opposed to 4.3 kg/m$^2$ for a conventional GCL) and the prehydration treatment (Kolstad et al. 2004). Kolstad et al. (2004) permeated both a conventional GCL and a DPH-GCL with deionized water (DIW) and a series of aggressive chemical solutions, as shown in Table 2.2. The results show that the hydraulic conductivity to DIW of DPH-GCL was approximately three times lower than that of the conventional GCL ($4.1 \times 10^{-12}$ m/s versus $1.2 \times 10^{-11}$ m/s). Also, the ratios, $K_{CONV}/K_{DPH}$, representing the ratios of hydraulic conductivity of the conventional GCL to the DPH-GCL, ranged from 66,700 to 219,000 for solutions containing 1 M NaCl, 1 M $CaCl_2$, and hydrochloric acid (pH = 1.2). These results indicate that the conventional GCL was 66,700 to 219,000 times more permeable to these solutions than the DPH-GCL. In these cases, the final hydraulic conductivities for the conventional GCL specimens ranged from $1.5 \times 10^{-7}$ m/s to $8.1 \times 10^{-7}$ m/s, values more than two orders of magnitude higher than the hydraulic conductivity typically required for clay liners in waste containment applications (i.e., $10^{-9}$ m/s). One of the primary reasons for the lower hydraulic conductivities shown in Table 2.2 for the DPH-GCL specimens is that the bentonite in the DPH-GCL is factory prehydrated, whereas the bentonite in the conventional GCL is not. When a GCL is prehydrated in water (or a dilute chemical solution), the bentonite undergoes up to two distinct phases of swell, i.e., a crystalline phase and an osmotic phase (Norrish 1954; Scalia and Benson 2011). Crystalline

**Table 2.2 Hydraulic conductivity of conventional GCL and DPH-GCL to various chemical solutions at 20 kPa effective stress (data from Kolstad et al. 2004).**

| Permeant liquid | DPH-GCL | | Conventional GCL[(b)] | | $K_{CONV}/K_{DPH}$ [(c)] |
|---|---|---|---|---|---|
| | $K$ (m/s) | $K/K_{DIW}$[(a)] | $K$ (m/s) | $K/K_{DIW}$ [(a)] | |
| 1 M NaCl | $4.2x10^{-12}$ | 1.02 | $7.9x10^{-7}$ | 65,800 | 188,000 |
| 1 M $CaCl_2$ | $3.7x10^{-12}$ | 0.90 | $8.1x10^{-7}$ | 67,500 | 219,000 |
| Base[(d)] | $5.2x10^{-12}$ | 1.27 | $2.2x10^{-11}$ | 1.83 | 4.23 |
| Acid[(e)] | $1.6x10^{-10}$ | 39.0 | $1.5x10^{-7}$ | 12,500 | 66,700 |
| DIW | $4.1x10^{-12}$ | 1.00 | $1.2x10^{-11}$ | 1.00 | 2.93 |

(a) $K$ is hydraulic conductivity to permeant solution, and $K_{DIW}$ is hydraulic conductivity to DIW. GCL was not prehydrated.
(b) $K_{CONV}$ is hydraulic conductivity of conventional non-prehydrated GCL and $K_{DPH}$ is hydraulic conductivity of DPH-GCL.
(c) HCl with pH 1.2.
(d) NaOH with pH 13.1.

swelling is characterized by water molecules entering the interlayer space hydrating the mineral surface and adjacent cations (Scalia and Benson 2011). In this case the movement of the water molecules is driven by the electric fields associated with the clay particle surfaces. Crystalline swelling creates a separation of the interlayers that is equivalent to the size of several water molecules (McBride 1994). In the end of crystalline swelling the bentonite water content is typically 35% (Mooney et al. 1952; Norrish and Quirk 1954; Martin 1960). Crystalline swelling is followed by osmotic swelling which occurs as a result of the water molecules flowing into the interlayer region due to the concentration gradient between the pore water and the interlayer region (Scalia and Benson 2011). Upon completion of osmotic swelling the bentonite water content exceeds 35% and in many cases exceeds 100% (Scalia and Benson 2011). Bentonite can swell to a much greater extent when undergoing osmotic swell as opposed

to experiencing crystalline swell only (Scalia and Benson 2011). Some salt solutions of certain concentrations can limit the swelling process to crystalline swell only, which can increase hydraulic conductivity of bentonite and reduce the efficiency of this material. The polymer treatment is designed to promote osmotic swelling of bentonite even in the presence of chemical solutions. Thus the absence of polymers in conventional GCLs to promote osmotic swell in the presence of chemical solutions may serve as an explanation for significantly higher hydraulic conductivities observed in conventional GCLs.

Hence, the first exposure effect can also be explained in terms of the various stages of swelling, i.e., prehydration allows bentonite to experience crystalline and osmotic swell, whereas chemical solutions can limit the swelling of the bentonite to crystalline swell only. This effect at least partly explains the superior barrier performance of DPH-GCLs in the presence of strong electrolyte solutions when compared to conventional GCLs. The conventional GCL tested by Kolstad et al. (2004) was not prehydrated with water, which prevented the bentonite from reaching its full swell potential. DPH-GCLs, on the other hand, are prehydrated during the manufacturing stage, which initially puts them at an advantage.

Finally, DPH-GCLs were found to be resilient to severe desiccation as indicated by insignificant changes in permeability to distilled water measured before and after dry/wet cycles (Mazzieri 2011). On the other hand, dramatic increases in hydraulic conductivity were observed for DPH-GCLs subjected to 0.0125 M $CaCl_2$ solutions and severe

desiccation (Mazzieri 2011). This increase in permeability was caused by a reduction in self-healing capacity that resulted from the cation exchange (Mazzieri 2011).

## 2.3 Membrane Behavior in Clay Soils

### *2.3.1 Background*

Membrane behavior is the ability of clays to inhibit the transport of ions while allowing for a relatively unrestricted flow of water. The anions are repelled by the electric fields associated with the DDLs of clay particles (Malusis and Shackelford 2002a). Chemico-osmotic pressure, a consequence of membrane behavior, causes liquid to flow in the

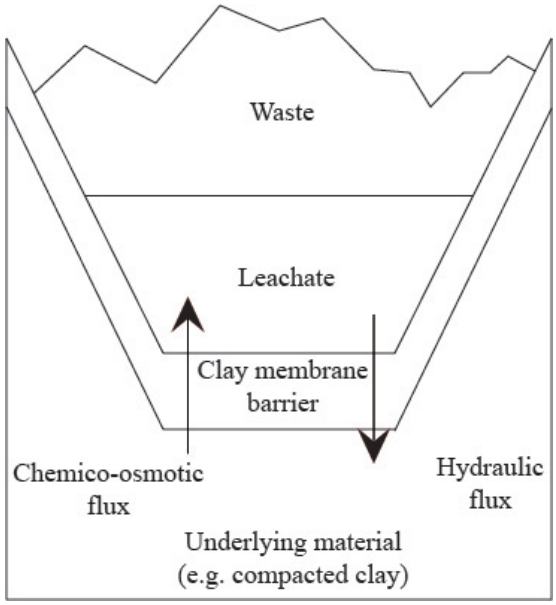


**Figure 2.2 Landfill cross-section and chemico-osmotic flux (redrawn after Malusis et al. 2003).**

direction from low concentration to high concentration (opposite to the concentration gradient). Chemico-osmotic flow of liquid can be beneficial in typical waste containment scenarios, such as the landfill liner system illustrated in Figure 2.2, because this flow opposes the advective (hydraulically driven) and diffusive contaminant flows that tend to drive contaminants out of the containment facility (Malusis et al. 2003).

### *2.3.2 Membrane Efficiency*

Quantitatively, membrane behavior is expressed as chemico-osmotic (membrane) efficiency coefficient, $\omega$, which ranges from zero to unity ($0 \leq \omega \leq 1$). An ideal membrane ($\omega = 1$) is a membrane that would not allow any ion to enter the pore spaces, whereas a non-membrane ($\omega = 0$) would not restrict any ion transport. As illustrated conceptually in Figure 2.3a, the electric fields associated with adjacent clay particles overlap in the pores of an ideal membrane, such that all cations attempting to pass through the pores are electrostatically repelled. The accompanying anions also are repelled, as the anions must travel with the cations to maintain electroneutrality in solution. Therefore, no ions are able to pass through the pores of an ideal membrane. In general, clay soils are considered as non-ideal membranes, because at least some of the pores of a clay soil are sufficiently large that the adjacent electric fields do not overlap (see Figure 2.3b). Ions are able to pass through the free solution in the center of these pores. As a result, $\omega$ values for clay soils generally lie within the range of $0 < \omega < 1$ depending on factors such as the clay type, clay content, dry density, applied stress, and the types and concentrations of ions attempting to pass through the pores.

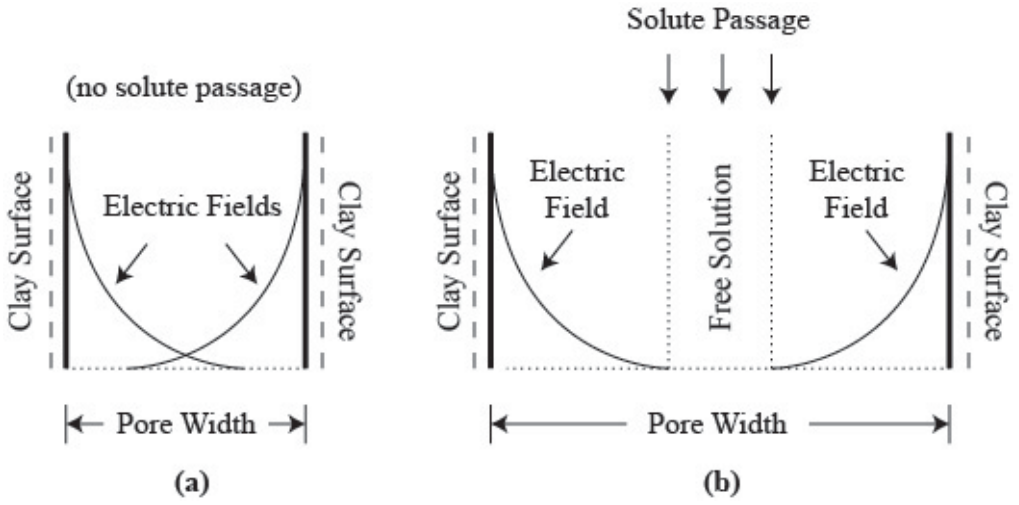


**Figure 2.3 Schematic membrane pores: (a) "ideal" membrane; (b) "non-ideal" membrane (redrawn after Shackelford et al. 2003).**

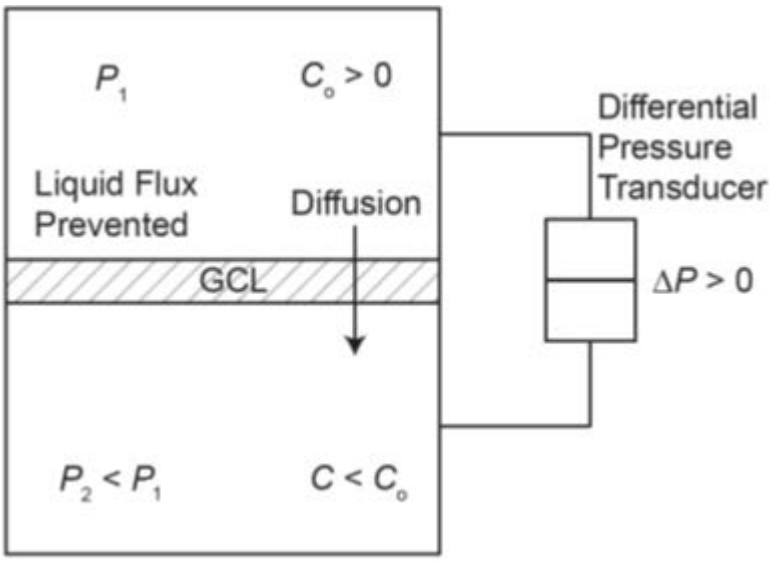


**Figure 2.4 Salt-diffusion testing apparatus for clayey soils.**

The most common test method used to measure membrane efficiency is a salt diffusion test in which a clay specimen is placed between two closed reservoirs, as illustrated conceptually in Figure 2.4. Liquid flux cannot occur across the specimen in this system, because the reservoirs are closed and completely filled. The top reservoir contains a salt (e.g., KCl) solution ($C_o > 0$), whereas the bottom reservoir contains DIW ($C < C_o$), such that downward diffusion of the salt would tend to occur through the specimen.

If the specimen in Figure 2.4 acts as a membrane ($\omega > 0$), diffusion would be at least partially restricted, and a differential pressure ($\Delta P$) would be induced across the specimen due to the prevention of chemico-osmotic flow. The induced differential pressure can be used to compute the membrane efficiency coefficient for the specimen, as follows:

$$\omega = \Delta P/\Delta\pi \tag{2.1}$$

where $\Delta\pi$ is the theoretical chemico-osmotic pressure difference that would be induced across an ideal membrane ($\omega = 1$). The value of $\Delta\pi$ can be calculated for dilute solutions using the van't Hoff equation, i.e.,

$$\Delta\pi = \nu RT\Delta C = \nu RT(C_1 - C_2) \tag{2.2}$$

where $\nu$ is the number of ions per molecule of salt; $R$ is the universal gas constant [8.314 J $mol^{-1}K^{-1}$]; $T$ is absolute temperature [K]; $C$ is salt concentration [M]; and subscripts 1 and 2 represent the upper and lower boundaries of the specimen, respectively (Malusis and Shackelford 2002a).

A primary advantage of the test method described above is that the effective salt-diffusion coefficient, $D_s^*$, also can be determined using the steady-state method

(Shackelford 1991), provided that the boundary concentrations are well controlled such that $\Delta C$ is maintained constant. This is explained further in Section 2.4.2.

### *2.3.3 Factors Affecting Membrane Efficiency*

Membrane behavior is affected by the effective stress, type of solution (valence of the cation), ion concentration, porosity and the types and the amount of clay minerals comprising the soil (Kemper and Rollins 1966; Olsen et al. 1990; Malusis et al. 2001; Malusis and Shackelford 2002a). Bentonite content is one of the most important factors affecting membrane behavior. Kang and Shackelford (2010) showed that a natural CCL with no bentonite content exhibited virtually no membrane behavior. In contrast, several studies have shown that specimens of pure bentonite can produce a wide range of membrane efficiency coefficients ($0 < \omega < 1$) when subjected to a certain range of electrolyte concentrations (Kemper and Rollins 1966; Kemper and Quirk 1972; Kang and Shackelford 2011; Malusis and Shackelford 2002a).

For example, Malusis and Shackelford (2002a) and Kang and Shackelford (2011) presented the relationship between membrane efficiency at steady-state and salt concentration for a conventional GCL subjected to KCl solutions of various concentrations. The relationship is approximately semi-log-linear, as illustrated in Figure 2.5. It is obvious from the graph that an increase in KCl concentration causes a decrease in membrane efficiency provided that the porosity values (shown in legend of Figure 2.5) are similar. The membrane efficiencies reported in these studies will be used as the main mean of comparison to the findings of this research.

The findings of Kemper and Rollins (1966) and Kemper and Quirk (1972) suggest that a decrease in porosity causes an increase in membrane efficiency, all the other things being equal (see Figure 2.6). These studies also support the idea that an increase in concentration produces a decrease in membrane efficiency. Likewise, an increase in valence of the cation causes a decrease in membrane efficiency. The clay structure and Gouy-Chapman theory described below explain the trends observed in Figures 2.5 and 2.6.

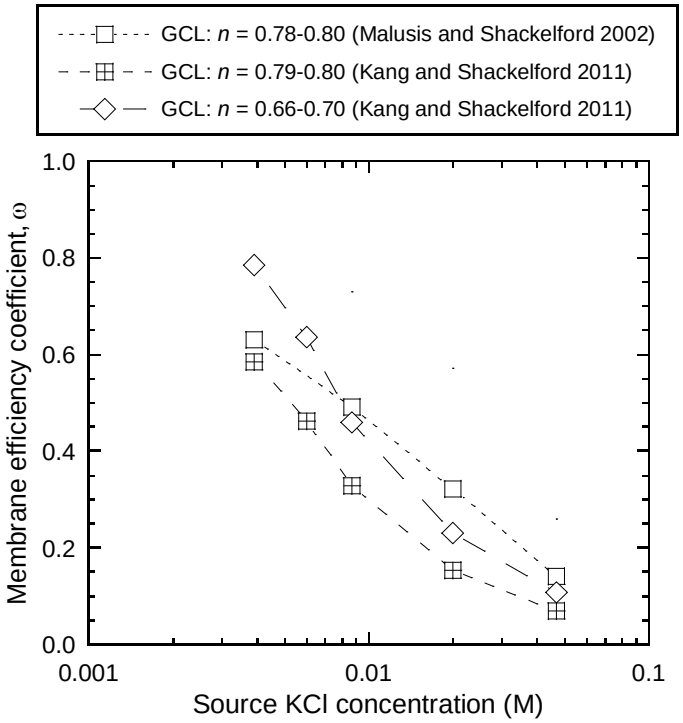


**Figure 2.5 Membrane efficiency of a GCL subjected to KCl solution (data from Malusis and Shackelford 2002a and Kang and Shackelford 2011).**

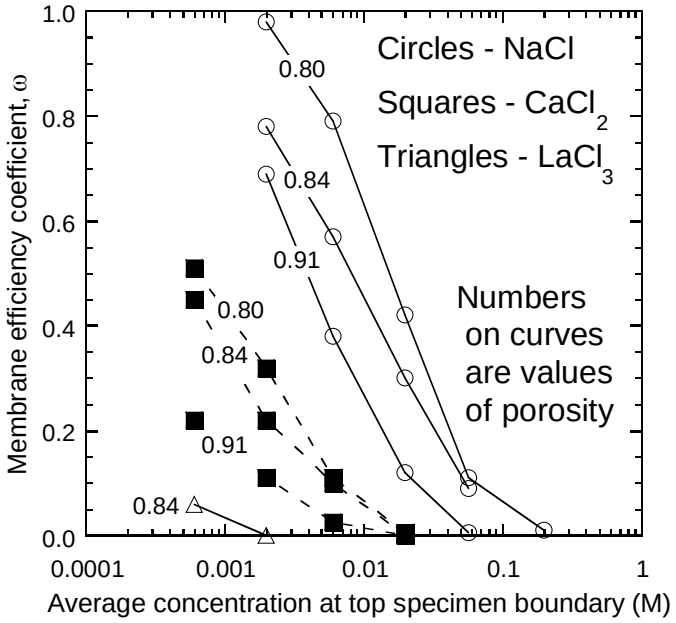


**Figure 2.6 Effect of concentration, valence and porosity on membrane efficiency (ω). Tests conducted by Kemper and Rollins (1966) and Kemper and Quirk (1972) (replotted after Malusis et al. 2001).**

Sodium-montmorillonite (bentonite), the clay that is used in most of GCLs (including DPH-GCL), is composed of one gibbsite sheet sandwiched between two silica sheets. Particles of montmorillonite have film-like shape and negative charge. The thickness of montmorillonite ranges from 10 Å to about 1/100 of the width. The long axis of the particle is typically not greater than 1 or 2 μm. In dry state of clay, the negatively charge of clay particles is balanced by exchangeable cations (e.g., $Ca^{2+}$, $Na^{+}$ and $K^{+}$) which are attracted to clay particles by electrostatic forces (Mitchell and Soga 2005). Once water is added to clay, some of these cations (and some anions) flow slightly further away from

the clay particle surface. This occurs due to concentration gradient between the free water (water that is far enough from clay particle surface for the electrostatic forces to be neglected) with low ion concentration and the clay particle surface where the concentration is high. The concentration gradient creates a diffusive transport of cations from the clay particle surface to the free water, which is counteracted by the electrostatic attraction of cations to negatively charged clay particle. As a result the ions are kept in suspension next to clay particle surface forming the diffuse-double layer (DDL); the water within this layer is called double layer water (DLW) (Mitchell and Soga 2005). Increase in DDL thickness promotes dispersion and, thus, impermeability. On the other hand, decrease in DDL promotes flocculation that is responsible for increases in permeability (Shackelford 1994). The DDL theory was first described by Gouy-Chapman and assumes that the DLW must carry a net positive charge to balance out the negative charge on clay particle surface for electroneutrality condition to be met. The factors that affect DDL thickness, *t*, are described by the following equation:

$$t = \sqrt{\frac{\epsilon\, k\, T}{8\, \pi\, \eta\, e^2 z^2}} \tag{2.3}$$

where $\epsilon$ is dielectric constant, $k$ is Boltzman's constant, $T$ is temperature, $\pi$ is osmotic pressure, $\eta$ is the concentration of the cation (number of ions per $cm^3$), $e$ is a unit electric charge, and $z$ is the valence of the cation (van Olphen 1963 and Mitchell and Soga 2005). Thus, an increase in the valence of the cation ($z$) and concentration of the electrolyte solution cause a decrease in DDL thickness; $t$. A decrease in DDL thickness will create a shorter path for the contaminants to travel across the clay membrane barrier that will

increase permeability. Whitworth and Fritz (1994) correlated an increase in permeability with a decrease in membrane efficiency of compacted smectitic membranes subjected to NaCl solutions. This correlation suggests that reduction in DDL thickness is the mechanism responsible for a reduction in membrane efficiency observed in Figures 2.5 and 2.6.

Cation exchange capacity is another factor that is considered to have an impact on membrane efficiency. The cations responsible for balancing the net negative charge of the clay particle surface are called exchangeable cations. Exchangeable cations are predominantly located within the DDL. When an electrolyte solution is introduced to clay, the exchangeable cations have the capability of being swapped for the cations in the solution if the exchange is thermodynamically favorable. The exchangeable cations that are typically present in naturally occurring clays are $Ca^{2+}$, $Mg^{2+}$, $Na^{+}$ (the primary exchangeable cation in sodium bentonite), and $K^{+}$ (Mitchell and Soga 2005). The propensity of a cation to exchange another cation depends on the relative valence, size, hydration energy and concentration (Mitchell and Soga 2005). Provided that the solution concentrations are the same, the ability of one cation to replace the other can be represented by the following hierarchy:

$$Li^{+} < Na^{+} < K^{+} < Mg^{2+} < Ca^{2+} < Al^{3+} < Fe^{3+} \quad (2.4)$$

## 2.4 Salt-diffusion in Clay Membranes

Diffusion is described as contaminant (ion) transport due to concentration gradient. When acting as waste containment barriers, GCLs separate highly concentrated (contaminant) solutions from clean ground water (see Figure 2.2); this creates high concentration gradient across the barrier and an inclination for contaminants to travel in the direction of decreasing concentration. There are several studies suggesting that diffusion is an important transport process, and possibly the prevailing transport process in fine-grained soils (e.g., Crooks and Quigley 1984 Goodall and Quigley 1987;; Johnson et al. 1989; Lake and Rowe 2000). Nevertheless, advective transport is often treated as the dominant process in the design of waste containment facilities, which poses a problem. Shackelford (1991) notes that laboratory diffusion testing needs to be implemented in the design of waste containment facilities for effective results.

### *2.4.1 Theoretical Background*

The ability of certain ions to diffuse across specific materials can be quantitatively represented in terms of effective salt-diffusion coefficient, $D_s$*:

$$D_s^* = \tau_a D_{so} \tag{2.5}$$

where $D_{so}$ is the diffusion coefficient of the salt in free solution and $\tau_a$ is the apparent tortuosity factor that accounts for the properties of the porous medium through which the diffusion is occurring. Diffusion through soils is a lot more complex and slower than through a free solution, particularly when adsorptive clay particles are present (Mitchell

and Soga 2005). The apparent tortuosity factor accounts for the mechanisms inhibiting the diffusion and takes values between zero and unity ($0 < \tau_a < 1$).

The $D_{so}$ values can be found in chemistry handbooks, while $D_s^*$ can be determined in laboratory following the methods described by Shackelford (1991). With $D_{so}$ and $D_s^*$ available, apparent tortuosity, $\tau_a$, can be determined using Equation 2.5. Based on Equation 2.5 and properties affecting apparent tortuosity, it can be concluded that effective salt-diffusion in soils is dependent on the solution type, concentration gradient and fabric.

Apparent tortuosity can also be expressed as a product of matrix ($\tau_m$) and restrictive ($\tau_r$) tortuosity factors:

$$\tau_a = \tau_m \tau_r \tag{2.6}$$

Matrix tortuosity, $\tau_m$, accounts for the diffusion restriction resulting from the geometry of the interconnected pores. On the other hand, restrictive tortuosity is responsible for all the remaining mechanisms (predominantly membrane behavior for clays) that restrict diffusion (Malusis et al. 2013).

### *2.4.2 Steady-state Diffusion Testing*

As was briefly discussed in Section 2.3.2, effective salt-diffusion coefficients, $D_s^*$, for GCL specimens can be measured using the setup shown in Figure 2.4 (with slight modifications) and the steady-state method described by Shackelford (1991).

The modifications to the system depicted in Figure 2.4 must allow for the systematic collection of the samples from both of the reservoirs for the chemical analysis. Another feature that is required by the steady-state method is that the top reservoir depicted in Figure 2.4 must be continuously replenished so that the concentration at the boundary of the specimen is kept approximately constant. On the other hand, the ions migrating across the membrane as a result of diffusion must be continuously removed from the bottom specimen boundary to maintain a constant concentration gradient. The complexity associated with maintaining the concentration boundaries at constant levels is the main disadvantage of steady-state method of diffusion testing (Shackelford 1991).

The advantage of the steady-state method is that $D_s$* can be measured without the knowledge of the retardation coefficient, $R_d$, as steady-state implies the absence of retardation (Shackelford 1991). That being said, attaining steady-state diffusion may take a long time. The ions that are less likely to participate in ion exchange or to exhibit adsorptive behavior (e.g., $Cl^-$) will take shorter time to reach steady-state condition.

There are several other methods that can be used to determine $D_s$* (e.g., time-lag, transient, column and half-cell methods; described by Shackelford 1991). The steady-state method was chosen because it allows for a simultaneous determination of $D_s$* and membrane efficiency, ω.

### *2.4.3 Influence of Membrane Efficiency on Salt-diffusion in GCLs*

The results of experimental research on conventional GCLs indicate that an increase in membrane efficiency results in a decrease in effective salt-diffusion coefficient (Malusis and Shackelford 2002b, Di Emidio 2010, Dominijanni et al. 2013). For example, the results in Figure 2.7 illustrate that $D_s^*$ generally decreases toward zero as the membrane efficiency increases toward the ideal condition ($\omega = 1$). These results are consistent with expected behavior in that, by definition, $D_s^*$ should be zero for an ideal membrane ($\omega = 1$) that completely restricts the passage of ions.

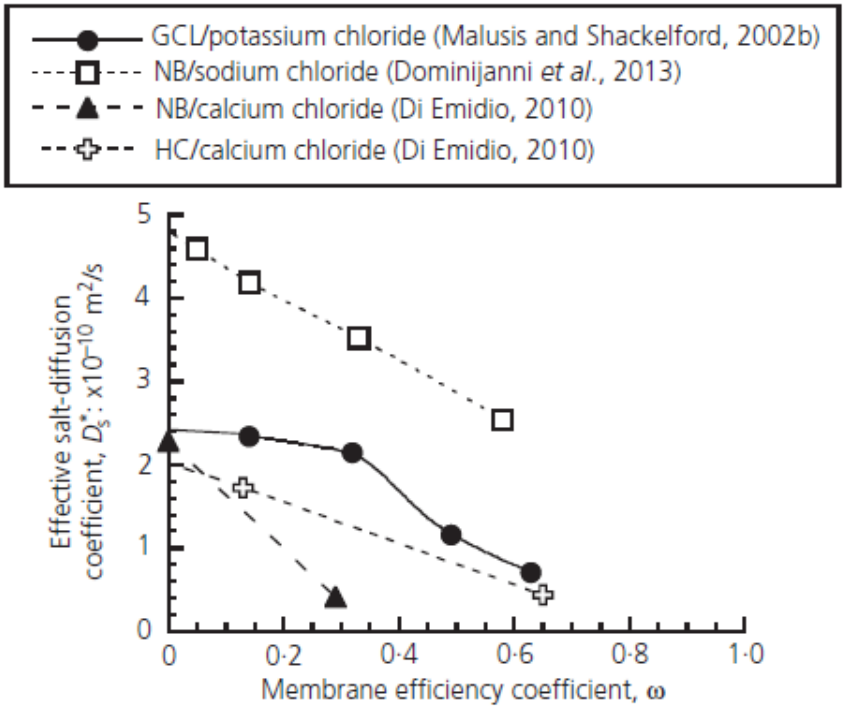


**Figure 2.7 Values of the salt-diffusion coefficient reported in the literature for bentonite specimens subjected to different electrolyte solutions, plotted as a function of membrane efficiency (NB = Na bentonite, HC = HYPER Clay, a polymer-treated Na bentonite) (from Malusis et. al 2014).**

While there has been some research done to determine $D_s^*$-ω relationship for conventional GCLs there is no documented attempt to determine such relationship for DPH-GCLs. A recent study (Malusis et al. 2014) has shown that the relationship between membrane efficiency and $D_s^*$ can be approximated as linear (see Figure 2.8). However, since Malusis et al. (2014) tested only conventional GCLs, it is unknown whether the linear relationship between membrane efficiency and $D_s^*$ will also hold for DPH-GCLs.

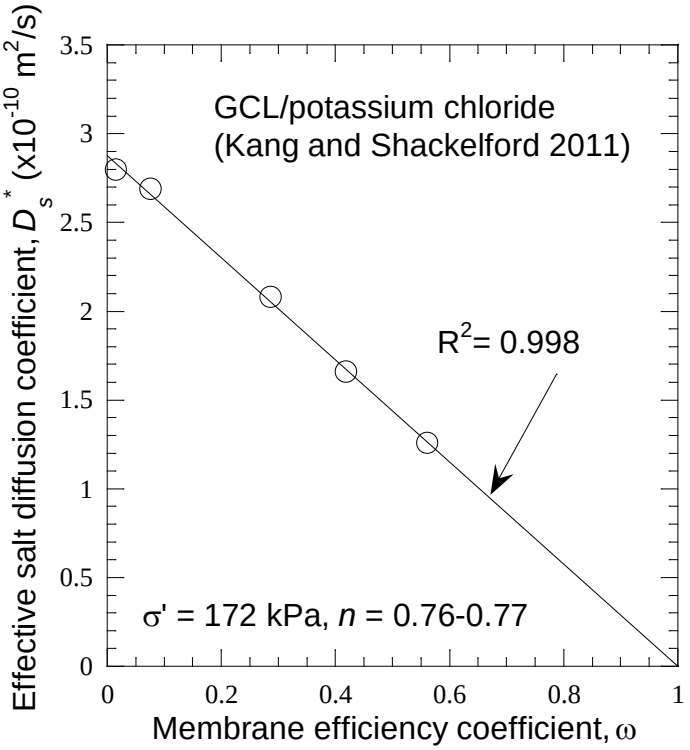


**Figure 2.8 Effective diffusion coefficient versus membrane efficiency for conventional GCL tested under an effective stress of 172 kPa and subjected to KCl solutions (replotted after Malusis et al. 2014).**

The data from Dominijanni et al. (2013) also suggest that the $D_s^*$-ω relationship is linear (see Figure 2.7),Based on these results, it is possible that DPH-GCLs will exhibit a linear $D_s^*$-ω relationship. However, no comprehensive testing has been performed to evaluate this relationship for DPH-GCLs.

Di Emidio (2010) is the only researcher to document membrane efficiency results for DPH-GCLs. This study reports the steady-state membrane efficiency of 0.27 for DPH-GCLs subjected to 1 mM $CaCl_2$ solution. Because Di Emidio (2010) used the salt of higher cation valence, based on the DDL theory it is expected that the membrane efficiency of DPH-GCLs subjected to KCl solutions of the same concentration will be significantly greater, while the effective salt-diffusion will be significantly less.

# 3. MEMBRANE EFFICIENCY OF A DENSE, PREHYDRATED GCL

One of the objectives of this thesis was to investigate the membrane efficiency of DPH-GCL specimens in the presence of monovalent salt (KCl) solutions. Membrane efficiency coefficients, ω, were determined for 5-mm-thick DPH-GCL specimens subjected to five different source KCl solutions (source concentration, $C_{ot}$ = 8.7, 20, 47, 80, and 160 mM) in rigid-wall (acrylic) diffusion cells under no-flow conditions. This chapter describes the testing methods and materials employed in this study. The results of the membrane efficiency testing and a comparison of measured ω values to those of the conventional GCLs are also provided herein.

## 3.1 Introduction

The potential for engineered soils and geosynthetic barriers containing sodium bentonite to act as semipermeable membranes, restricting the passage of ions while allowing relatively unrestricted flow of water, has been well documented in studies conducted over the past decade (e.g., Malusis and Shackelford 2002a,b; Yeo et al. 2005; Henning et al. 2006; Kang and Shackelford 2010, 2011; Mazzieri et al. 2010; Shackelford 2013). The results of these studies indicate that, among the different types of bentonite-rich barriers used in geoenvironmental containment applications, geosynthetic clay liners (GCLs) are most likely to exhibit significant membrane behavior (i.e., high membrane efficiency) due to the high bentonite content (~100 %) in these barriers. Such behavior can improve the containment performance of a GCL by limiting the migration of solutes through the GCL due to chemico-osmosis and restricted diffusion (Malusis et al. 2003).

The vast majority of studies conducted to investigate the membrane behavior of GCLs have been performed on conventional GCL specimens consisting of loose, granular bentonite held between two geotextiles (e.g., by stitching or needle-punching), such as the Bentomat® DN GCL (CETCO, Hoffman Estates, IL) shown in Figure 3.1a (see Malusis and Shackelford 2002a, b; Shackelford and Lee 2003; Kang and Shackelford 2011). However, a relatively new GCL product known as a dense, prehydrated GCL (DPH-GCL; see Figure 3.1b) has emerged as a potentially attractive alternative to conventional GCLs. Whereas conventional GCLs are typically ~10 mm thick and contain naturally dry (non-prehydrated) granular bentonite, the DPH-GCL in Figure 3.1b is ~5 mm thick and contains a calendered layer of powdered bentonite that has been factory prehydrated with a treatment solution designed to improve the flexibility and resilience of the bentonite (Di Emidio 2010).

The combination of the smaller manufactured thickness and the higher bentonite mass per unit area (i.e., ~5 kg/m$^2$ for the DPH-GCL versus ~4 kg/m$^2$ for the conventional GCL) yields a considerably higher as-received dry density for the DPH-GCL (~1.2 Mg/m$^3$) relative to a conventional GCL (~0.43 Mg/m$^3$). Consequently, the DPH-GCL exhibits extremely low hydraulic conductivities, $k$, to water ($1 \times 10^{-12}$ to $4 \times 10^{-12}$ m/s; e.g., see Kolstad et al. 2004), approximately an order of magnitude lower than a conventional GCL. Also, DPH-GCL specimens have been shown to exhibit little or no degradation in $k$ when permeated with highly concentrated salt solutions (Kolstad et al. 2004; Katsumi et al. 2008).

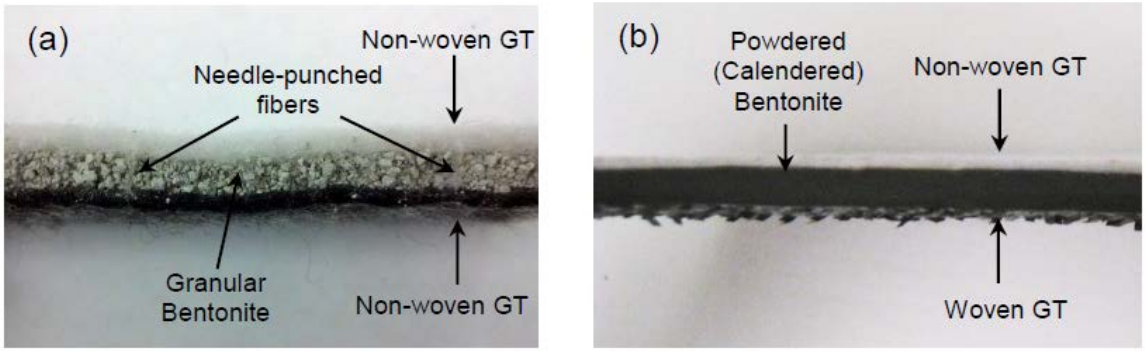


**Figure 3.1 Photographs of GCL cross sections: (a) conventional GCL (Bentomat® DN); (b) DPH-GCL (GT= geotextile).**

Quantitatively, membrane behavior is expressed in terms of a membrane efficiency coefficient, ω, which ranges from zero to unity ($0 \leq \omega \leq 1$). An ideal membrane ($\omega = 1$) is a membrane that would not allow any ion to enter the pore spaces, whereas a non-membrane ($\omega = 0$) would not restrict any ion transport. In general, GCLs act as non-ideal membranes, with ω values varying over nearly the full range of $0 < \omega < 1$ depending on factors such as the dry density (or porosity), applied stress, and the types and concentrations of ions attempting to pass through the pores (e.g., Malusis and Shackelford 2002a, b; Shackelford and Lee 2003; Kang and Shackelford 2011). Given the higher dry density of the bentonite in a DPH-GCL, higher values of ω may be expected for DPH-GCLs relative to conventional GCLs tested under similar conditions. However, only one value of ω has been reported in the literature for a DPH-GCL specimen (Di Emidio 2010). Thus, one of the purposes of this study was to perform membrane tests on DPH-GCL specimens using monovalent salt (KCl) solutions over a range of concentrations (i.e., 8.7 – 160 mM) to facilitate comparison of ω for the DPH-

GCL relative to ω for conventional GCL specimens tested previously by Malusis and Shackelford (2002a) and Kang and Shackelford (2011).

## 3.2 Materials and Methods

### *3.2.1 DPH-GCL*

The DPH-GCL being tested in this study, shown in Figure 3.1b, is manufactured by Rawell Environmental Ltd. (Hoylake, UK) and is commercially available under the trade name Rawmat®. This DPH-GCL is fabricated by blending (prehydrating) Na bentonite with a dilute polymeric solution (containing sodium carboxymethyl cellulose [CMC], sodium polyacrylate [SPA], sodium hexametaphosphate) in a high speed mixer, and then calendaring the bentonite under vacuum into a thin, dense sheet (Flynn and Carter 1998; Di Emidio 2010). The detailed manufacturing process and the role/amounts of the polymeric solutions are provided earlier in the literature review of this thesis (Chapter 2). As reported by Di Emidio (2010), the bentonite in this DPH-GCL exhibits a cation exchange capacity of 52 meq/100 g (52 $cmol_c/kg$) and contains primarily sodium ions (~78 %) on the exchange complex.

The DPH-GCL sheets acquired for this study measured 4.9-5.6 mm in thickness excluding the geotextiles (1.0-1.5 mm), and the average dry bentonite mass per original unit area (i.e., area prior to drying) was determined to be 4.88 $kg/m^2$ based on seven replicate measurements. Note that Kolstad et al. (2004) reports 6.0 $kg/m^2$ as the dry bentonite mass per unit area. It is likely that Kolstad et al. (2004) performed calculations

based on the dry bentonite area as opposed to prehydrated area. The calculations performed by the author suggest that the dry bentonite mass per unit dry area (post oven-drying) was indeed approximately 6 kg/m$^2$.

Specific gravity, $G_s$, of 2.69, was measured for the bentonite following the procedure given by ASTM D 854-10 (water pycnometer test). Two successful water pycnometer tests were conducted using 13.5 and 14.7 g of dry, crumbled DPH-GCL bentonite (see Figure 3.2; see Appendix B for more details). The DIW-bentonite mixture was de-aired for more than 6 months.


**Figure 3.2 (a) Dry, crumbled DPH-GCL bentonite; (b) De-airing station.**

Based on the mass/area, thickness, and $G_s$ values reported above, the average porosity and dry density of the as-received DPH-GCL sheets were estimated to be 0.60 and 1.2 Mg/m$^3$, respectively. Initial degrees of saturation, $S_{av}$, of the as-received samples averaged 88 %, indicating that the sheets were well hydrated but not fully hydrated in the as-received condition.

Table 3.1 below summarizes some of the initial properties of the tested DPH-GCL specimens. Although the initial saturation of one of the test specimens in Table 3.1 (Test 1) was much lower than that of the other tested specimens (28 %), this saturation was not representative of the as-received saturation. This particular specimen was part of a larger sample sheet that had partially dried during ~2 years of storage prior to testing. All of the specimens were permeated with de-ionized water (DIW) prior to membrane/diffusion tests to ensure that the specimens were fully hydrated at the start of the tests.

**Table 3.1 Initial specimen properties.**

| Test No. | $C_{ot}$ (mM) | $L$ (mm) | $w$ (---) | $S$ (%) | $e$ (---) | $\rho_d$ (g/cm$^3$) | $n$ (---) |
|---|---|---|---|---|---|---|---|
| 1 | 8.7 | 5.2 | 0.12 | 28 | 1.15 | 1.25 | 0.53 |
| 2 | 20.0 | 5.6 | 0.54 | 82 | 1.76 | 0.97 | 0.64 |
| 3 | 47.0 | 5.0 | 0.54 | 95 | 1.52 | 1.07 | 0.60 |
| 4 | 80.0 | 5.1 | 0.54 | 84 | 1.73 | 0.99 | 0.63 |
| 5 | 160.0 | 4.9 | 0.54 | 88 | 1.66 | 1.56 | 0.62 |

$C_{ot}$ = source KCl concentration, $L$ = specimen thickness, $w$ = water content, $S$ = degree of saturation, $e$ = void ratio, $\rho_d$ = dry density and $n$ = porosity.

### *3.2.2 Liquids*

The liquids used in this study include de-ionized water (DIW) and 8.7, 20, 47, 80, and 160 mM potassium chloride (KCl) (certified A.C.S., Fisher Scientific, Rochester, NY) solutions created by dissolving the KCl in DIW. Table 3.2 lists some of the measured properties for the solutions. Most of the KCl concentrations were chosen to be the same as those used by Malusis and Shackelford (2002) and Kang and Shackelford (2011) in membrane tests on conventional GCL (Bentomat® DN) specimens. In all tests except for Test 1, the DIW and KCl solutions were amended with 500 ppm of DOWICIL® QK-20

biocide (Dow Chemical Company, Midland, MI) to minimize gas generation in the DPH-GCL due to biological activity (see Jo et al. 2005; Di Emidio et al. 2008). Jo et al. (2005) notes that 500 ppm Dowicil QK-20 is effective for controlling microbial activity without significantly altering the clay fabric. During the DIW permeation stage of Test 1, gas bubbles were observed in the inflow/outflow lines connecting the testing cell to the pressure panel burettes. Therefore, the biocide was added to the DIW and KCl solutions used in the remaining tests (no gas bubbles were observed in these tests). The presence of the biocide resulted in only a minor increase in the EC of the solutions (i.e., maximum 4.8 mS/m).

**Table 3.2 Measured chemical properties of solutions used in study.**

| Liquid | Concentrations | | | EC at 25°C (mS/m) |
|---|---|---|---|---|
| | KCl | | Biocide | |
| | mM | mg/L | mg/L | |
| DIW | 0 | 0 | 0 | 0.4 |
| DIW + biocide | 0 | 0 | 500 | 4.7 |
| KCl solutions | 8.7 | 645 | 0 | 129 |
| | 20 | 1,491 | 500 | 288 |
| | 47 | 3,504 | 500 | 606 |
| | 80 | 5,964 | 500 | 1,024 |
| | 160 | 11,928 | 500 | 1,975 |

EC = electrical conductance

### *3.2.3 Specimen Preparation and Testing Apparatus*

Circular specimens (diameter = 71 mm) of the DPH-GCL were cut from larger sheets, and the lower woven geotextile (see Figure 3.1b) was removed and replaced with a piece of the upper non-woven geotextile for greater protection against erosion of the bentonite during the tests. The specimens then were placed inside of rigid-wall testing cells. Each

cell consisted of an acrylic cylinder with a base pedestal and top piston that enclosed the specimen between two porous stones, as depicted in Figure 3.3. Filter papers were placed at each end, between the specimens and the porous stones. The top piston was fixed in place to prevent outward swelling, thereby maintaining a constant specimen thickness. Both the top piston and base pedestal of the rigid-wall cell contained three bored flow channels. Two of these channels were used to circulate fluids across the specimen boundaries, while the third channel was used to monitor differential pressure induced across the specimen.

Prior to membrane testing, the specimens were permeated with DIW to further hydrate and saturate the specimens and to measure the baseline hydraulic conductivity to water ($k_w$). The specimens were permeated by applying a pressure difference of 34.5 kPa (5 psi) to induce upward flow. There was no attempt to flush the majority of the soluble salts from the specimens, as has been done in several previous studies on membrane behavior of GCLs (e.g., Malusis and Shackelford 2002a, b; Kang and Shackelford 2009, 2011; Di Emidio 2010). For example, the DPH-GCL specimen tested by Di Emidio (2010) was permeated with DIW for 3.8 years (17 pore volumes of flow [PVF]) to remove most of the soluble salts prior to testing for membrane efficiency. In contrast, the specimens in this study were permeated for 4-6 months (~2 PVF). Thus, the overall test durations in this study were much shorter, and the specimens were considered to be a better representation of typical field conditions (i.e., GCLs are not purged of soluble salts prior to being put into service). Permeability tests were terminated once the outflow approached a steady condition and a baseline hydraulic conductivity could be estimated.

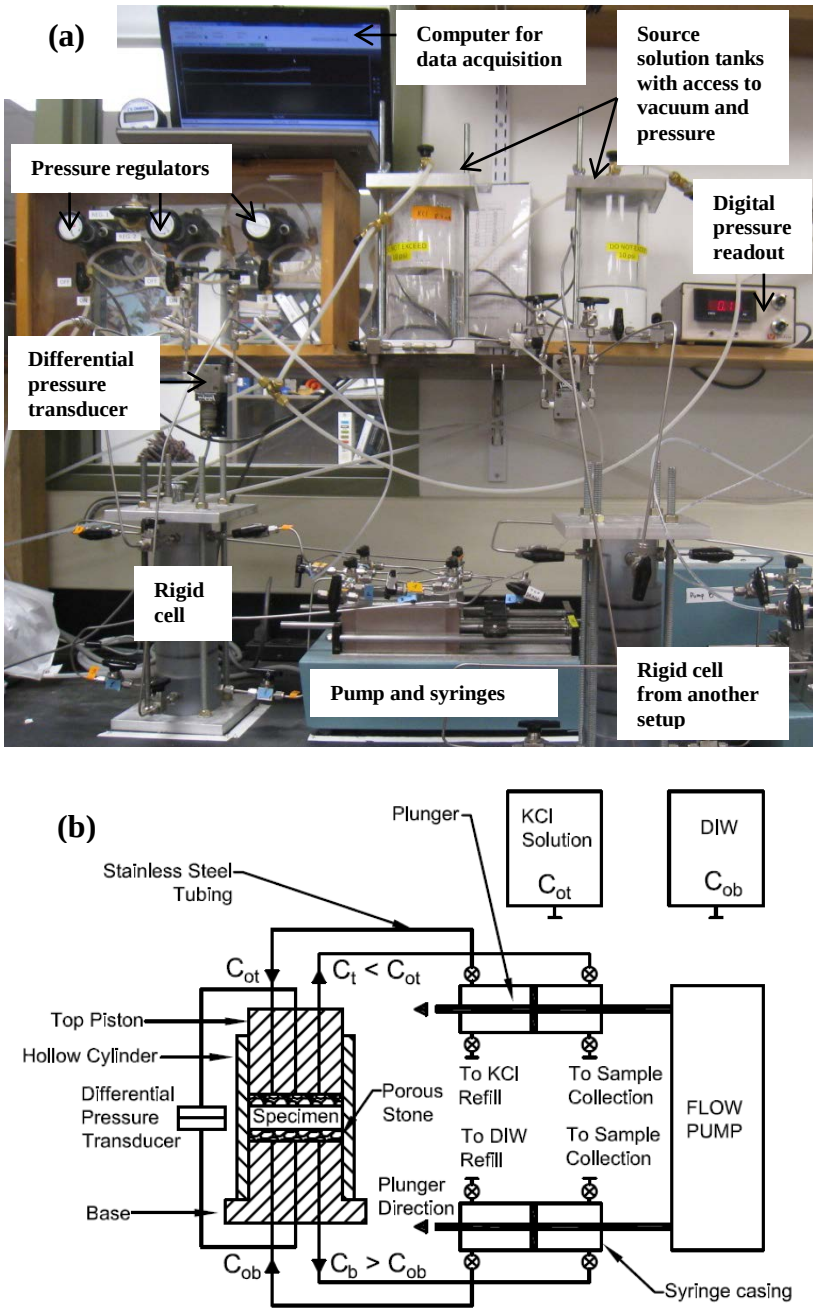


**Figure 3.3 Membrane/diffusion testing apparatus: (a) photograph; (b) schematic diagram (redrawn after Malusis and Shackelford 2002a).**

Each membrane test was performed on a separate DPH-GCL specimen and utilized a different source KCl concentration ($C_{ot}$ = 8.7, 20, 47, 80, or 160 mM). Each test was performed using the apparatus illustrated in Figure 3.3, in general accordance with the procedures described by Malusis and Shackelford (2002a). A syringe pump was used to continuously circulate DIW or KCl solution across the top and bottom specimen boundaries at rate of $4.6 \times 10^{-10}$ $m^3/s$ to establish constant solute concentration difference across the specimen while maintaining a closed system (i.e., no volumetric flux of liquid could occur across the specimens). All the solutions were stored under vacuum to keep the solutions de-aired. All of the tubing, valves, fittings and actuators were made of stainless steel to minimize volume changes and corrosion.

To determine the membrane efficiency, DIW was circulated across the bottom boundary, whereas the KCl solution was circulated across the top boundary. The circulated solutions, collected daily from both boundaries, were analyzed for ion concentrations using ion chromatography (IC). The applied concentration difference induced a pressure difference across the specimen (i.e., due to prevention of chemico-osmotic liquid flux through the specimen), which was measured at 15-minute intervals using a differential pressure transducer.

### *3.2.4 Measurement of Membrane Efficiency*

As it was mentioned in Chapter 2, values of the membrane efficiency coefficient, $\omega$, were determined using the following equation (Malusis et al. 2001):

$$\omega = \Delta P/\Delta\pi \tag{3.1}$$

where $\Delta P$ is the induced differential pressure and $\Delta\pi$ is the theoretical chemico-osmotic pressure difference for an "ideal" membrane ($\omega = 1$). Values of $\Delta\pi$ were computed from the applied KCl concentration difference ($\Delta C$) using the van't Hoff equation (Katchalsky and Curran 1965), or

$$\Delta\pi = \nu RT\Delta C = \nu RT(C_2 - C_1) \tag{3.2}$$

where $\nu$ is the number of ions per molecule of salt ($\nu = 2$ for KCl), $R$ is the universal gas constant (8.314 J $mol^{-1}K^{-1}$), and $T$ is absolute temperature (K), $C$ is salt concentration (M); and subscripts 1 and 2 represent the upper and lower boundaries of the specimen.

The van't Hoff equation is based on the assumption that the electrolyte solutions are ideal and dilute and, thus, is an approximation of the true chemico-osmotic pressure. According to Fritz (1986), the approximation error is small (<5%) for monovalent salts (e.g., NaCl, KCl) at concentrations less than 1 M. The tests were conducted at an average ambient temperature of 22 °C (295 K) as measured by a thermocouple placed next to the experimental setup.

Although the circulation rate of $4.6\text{x}10^{-10}$ $m^3/s$ was sufficient to establish a reasonably constant KCl concentration difference across the specimens, diffusion of KCl through the specimen (i.e., from top to bottom) resulted in small but measurable differences between the inflow concentrations ($C_{ot}$ and $C_{ob}$) and outflow concentrations ($C_t$ and $C_b$) in the circulation loops at the specimen boundaries (i.e., $C_t < C_{ot}$ and $C_b > C_{ob}$; see Figure 3.3b).

Also, since sodium was the predominant soluble salt species and the predominant exchangeable cation species in the bentonite (Di Emidio 2010), the specimens were expected to elute appreciable concentrations of sodium ions ($Na^+$) during the tests. Therefore, the outflow solutions from each specimen boundary were collected and analyzed for electrical conductivity (EC) and for $K^+$, $Na^+$, and $Cl^-$ concentrations using ion chromatography (IC). Other cation and anion species also were monitored ($NH_4^+$, $Ca^{2+}$, $Mg^{2+}$, $Br^-$, $F^-$, $NO_3^-$, $PO_4^{3-}$ and $SO_4^{3-}$), but the concentrations of these species were minor relative to $K^+$ , $Na^+$, and $Cl^-$. The membrane tests were carried out until the transport of both $K^+$ and $Cl^-$ into the bottom boundary approached steady-state conditions, after which the specimens were permeated with the source KCl solution (the same source KCl solution used in the membrane test) to determine the final hydraulic conductivity, $k_c$.

## 3.3 Results and Discussion

### *3.3.1 Induced Differential Pressures*

The differential pressures ($-\Delta P$) measured in the tests are presented in Figure 3.4. At the start of each test, DIW was circulated across both the bottom and top boundaries to establish a baseline differential pressure, $-\Delta P_o$, across the specimen. Despite the absence of an applied concentration difference during this stage, non-zero values of $-\Delta P_o$ are possible due, at least in part, to slight differences in hydraulic conductivity of the porous stones at the specimen boundaries (e.g., see Malusis et al. 2001). In this study, values of $-\Delta P_o$ = 1.7, 0.7, 1.7, 7.0 and 3.0 kPa (listed in the order of increasing source

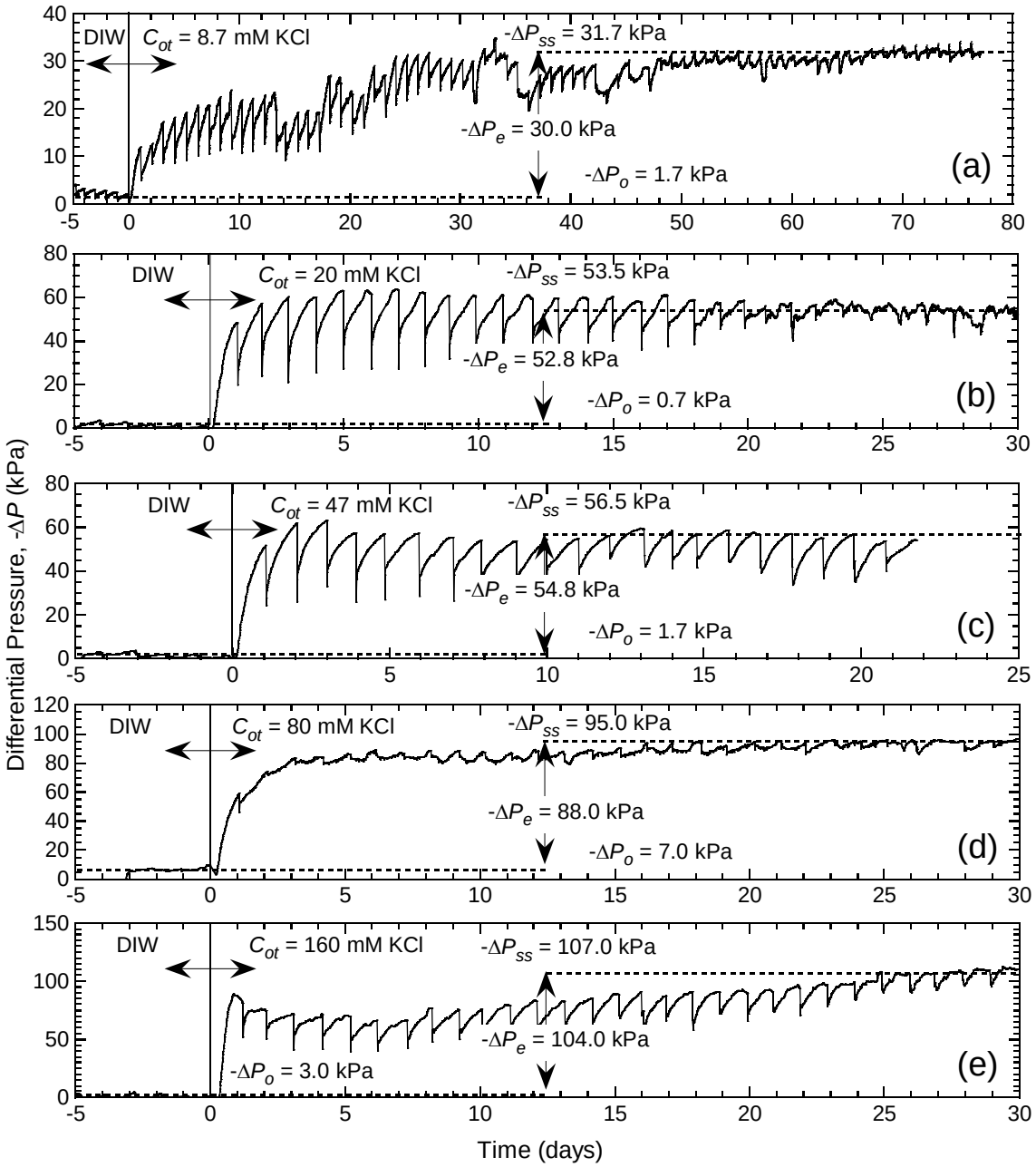


**Figure 3.4 Chemico-osmotic induced differential pressures across DPH-GCL specimens: (a) $C_{ot}$ = 8.7 mM KCl; (b) $C_{ot}$ = 20 mM KCl; (c) $C_{ot}$ = 47 mM KCl; (d) $C_{ot}$ = 80 mM KCl ; (e) $C_{ot}$ = 160 mM KCl; Note: 500 ppm biocide not introduced in test involving 8.7 mM KCl.**

concentration) were measured (see Figure 3.4). Positive -$\Delta P$ indicates that the pressure at the top of the specimen boundary is greater than that at the bottom.

Upon introduction of the KCl solution at the top specimen boundary (on day 0), -$\Delta P$ increased and eventually approached a steady value over time. After approximately two or three days of testing, most of the DIW present initially in the top porous stone was displaced by the KCl solution, such that the top boundary concentration approached the source concentration, $C_{ot}$ (see Figure 4). This short delay in establishing a fairly constant concentration difference across the specimens explains the slight delay in the measured differential pressure response. Daily variations in -$\Delta P$ illustrated in Figure 3.4 result from temporary release of some of the pressure during the daily process of refilling the syringes.

As shown in Figure 3.4, the differential pressures at steady state, -$\Delta P_{ss}$, increased with increasing $C_{ot}$ and were estimated to be 31.7, 53.5, 56.5, 95.0 and 107.0 kPa (in the order of increasing source concentration). Thus, the net (effective) differential pressures attributed to membrane behavior, $-\Delta P_e = (-\Delta P_{ss} + \Delta P_o)$, were 30.0, 52.8, 54.8, 88.0 and 104.0 kPa, respectively. Although the trends of -$\Delta P$ over time were similar in each test, the trend was more erratic throughout much of the test conducted using the 8.7 mM KCl solution (Figure 3.4a), which did not contain the biocide. Because the suspected cause of the erratic behavior was gas generation by microbial activity in the specimens, biocide was added to both the DIW and the KCl solutions for the tests in Figures 3b-e. The -$\Delta P$

trends in these tests were more consistent over time, indicating that microbial activity may have been responsible for the more erratic behavior illustrated in Figure 3.4a.

### *3.3.2 Determination of* $\Delta\pi$

The ion concentrations in the outflows from each specimen boundary are presented as a function of time in Figure 3.5. The circulation rate for specimens subjected to concentrations 8.7, 20 and 47 mM KCl was $4.7 \times 10^{-10}$ $m^3/s$, whereas the circulation rate per specimen exposed to 80 and 160 mM KCl was $4.4 \times 10^{-10}$ $m^3/s$. This slight difference in the circulation rate resulted from the use of the two different pumps and is considered to have an insignificant effect on the results of this study.

The $Na^+$ concentrations in Figure 3.5 indicate that the DPH-GCL specimens tested contained appreciable soluble salts that were not flushed during the initial permeation stage. In addition, cation exchange of $K^+$ for $Na^+$ contributed much of $Na^+$ eluted at both boundaries during the transient portion of the tests. In the first few days of testing, the concentrations of $Na^+$ exceeded the concentrations of both $Cl^-$ and $K^+$ at the bottom specimen boundary. However, the eluted $Na^+$ concentrations decreased over time and generally were at least 10 times lower than the eluted $Cl^-$ and $K^+$ concentrations at the end of each test. Chloride concentrations approached the steady state condition much faster than $K^+$ at both the top and bottom boundaries, due to the greater reactivity of $K^+$ with the bentonite (see Figure 3.5). However, as cation exchange neared completion (as indicated

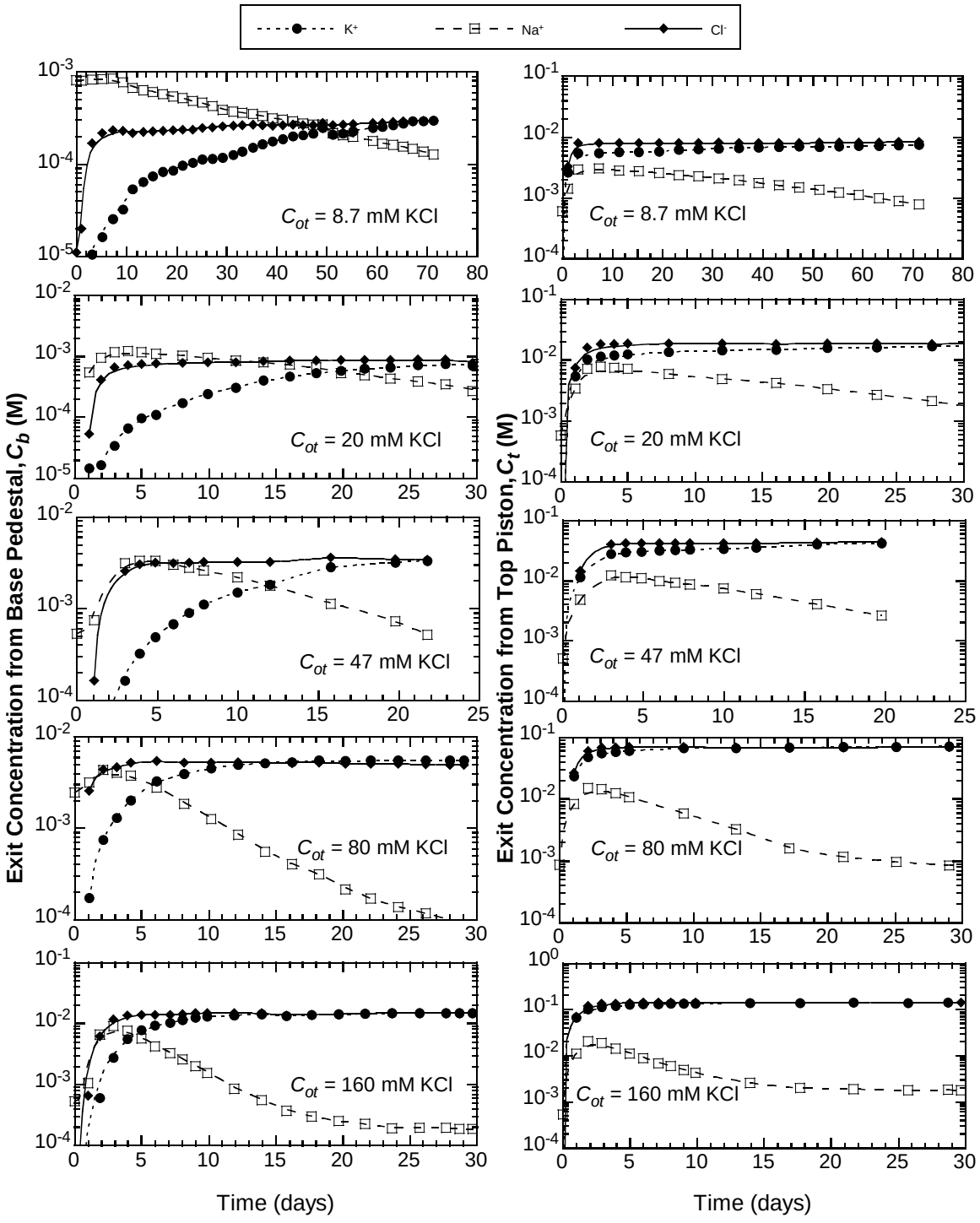


**Figure 3.5 Measured ion concentrations as function of time at bottom (left set of plots) and at top (right set of plots) specimen boundaries (KCl is added on day 0).**

by the significant decrease in eluted $Na^+$ concentrations), the $K^+$ concentrations at both boundaries approached the respective $Cl^-$ concentrations. The maximum chemico-osmotic pressure difference, termed initial difference in chemico-osmotic pressure ($\Delta\pi_o$), occurs when the $C_2 = C_{ob}$ and $C_1 = C_{ot}$, and can be computed using the Equation 2.2. Because $C_{ob} = 0$ in each test, the expression used to determine $\Delta\pi_o$ is reduced to:

$$\Delta\pi_o = -2RTC_{ot} \qquad (3.3)$$

The use of $\Delta\pi_o$ in determining the membrane efficiency, $\omega$, can only be justified under the "perfectly flushing" scenario in which the liquid circulation rate at each boundary is sufficiently fast to completely mask the contribution of ions diffusing into and out of the specimens. Otherwise, a measureable diffusive flux will persist which will result in a loss and gain of ions at the top and bottom boundaries, respectively ($C_t < C_{ot}$ and $C_b > C_{ob}$ in Figure 3.3b). In this case, the actual $\Delta\pi$ is lower than $\Delta\pi_o$ (Malusis et al. 2001). To account for impact of diffusion, $\Delta\pi$ was more accurately computed based on the average boundary KCl concentrations, $C_{t,av}$ and $C_{b.av}$ as follows (Malusis et al. 2001):

$$C_{t,av} = (C_{ot} + C_t)/2; \qquad C_{b,av} = (C_{ob} + C_b)/2 \qquad (3.4)$$

Thus, the average chemico-osmotic pressure difference at steady state, $\Delta\pi_{av}$, was estimated using the average concentrations as follows:

$$\Delta\pi_{av} = 2RT(C_{b.av} - C_{t.av})_{ss} \qquad (3.5)$$

where the subscript "ss" indicates that the values were measured at steady state. The resulting values of $\Delta\pi_o$ and $\Delta\pi_{av}$ are presented in Table 3.3.

**Table 3.3 Summary of membrane test results.**

| Test No. | $C_{ot}$ (mM) | Membrane test results (based on $Cl^-$ concentrations at steady state) | | | | | | | | | | Hydraulic conductivities |
|---|---|---|---|---|---|---|---|---|---|---|---|---|
| | | $-\Delta P_o$ (kPa) | $-\Delta P_{ss}$ (kPa) | $-\Delta P_e$ (kPa) | $C_{b.av}$ (mM) | $C_{t.av}$ (mM) | $\Delta C_{av}$ (mM) | $-\Delta\pi_o$ (kPa) | $-\Delta\pi_{av}$ (kPa) | $\omega_o = \Delta P_e / \Delta\pi_o$ | $\omega_{av} = \Delta P_e / \Delta\pi_{av}$ | $k_w, k_c$ (x$10^{-12}$ m/s) |
| 1 | 8.7 | 1.7 | 31.7 | 30.0 | 0.3 | 8.3 | 8.4 | 42.6 | 40.9 | 0.70 | 0.73 | 1.4, 1.8 |
| 2 | 20 | 0.7 | 53.5 | 52.8 | 0.8 | 18.4 | 18.8 | 98.0 | 92.1 | 0.54 | 0.57 | 1.1, 1.3 |
| 3 | 47 | 1.7 | 56.5 | 54.8 | 3.2 | 41.3 | 42.5 | 230.3 | 208.5 | 0.24 | 0.26 | 2.0, 1.9 |
| 4 | 80 | 7.0 | 95.0 | 88.0 | 4.9 | 69.4 | 72.2 | 392.0 | 352.9 | 0.22 | 0.25 | 1.2, 1.0 |
| 5 | 160 | 3.0 | 107.0 | 104.0 | 14.7 | 138.4 | 141.9 | 785.2 | 696.2 | 0.13 | 0.15 | 0.7, 1.2 |

$C_{ot}$ = source KCl concentration, $\Delta P_o$ = background differential pressure, $\Delta P_{ss}$ = steady-state differential pressure at presence of chemical solution, $\Delta P_e$ = net (effective) differential pressure, $C_{b.av}$ and $C_{t.av}$ = molar Cl concentrations in outflows form top and bottom specimen boundaries at steady state, respectively, $\Delta C_{av}$ = average molar specimen boundary concentration difference, $\Delta\pi_o$ = chemico-osmotic pressure difference based on input (source) concentrations at specimen boundaries, $\Delta\pi_{av}$ = chemico-osmotic pressure difference based on average concentrations at specimen boundaries, $\omega_o$ = membrane efficiency coefficient based on source concentration difference, $\omega_{av}$ = membrane efficiency coefficient based on average concentration difference, $k_w$ = hydraulic conductivity to water (measured prior to testing), $k_c$ = hydraulic conductivity to source KCl solution (measured after testing).

### *3.3.3 Membrane Efficiency Coefficients*

Membrane efficiency coefficients, ω, for each of the five specimens (based on the steady-state $-\Delta P_e$ values in Figure 3.4) are presented in Table 3.3. The values designated $\omega_o$ represent membrane efficiency coefficients computed based on $\Delta\pi = \Delta\pi_o$ (see Equation 3.3). Values of ω computed using $\Delta\pi = \Delta\pi_{av}$ (designated as $\omega_{av}$ in Table 3.3) as given by Equation 3.5 are slightly higher than $\omega_o$, because $\Delta\pi_{av}$ is slightly lower than $\Delta\pi_o$. However, the differences between $\omega_{av}$ and $\omega_o$ are small (<12 %).

### *3.3.4 Results Based on Electrical Conductivity Measurements*

As previously mentioned, the electrical conductivity (EC) of the circulated solutions was measured using a portable EC meter that automatically corrects for temperature effects. The EC results for the bottom and top specimen boundary outflows are presented in Figure 3.6. Previous research suggests that the concentrations of KCl solutions can be well approximated by the EC values (see Malusis and Shackelford 2002a) as the relationship between the two is linear (see Figure 3.7). The relationship depicted in Figure 3.7a was used to determine the EC-based KCl concentrations for solutions with low EC range (0 – 140 mS/m) whereas the regression equation shown in Figure 3.7b was used to determine the EC-based KCl concentrations with relatively high EC range (140-2500 mS/m).

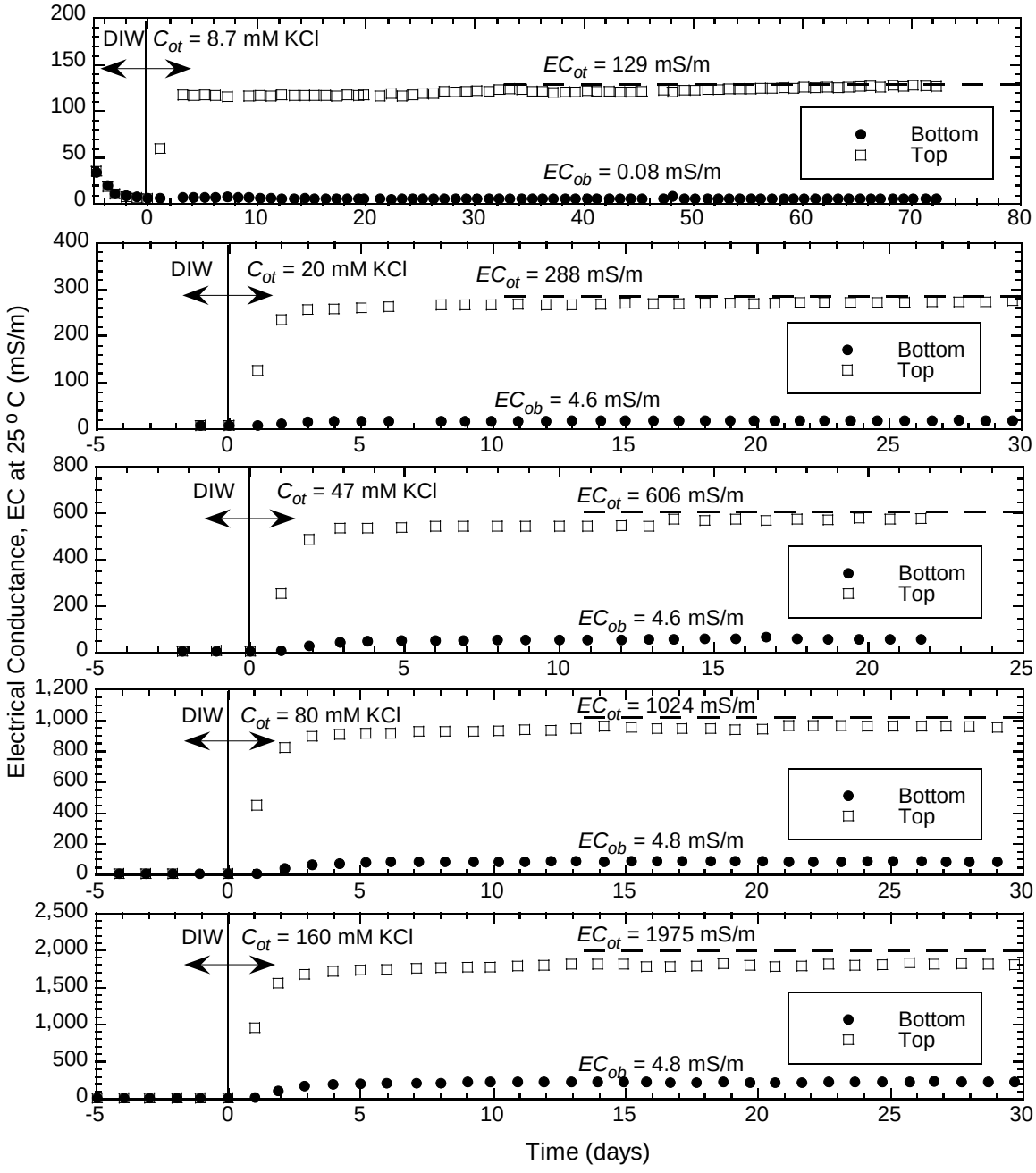


**Figure 3.6 Electrical conductance at 25°C as function of time.**

Malusis and Shackelford (2002a) and Malusis et al. (2014) indicate that membrane efficiencies can be well approximated by estimating $\Delta\pi_{av}$ from EC measurements using the correlations in Figure 3.7. The reason behind this successful approximation is that $K^+$ and $Cl^-$ ions are practically the only ions contributing to the EC when at steady state.

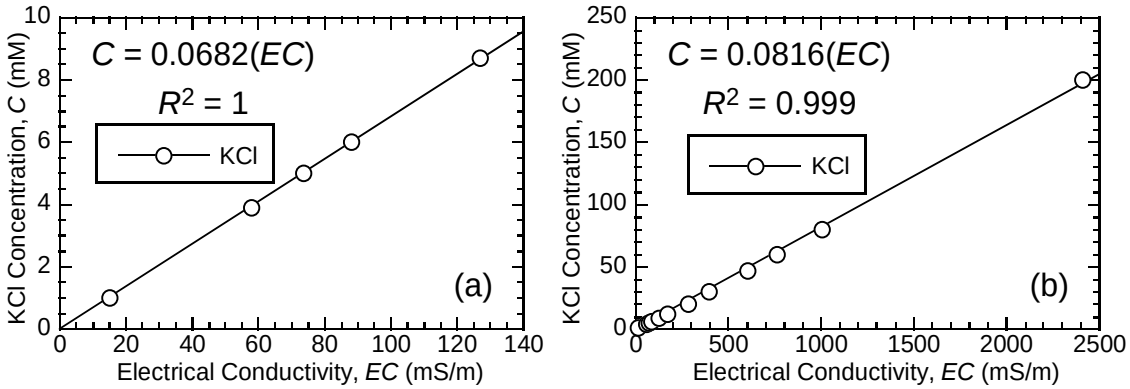


**Figure 3.7 Concentration of KCl in DIW (no biocide added) as function of electrical conductivity at 25°C (EC): (a) for low concentrations (1.0-8.7 mM KCl); (b) for high concentrations (8.7-200 mM KCl).**

The steady-state EC values ($EC_b$ and $EC_t$) as well as the EC-based KCl concentrations ($C_{b.EC}$ and $C_{t.EC}$) derived from the ECs for bottom and top outflows are presented in Table 3.4. Note that before converting the ECs to concentrations, the electrical conductivity of biocide in DIW (4.6-4.8 mS/m) was subtracted from the measured total ECs. This action was taken to better estimate the outflow concentrations. The exception form this method was test with the lowest source concentration (Test 1; $C_{ot}$ = 8.7 mM) since it was not exposed to biocide. The converted steady-state concentration values were used to determine $\Delta C_{av.EC}$, $\Delta\pi_{av.EC}$ and, subsequently, $\omega_{av.EC}$ (presented in Table 3.4) following the methods employed to determine $\Delta C_{av}$, $\Delta\pi_{av}$ and $\omega_{av}$ (shown in Table 3.3). The

**Table 3.4 Summary of membrane test results based on the electrical conductivity (EC) measurements.**

| Test No. | $C_{ot}$ (mM) | Membrane test results (based on KCl concentrations derived from EC measurements at steady state) | | | | | | | | | Membrane test results from Table 3.3 (based on $Cl^-$ concentrations at steady state) | | |
|---|---|---|---|---|---|---|---|---|---|---|---|---|---|
| | | $EC_{ob}$ (mS/m) | $EC_{ot}$ (mS/m) | $EC_b$ (mS/m) | $EC_t$ (mS/m) | $C_{b.av.EC}$ (mM) | $C_{t.av.EC}$ (mM) | $\Delta C_{av.EC}$ (mM) | $-\Delta\pi_{av.EC}$ (kPa) | $\omega_{av.EC} = \Delta P_e / \Delta\pi_{av.EC}$ | $C_{b.av}$ (mM) | $C_{t.av}$ (mM) | $\omega_{av} = \Delta P_e / \Delta\pi_{av}$ |
| 1 | 8.7 | 0.1 | 129 | 6.0 | 127.2 | 0.4 | 8.7 | 8.5 | 41.6 | 0.72 | 0.3 | 8.3 | 0.73 |
| 2 | 20 | 4.6 | 288 | 19.3 | 278.0 | 1.0 | 22.4 | 20.7 | 101.4 | 0.52 | 0.8 | 18.4 | 0.57 |
| 3 | 47 | 4.6 | 606 | 47.9 | 536.8 | 3.3 | 43.8 | 43.8 | 214.4 | 0.26 | 3.2 | 41.3 | 0.26 |
| 4 | 80 | 4.8 | 1024 | 86.7 | 960.5 | 5.5 | 77.9 | 76.2 | 373.4 | 0.24 | 4.9 | 69.4 | 0.25 |
| 5 | 160 | 4.6 | 1975 | 228.0 | 1814.0 | 15.0 | 147.7 | 146.3 | 718.3 | 0.14 | 14.7 | 138.4 | 0.15 |

$C_{ot}$ = source KCl concentration, $EC_{ob}$ and $EC_{ot}$ = electrical conductivities of top and bottom solutions (biocide included), $EC_b$ and $EC_t$ = electrical conductivities of top and bottom specimen boundaries at steady state, respectively (biocide included), $C_{b.av.EC}$ and $C_{t.av.EC}$ = EC-derived molar Cl concentrations in outflows from top and bottom specimen boundaries at steady state, respectively, $\Delta C_{av.EC}$ = average molar specimen boundary concentration difference computed based on EC-derived steady-state concentrations, $\Delta\pi_{av.EC}$ = chemico-osmotic pressure difference based on $\Delta C_{av.EC}$, $\omega_{av.EC}$ = membrane efficiency coefficient based on average concentration difference.

pressure values and the source concentrations (and therefore $\omega_o$) remained unchanged from the values shown in Table 3.3.

It can be seen from Table 3.4 that the EC-based concentrations ($C_{b.EC}$ and $C_{t.EC}$) generally are at least slightly greater than those determined using ion chromatography (IC) (see Table 3.3). This difference can be explained by the elution of the soluble salts from the specimens,which contributes to the measured EC values. This does not pose a serious problem when determining $\omega$, because the soluble salts are eluted at both at the top and the bottom specimen boundaries. When the differences in concentration ($\Delta C_{av.EC} = C_{b.av.EC} - C_{t.av.EC}$) are computed, the contribution of the soluble salts is essentially canceled out. Hence the membrane efficiency values computed using the EC measurements ($\omega_{av.EC}$) closely match the membrane efficiency values produced using the ion chromatography ($\omega_{av}$) (see Figure 3.8).

## 3.4 Comparison to Conventional GCLs

The $\omega_{av}$ and $\omega_{av.EC}$ values in Tables 3.3 and 3.4 are plotted as a function of source KCl concentration ($C_{ot}$) in Figure 3.8, along with those reported previously for the Bentomat® DN conventional GCL by Malusis and Shackelford (2002) and Kang and Shackelford (2011). The results show that $\omega_{av}$ decreases with increasing source concentration for both the conventional GCL and the DPH-GCL. These trends are consistent with expected behavior for bentonite based on DDL theory (Kemper and Rollins 1966; Shackelford et

al. 1999; Malusis and Shackelford 2002a, b) and suggest that the presence of the polymers in the DPH-GCL did not completely prevent DDL shrinkage upon exposure to

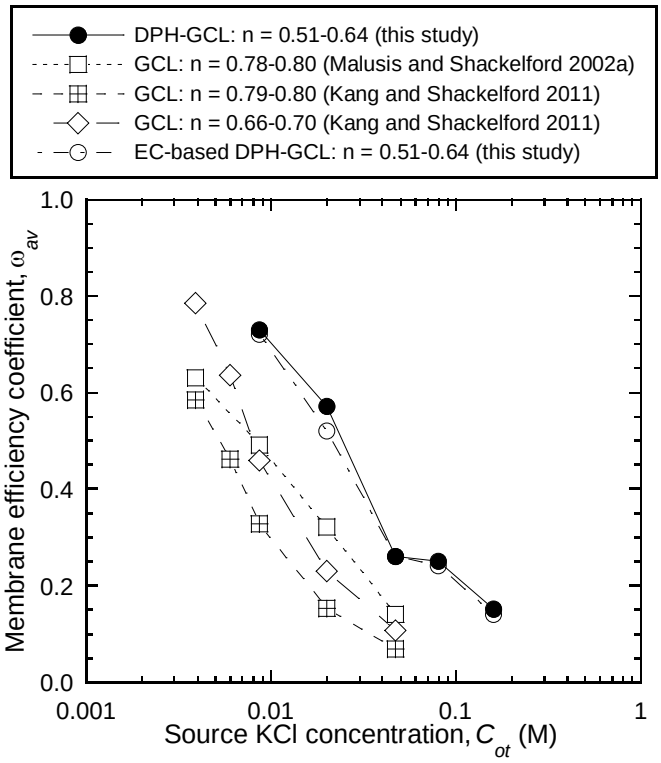


**Figure 3.8 Membrane efficiency as function of source KCl concentration ($C_{ot}$) for DPH-GCL specimens and conventional (Bentomat® DN) GCL specimens.**

the KCl solutions, even though the hydraulic conductivities to the KCl solutions (measured after testing) were nearly the same as the hydraulic conductivities to DIW (measured before testing; see Table 3.3). Nonetheless, the DPH-GCL specimens exhibited higher $\omega_{av}$ for a given source concentration relative to the conventional GCL specimens. The higher ω values for the DPH-GCL specimens are attributed primarily to the lower porosity (or higher dry density) of these specimens (see Table 3.1). There are several studies showing the inverse relationship between porosity and membrane

efficiency (e.g. Olsen 1969; Malusis and Shackelford 2002a). Reduced pores create shorter distances between clay particles and the electric fields associated with them (Shackelford 2003). As a result, diffusive transport is inhibited and membrane efficiency is increased.

However, the ω values for the conventional GCL compressed to porosities approaching those of the DPH-GCL specimens (i.e., $n$ = 0.66-0.70) are still appreciably lower than $\omega_{av}$ for the DPH-GCL specimens, indicating that factors other than porosity may be contributing to the differences in ω. For example, it is possible that the presence of the CMC and SPA in the DPH-GCL provided some benefit in terms of mitigating DDL shrinkage. Also, the DPH-GCL was fabricated using powdered bentonite, whereas the conventional GCL contained granular bentonite. As noted by Malusis and Shackelford (2002a), the coarse granules in a conventional GCL may contribute to larger pore sizes and, thus, lower membrane efficiencies relative to powdered bentonite specimens. Finally, the tests by Kang and Shackelford (2011) were conducted in flexible wall cells, whereas the tests in this study were conducted in rigid wall cells. Additional research is needed to further investigate the impacts of these differences on membrane efficiency.

## 3.5 Conclusions

This study reports the results of an experimental investigation conducted to determine the membrane efficiency coefficients (ω) for DPH-GCL specimens subjected to potassium chloride (KCl) solutions with source concentrations of 8.7, 20, 47, 80 and 160 mM.

Values of ω for the DPH-GCL specimens decreased with increasing KCl concentration, as expected based on diffuse-double layer theory, despite any potential mitigation of diffuse-double layer shrinkage that may have been provided by the polymeric treatment agents added to the DPH-GCL bentonite via the prehydration solution. Nonetheless, the ω values for the DPH-GCL specimens were shown to be greater (for a given source KCL concentration) relative to those for conventional GCL specimens containing non-prehydrated Na bentonite granules. The concentrations derived from the electrical conductivity measurements were proven to yield accurate membrane efficiencies despite the presence of biocide and elution of soluble salts. The biocide and the soluble salts contributed similar incremental increases to the EC values at both specimen boundaries, which were canceled out when the concentration differences across the specimens were computed. .

The superior membrane efficiencies of the DPH-GCL specimens relative to the conventional GCL specimens are attributed primarily to the higher dry density (and, therefore, lower porosity) of the specimens, although differences in bentonite texture (i.e., powdered bentonite in the DPH-GCL versus granular bentonite in the conventional GCL) and chemical treatment of the bentonite in the DPH-GCL also may have contributed to higher ω for the DPH-GCL. Additional research is needed to elucidate the relative significance of these different potential factors.

# 4. SALT-DIFFUSION THROUGH A DENSE, PREHYDRATED GCL

Determination of the relationship between the effective salt-diffusion coefficient, $D_s^*$, and membrane efficiency coefficient, ω, for a dense, prehydrated GCL (DPH-GCL) was one of the primary objectives of this thesis. This chapter covers (and references) the description of the testing equipment and methods employed to determine $D_s^*$ values for DPH-GCL specimens, which are presented herein and plotted as a function of source KCl concentration as well as ω. The factors affecting $D_s^*$ (i.e., tortuosity) are also discussed in this chapter. All of the results are compared against results reported for conventional GCLs in previous studies.

## 4.1 Introduction

As briefly discussed in the literature review (see Chapter 2), diffusion has been proven to be a critical factor in the chemical transport process within fine-grained soils (e.g., Goodall and Quigley 1987; Crooks and Quigley 1984; Johnson et al. 1989; Lake and Rowe 2000). These findings suggest that a careful consideration must be given to diffusive transport (e.g., laboratory testing) when designing waste containment facilities (Shackelford 1991). Thus, determining the effect of the solutes of certain type and concentration on $D_s^*$ can be of value to the geoenvironmental engineering profession.

### *4.1.1 Salt-diffusion – Background*

Salt-diffusion is a process in which the cations and anions of a miscible salt species diffuse in the same direction through a porous medium. For example, consider a simple

experiment in which a clay soil is placed between two sealed reservoirs, as shown in Figure 4.1. The source reservoir contains a binary salt (KCl) solution, whereas the collection reservoir contains de-ionized water (DIW). The salt cation ($K^+$) and the salt anion ($Cl^-$) will both diffuse through the soil from the source (left) reservoir into the collection (right) reservoir.

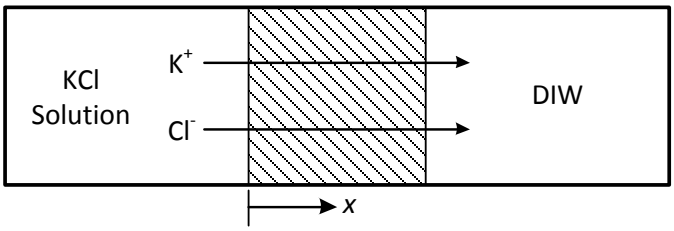


**Figure 4.1 Salt-diffusion of KCl through a clay soil in a closed system (DIW = de-ionized water) (Malusis et al. 2013).**

Provided there are no other solutes present in the system illustrated in Figure 4.1, the $K^+$ and $Cl^-$ will diffuse through the soil at the same rate, thereby maintaining electroneutrality in solution. Thus, the molar diffusive fluxes of both the $K^+$ and the $Cl^-$ will be the same, such that the diffusive flux of either solute may be described by the following form of Fick's first law for one-dimensional diffusion in a saturated porous medium (Shackelford 1991):

$$J_D = -nD_s^* \frac{dC}{dx} \tag{4.1}$$

where $J_D$ is the diffusive flux, $n$ is the soil porosity, $C$ is solute concentration, $D_s$* is the effective salt-diffusion coefficient, and $x$ is the distance into the soil specimen (i.e., in Figure 4.1, $x = 0$ at the left boundary and $x = L$ at the right boundary). When Fick's law is expressed in the form presented in Equation 4.1, $D_s$* is implicitly defined as follows:

$$D_s^* = \tau_a D_{so} \quad (4.2)$$

where $D_{so}$ is the salt-diffusion coefficient in free solution (values for KCl were obtained from Robinson and Stokes 1959) and $\tau_a$ is a dimensionless apparent tortuosity factor ($0 \leq \tau_a < 1$) that accounts for the geometry associated with the interconnectivity of the individual pores within the porous matrix as well as any other factors that may affect solute transport. Because $0 \leq \tau_a < 1$ and, therefore, $D_s^*$ is always less than $D_{so}$, the definition of $D_s^*$ in Equation 4.2 inherently accounts for the tortuous nature of solute diffusion pathways through the soil.

### *4.1.2 Impact of Membrane Behavior on Salt-diffusion Through GCLs*

Typically, $D_s^*$ is assumed to be constant in Equation 4.1. However, results of prior experimental studies on conventional GCLs have shown that (1) $D_s^*$ values for conventional GCLs are not constant, but rather tend to decrease as the source salt concentration ($C_o$) decreases, and (2) the decreasing trend in $D_s^*$ with decreasing $C_o$ correlates with an increase in the membrane efficiency coefficient, ω (Malusis and Shackelford 2002b; Di Emidio, 2010; Dominijanni et al. 2013). In fact, these studies indicate that $D_s^*$ will approach zero ($D_s^* \rightarrow 0$) in the limit as ω approaches unity ($\omega \rightarrow 1$), which is consistent with the theoretical consideration that no solutes can pass through the pores of an ideal membrane ($\omega = 1$). Malusis and Shackelford (2002b) attributed this effect to a decrease in the apparent tortuosity factor, $\tau_a$, with increasing ω, since $D_{so}$ in Equation 4.2 must be constant for a given salt species.

According to Shackelford and Daniel (1991), $\tau_a$ can be defined as the product of a matrix tortuosity factor, $\tau_m$, and a restrictive tortuosity factor, $\tau_r$, as follows:

$$\tau_a = \tau_m \tau_r = \tau_m \prod_{i=1}^{N} \tau_i \tag{4.3}$$

where $\tau_m$ accounts for the tortuosity associated with the geometry of the interconnected pores and $\tau_r$ is a lumped parameter that accounts for any number, $N$, of other mechanisms, represented individually by $\tau_i$, that restrict the diffusive solute flux, such as solute exclusion and solute drag near the surfaces of clay particles (Malusis et al. 2013). Based on Equation 4.3, $D_s^*$ can be expressed to reflect the separate influences of matrix tortuosity and restrictive tortuosity as follows:

$$D_s^* = \tau_a D_{so} = \tau_m \tau_r D_{so} \tag{4.4}$$

Whereas $\tau_m$ generally is considered to be constant for a given arrangement of soil particles (and, therefore, independent of solute concentration), $\tau_r$ for clay membranes may vary with solute concentration insofar as changes in solute concentration cause a change in $\omega$. Theoretically, $\tau_r = 0$ for ideal membranes (i.e., $\omega = 1$) that completely exclude solutes. However, higher solute concentrations will cause shrinkage of the diffuse-double layers and an increase in $\tau_r$, such that $\tau_r$ would approach unity as the membrane efficiency approaches zero ($\tau_r \rightarrow 1$ as $\omega \rightarrow 0$), assuming that all other potentially restrictive effects are insignificant. Under this assumption, $\tau_m$ would be equivalent to $\tau_a$ at zero membrane efficiency (i.e., $\tau_a = \tau_m$ when $\omega = 0$; based on Equation 4.4).

Over a decade ago, Manassero and Dominijanni (2003) proposed that the relationship between ω and the restrictive tortuosity factor, $\tau_r$ for clay membranes can be reasonably approximated as linear, i.e.,

$$\tau_r = 1 - \omega \tag{4.5}$$

In a more recent study by Malusis et al. 2013 the $\tau_r - \omega$ relationship for conventional GCLs subjected to KCl concentrations was proven to follow the trend described by Equation 4.5.

The $D_s^* - \omega_{av}$ relationship for DPH-GCLs, subjected to KCl solutions of various concentrations, established in this chapter was compared against the model developed by Manassero and Dominijanni (2003) and the results for conventional GCLs obtained by Malusis et al. 2013.

The $D_s^*$ values pertaining to DPH-GCLs were expected to be lower than the values for conventional GCLs tested under similar conditions due to a higher dry density of the bentonite in DPH-GCLs. The fact that DPH-GCLs have significantly higher membrane efficiencies, ω, per given source KCl concentrations, than conventional GCLs (see Chapter 3) also suggests the lower $D_s$* (and thus superior performance) for DPH-GCLs.

## 4.2 Materials and methods

Diffusion measurements were conducted simultaneously with the membrane efficiency tests, using the same apparatus, specimens, and KCl solutions described in Chapter 3.

Please refer to Sections 3.1 and 3.2 for detailed descriptions of the materials, equipment, specimen preparation procedures, and specimen properties.

### *4.2.1 Measurement of Diffusion Coefficient*

The measurements of the effective salt-diffusion coefficients, $D_s^*$, were made possible by the steady-state diffusion method described by Shackelford (1991). The calculations were performed based on the steady-state chloride ($Cl^-$) concentrations which were attained a lot faster than the steady-state concentrations for potassium, $K^+$, due to adsorptive behavior of $K^+$.

Diffusion, $J_D$, by definition, is the ratio of the cumulative amount of mass passed through unit area of a material over a certain interval of time. Thus, $J_D$, at steady state can be expressed as:

$$J_D = \frac{\Delta m}{A\Delta t} = \frac{\Delta Q_t}{\Delta t} \tag{4.6}$$

were $m$ is mass (of an ion or salt), $A$ is the specimen area through which diffusion is taking place, $t$ is time and $\Delta Q_t$ is the cumulative mass (of an ion or salt) per unit specimen area $A$ (Shackelford 1991).

Combining equation 4.1 and equation 4.6 at steady state yields:

$$D_s^* = -\frac{\Delta Q_t}{\Delta t}\frac{\Delta x}{n\Delta C} \tag{4.7}$$

Because the thickness of the soil specimen is $L$, the expression 4.7 can be reduced to:

$$D_s^* = -\frac{\Delta Q_t}{\Delta t}\frac{L}{n\Delta C} \tag{4.8}$$

Note that the expression 4.8 is only true for no-flow, steady-state (no retardation) conditions. Equation 4.8 and the $Cl^-$ and KCl (based on electric conductivity measurements) concentrations at steady state were used to determine the effective salt-diffusion coefficients.

The factors in equation 4.8 were determined experimentally. Diffusive flux ($\Delta Q_t / \Delta t$) was determined by plotting $Q_t$ as a function of time and evaluating the slope of the steady-state portion (beginning at time, $t = t_{ss}$) of the plot (see Figure 4.2)

Using the plot depicted in Figure 4.2 time lag, $t_L$, can also be computed as the x-intercept of the $\Delta Q_t / \Delta t$ slope. Time lag is an alternative method for determining effective salt-diffusion; this method requires the knowledge of $t_L$ and retardation, $R_d$ (see Shackelford 1991 for more information). Note that the concentration values (e.g. $\Delta C_{av}$) were determined using the same methods as discussed in Chapter 3.

## 4.3 Results and Discussion

### *4.3.1 Diffusive flux* ($dQ_t/dt$)

The diffusive flux, $J_D$ (or $dQ_t/dt$), values were determined based on the steady-state portion of the plot of relationship between cumulative molar mass of $Cl^-$ (determined using ion chromatography) collected at the bottom specimen boundary and time, *t*, during which diffusion was taking place.

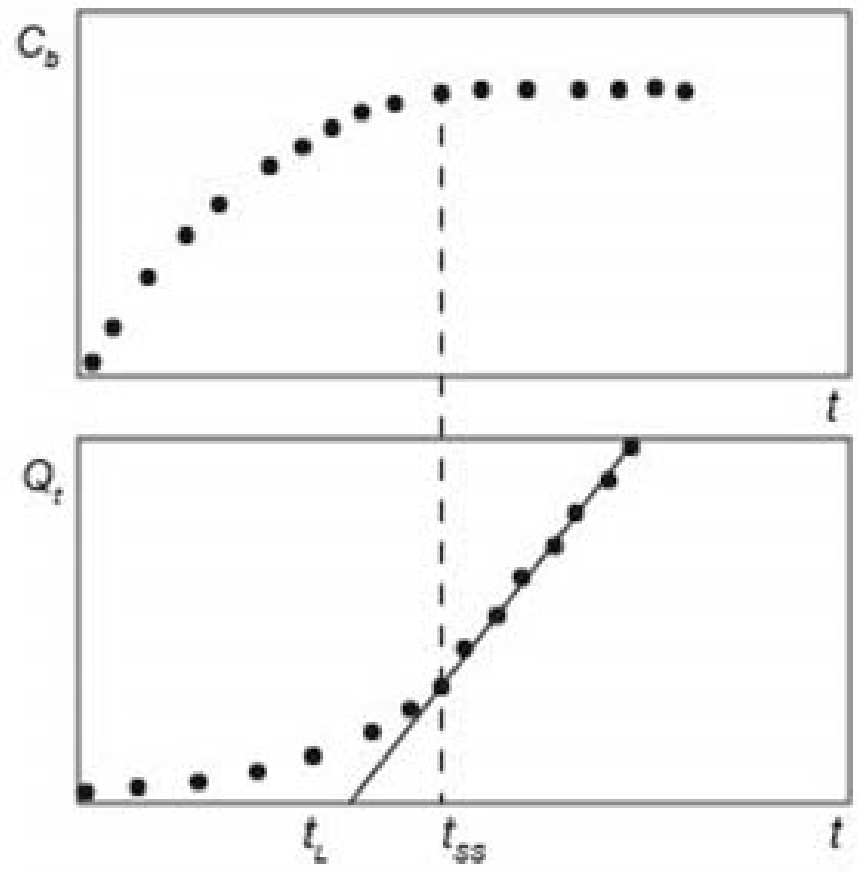


**Figure 4.2 Cumulative mass per unit area as function of time ($C_b$ is concentration at the bottom specimen boundary; redrawn after Shackelford 1991).**

The cumulative mass plots were produced from the $Cl^-$ concentration profiles at the bottom specimen boundary depicted in Figure 4.3. Figure 4.3 also presents the concentration profiles for $K^+$ and EC-based KCl (discussed later in this chapter). The results for $dQ_t/dt$ are presented in Figure 4.4. The start of the steady-state portion of the plot depicted in Figure 4.4 is defined by the time-to-steady-state, $t_{SS}$.

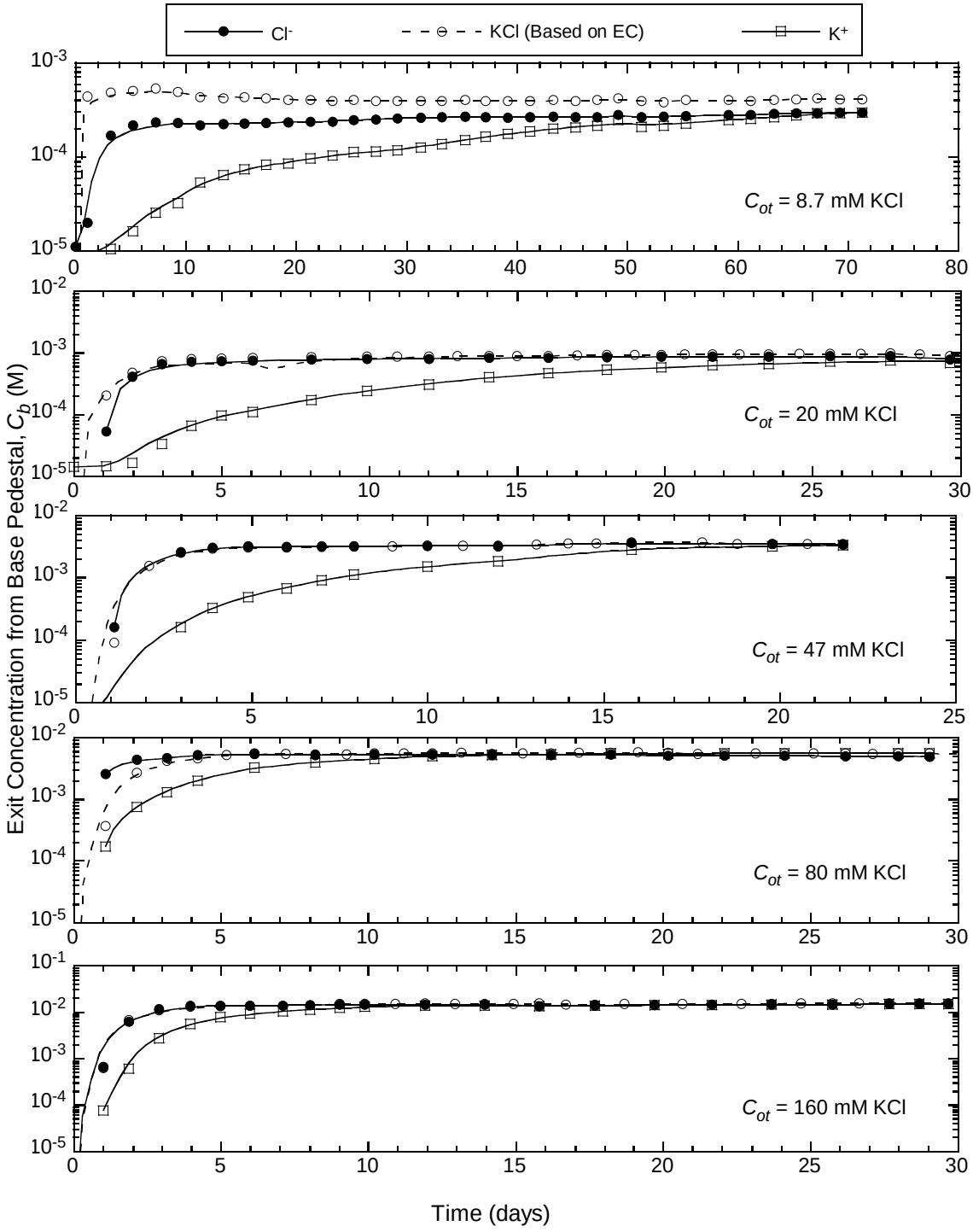


**Figure 4.3 Measured $Cl^-$ and EC-based KCl concentrations as a function of time at bottom specimen boundary (KCl is added on day 0).**

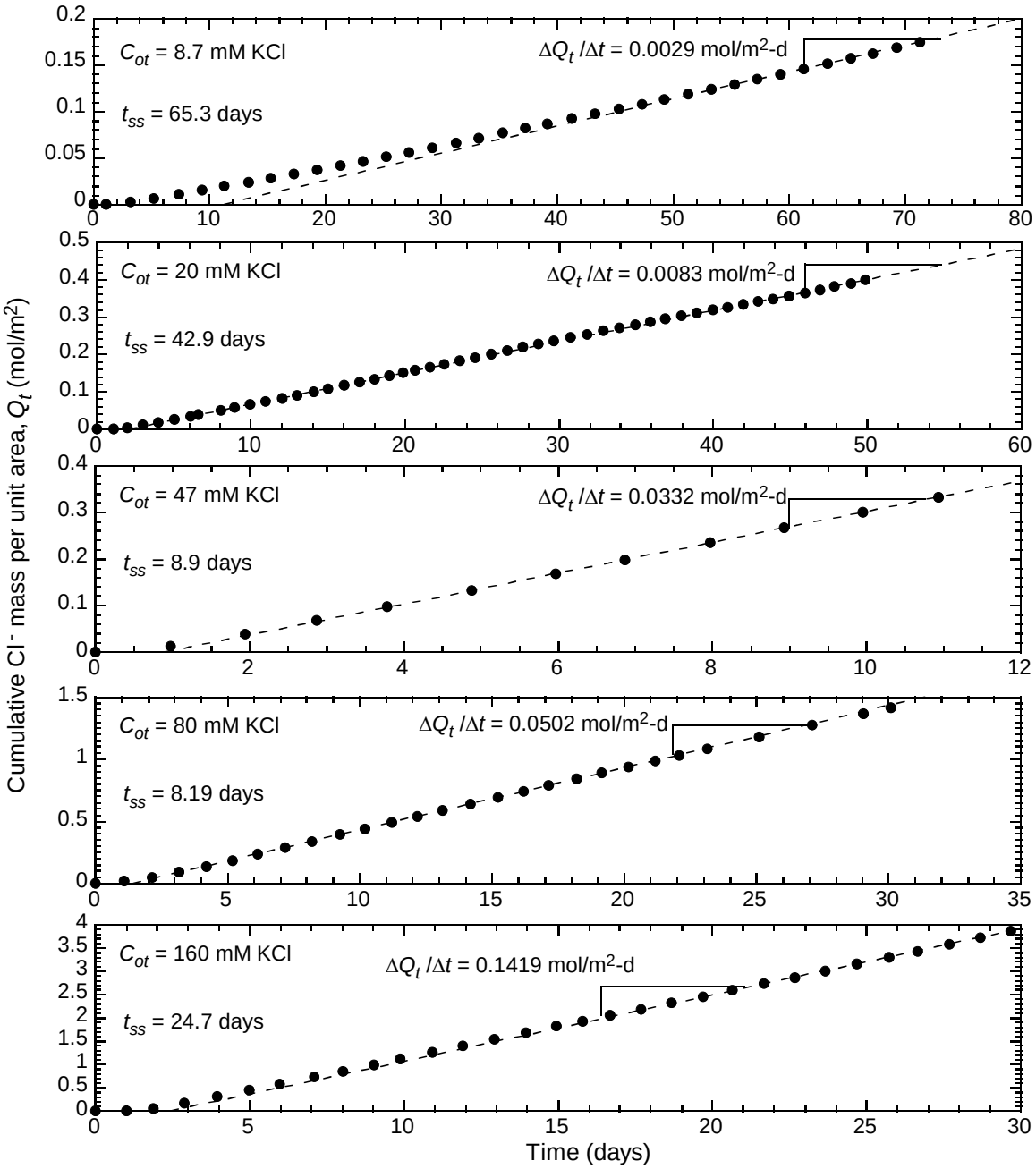


**Figure 4.4 Cumulative moles of $Cl^-$ diffused through a unit area of the DPH-GCL specimen, $Q_t$, as a function of time.**

### *4.3.2 Effective Salt-diffusion Coefficients*

The effective salt-diffusion coefficients, $D_s$*, were evaluated using the $dQ_t/dt$ values along with the initial specimen properties and steady state changes between the average boundary concentrations ($\Delta C_{av}$) determined in Chapter 3. The $D_s$* values are presented in Table 4.1 and are expressed as a function of source KCl concentration in Figure 4.5.

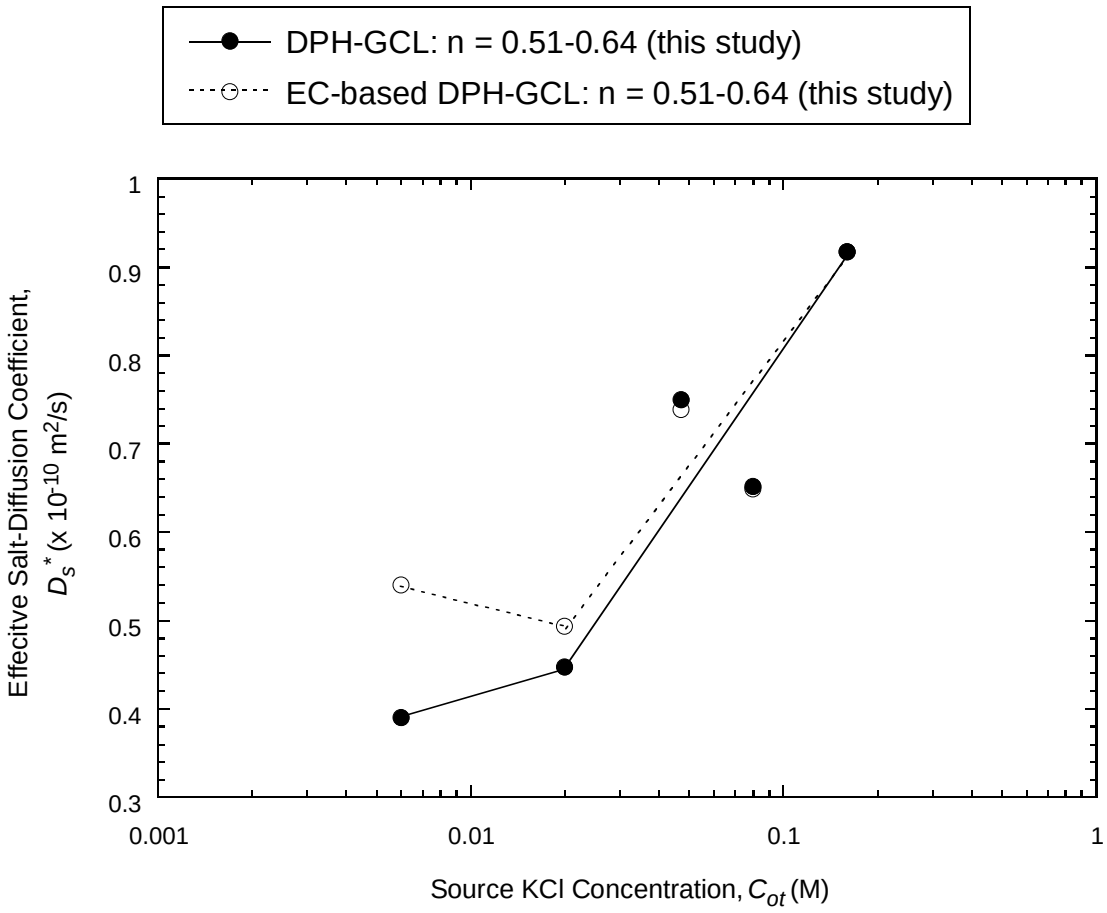


**Figure 4.5 Effective salt-diffusion coefficients as a function of source KCl concentration for DPH-GCLs.**

**Table 4.1 Summary of salt-diffusion test results based on ion chromatography (IC) measurements.**

| Test No. | Specimen properties | | | Salt-diffusion test results (based on $Cl^-$ concentrations at steady state) | | | | | Tortuosity results | | | |
|---|---|---|---|---|---|---|---|---|---|---|---|---|
| | $C_{ot}$ (mM) | $L$ (mm) | $n$ (---) | $C_b$ (mM) | $C_t$ (mM) | $\Delta C_{av}$ (mM) | $\Delta Q_t/\Delta t$ (mol/ $m^2$-d) | $D_s^*$ (x$10^{-10}$ $m^2$/s) | $D_{so}$ (x$10^{-10}$ $m^2$/s) | $\tau_a$ (---) | $D_{se}$ (x$10^{-10}$ $m^2$/s) | $\tau_r$ (---) |
| 1 | 8.7 | 5.2 | 0.53 | 0.3 | 8.3 | 8.4 | 0.0029 | 0.39 | 19.93 | 0.020 | 0.96 | 0.41 |
| 2 | 20 | 5.6 | 0.64 | 0.8 | 18.4 | 18.8 | 0.0083 | 0.45 | 19.93 | 0.023 | 0.96 | 0.47 |
| 3 | 47 | 5.0 | 0.60 | 3.2 | 41.3 | 42.5 | 0.0332 | 0.75 | 19.93 | 0.038 | 0.96 | 0.78 |
| 4 | 80 | 5.1 | 0.63 | 4.9 | 69.4 | 72.2 | 0.0502 | 0.65 | 19.93 | 0.033 | 0.96 | 0.68 |
| 5 | 160 | 4.9 | 0.62 | 14.7 | 138.4 | 141.9 | 0.1419 | 0.92 | 19.93 | 0.046 | 0.96 | 0.96 |

$C_{ot}$ = source KCl concentration, $L$ = specimen thickness, $n$ = porosity, $C_{b.av}$ and $C_{t.av}$ = molar Cl concentrations in outflows form top and bottom specimen boundaries at steady state, respectively, $\Delta C_{av}$ = average molar specimen boundary concentration difference, $\omega_{av}$ = membrane efficiency coefficient based on average concentration difference, $\Delta Q_t/\Delta t$ = change in cumulative moles of $Cl^-$ per unit area, $Q_t$, per change in time, $D_s^*$ = true effective salt-diffusion coefficient, $D_{se}$ = effective salt-diffusion coefficient at zero membrane efficiency ($\omega_{av}$= 0), $D_{so}$ = salt-diffusion coefficient for KCl in free solution (from Robinson and Stokes 1959), $\tau_a$ = apparent tortuosity factor, $\tau_r$ = restrictive tortuosity factor.

As it can be seen from Figure 4.5, the $D_s$* values at 47 and 80 mM KCl source concentrations for DPH-GCL break the expected trend of increasing $D_s$* with increasing source solution concentration ($D_s$*[80 mM] < $D_s$*[47 mM]). This inconsistency could be attributed to specimen variability and warrants duplicate tests (with the same source concentrations).

### *4.3.3 Results Based on Electrical Conductivity (EC)*

The effective salt-diffusion coefficients determined using the KCl concentrations derived from EC measurements (see Chapter 3 Section 3.3.4 for EC method description) are presented in Table 4.2. Note that the exact same conversion techniques were used as in Chapter 3. Figure 4.5 depicts the relationship between EC-based effective salt-diffusion coefficients, $D_{s.EC}$*, and source KCl concentrations, $C_{ot}$. The $D_{s.EC}$* values were calculated using the same method as it was used to compute $D_s$* values. Figure 4.3 shows the EC-based KCl concentration profiles at the bottom specimen boundaries that were used to construct the cumulative molar mass plots depicted in Figure 4.6. The steady state portion of the cumulative mole of KCl plots (starting at time $t = t_{SS}$) was used to determine the $(dQ_t/dt)_{EC}$ (also shown in Figure 4.6). It is obvious from Figure 4.5 that $D_{s.EC}$* values closely resemble the effective salt-diffusion coefficients determined using the measured $Cl^-$ concentrations, $D_s$* (also depicted in Figure 4.3) which suggests that EC method can be effective in estimating $D_s$*.

**Table 4.2 Summary of salt-diffusion test results based on electric conductivity (EC) measurements.**

| Test No. | Specimen properties | | | Salt-diffusion test results (based on KCl concentrations at steady state determined from EC measurements) | | | | | Tortuosity results (EC-based) | | | |
|---|---|---|---|---|---|---|---|---|---|---|---|---|
| | $C_{ot}$ (mM) | $L$ (mm) | $n$ (---) | $C_{b.av.EC}$ (mM) | $C_{t.av.EC}$ (mM) | $\Delta C_{av.EC}$ (mM) | $(\Delta Q_t/\Delta t)_{EC}$ (mol/ $m^2$-d) | $D_{s.EC}^*$ ($x10^{-10}$ $m^2/s$) | $D_{so}$ ($x10^{-10}$ $m^2/s$) | $\tau_{a.EC}$ (---) | $D_{se.EC}$ ($x10^{-10}$ $m^2/s$) | $\tau_{r.EC}$ (---) |
| 1 | 8.7 | 5.2 | 0.53 | 0.4 | 8.7 | 8.5 | 0.0029 | 0.54 | 19.93 | 0.027 | 0.89 | 0.61 |
| 2 | 20 | 5.6 | 0.64 | 1.0 | 22.4 | 20.7 | 0.0103 | 0.49 | 19.93 | 0.025 | 0.89 | 0.55 |
| 3 | 47 | 5.0 | 0.60 | 3.3 | 43.8 | 43.8 | 0.0335 | 0.74 | 19.93 | 0.037 | 0.89 | 0.83 |
| 4 | 80 | 5.1 | 0.63 | 5.5 | 77.9 | 76.2 | 0.0528 | 0.65 | 19.93 | 0.033 | 0.89 | 0.73 |
| 5 | 160 | 4.9 | 0.62 | 15.0 | 147.7 | 146.3 | 0.1467 | 0.92 | 19.93 | 0.046 | 0.89 | 1.0 |

$C_{ot}$ = source KCl concentration, $L$ = specimen thickness, $n$ = porosity, $C_{b.av.EC}$ and $C_{t.av.EC}$ = EC-derived molar Cl concentrations in outflows from top and bottom specimen boundaries at steady state, respectively, $\Delta C_{av.EC}$ = average molar specimen boundary concentration difference computed based on EC-derived steady-state concentrations, $(\Delta Q_t/\Delta t)_{EC}$ = change in cumulative moles of $Cl^-$ per unit area, $Q_t$, per change in time (from EC-based diffusion data), $D_{s.EC}^*$ = true effective salt-diffusion coefficient(based on EC measurements), $D_{se.EC}$ = effective salt-diffusion coefficient at zero membrane efficiency ($\omega_{av} = 0$) (EC based), $D_{so}$ = salt-diffusion coefficient for KCl in free solution (from Robinson and Stokes 1959), $\tau_{a.EC}$ = apparent tortuosity factor (based on EC results), $\tau_{r.EC}$ = restrictive tortuosity factor (based on EC results).

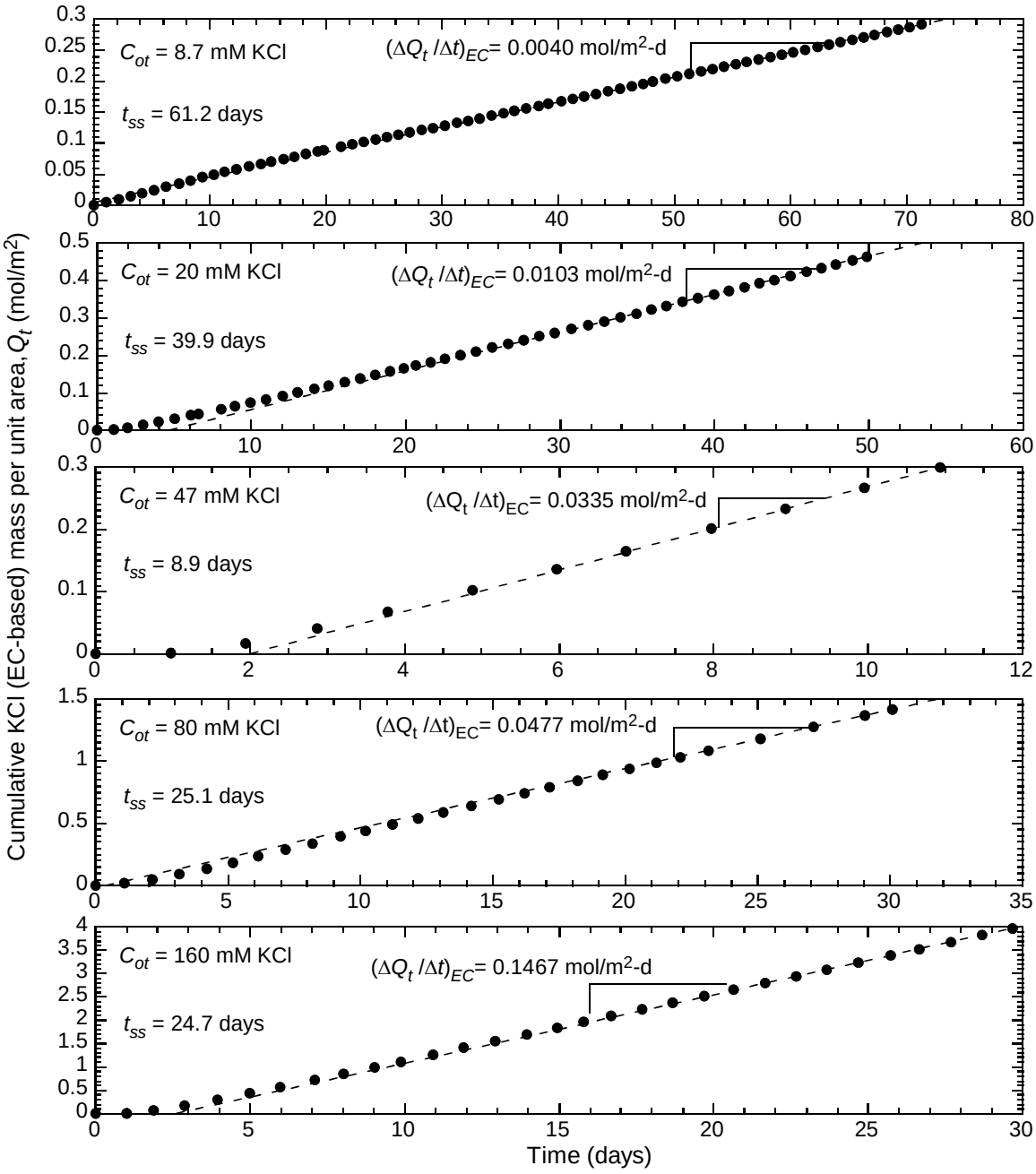


**Figure 4.6 Cumulative moles of KCl (EC-based) per unit area, $Q_t$, diffused through a DPH-GCL specimen as function of time.**

The graphs in Figure 4.6 also suggest that EC-based results tend to be more accurate with increasing source KCl concentration ($C_{ot} \geq 47$ mM KCl) as the gap between $D_s$* and $D_{s.EC}$* reduces with increasing $C_{ot}$. This is explained by the background effect of the soluble salts (see Chapter 3 for more details) on calculations of diffusive flux, $J_D$ ($\Delta Q_t / \Delta t$), estimated using the measured EC values. The tests involving low source concentrations ($C_{ot} < 47$ mM KCl) have the background EC (due to soluble salts) which heavily contributes to the total EC and, thus, exaggerates the $(\Delta Q_t / \Delta t)_{EC}$ values. Exaggerated $(\Delta Q_t / \Delta t)_{EC}$ values produce exaggerated $D_{s.EC}$*. High source KCl concentrations ($C_{ot} \geq 47$ mM) produced higher $K^+$ and $Cl^-$ (the main ion contributing to EC) concentrations at the bottom specimen boundary ($C_b$) which in turn increased the total EC at the bottom specimen boundary. As a result, the background EC associated with the soluble salts had a slight contribution to the total EC at the bottom specimen boundary which significantly reduced the possible error.

### *4.3.4 Relationship Between ω and $D_s$**

The effective salt-diffusion coefficients based on concentrations of $Cl^-$, $D_s$*, and EC-derived KCl, $D_{s.EC}$*, are plotted as functions of the respective membrane efficiency coefficients ($\omega_{av}$ and $\omega_{av.EC}$) (see Figure 4.7a and b).

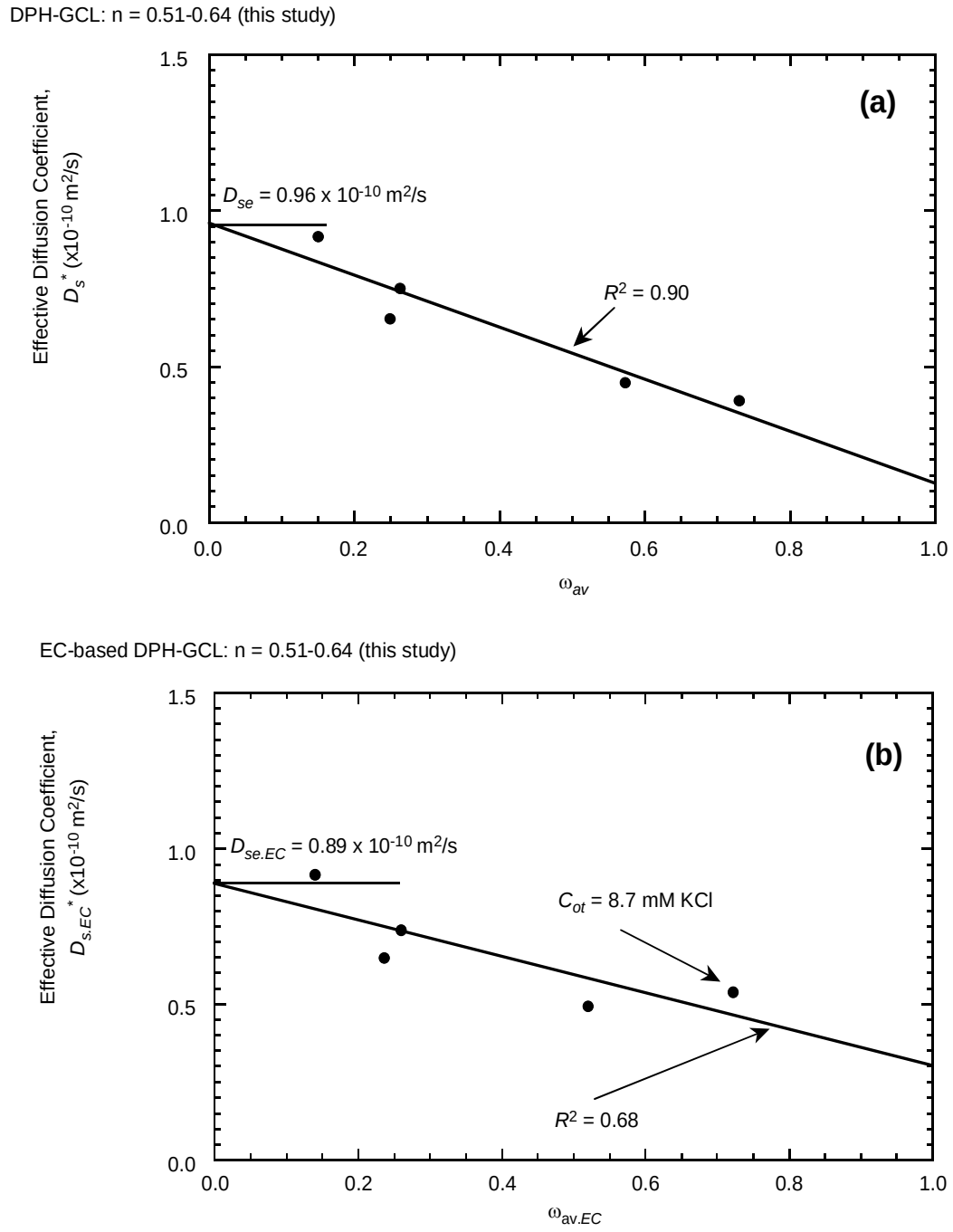


**Figure 4.7 Effective salt-diffusion coefficients as a function of membrane efficiency coefficient based on (a) $Cl^-$ and (b) EC-based KCl concentrations.**

The linear model for $D_{s.EC}$*- $\omega_{avEC}$ relationship ($R^2$ = 0.68) does not approximate the experimental data as well as the linear fit for $D_s$*- $\omega_{av}$ relationship ($R^2$ = 0.90). This can be explained by the fact that EC-based diffusion test results tend to be less accurate at lower concentrations (e.g. $C_{ot}$ = 8.7 mM). Nevertheless, the linear trends of decreasing effective salt-diffusion coefficient with increasing membrane efficiency are evident for both plots (Figure 4.7a and b). Another trend that can be observed from Figure 4.7 is that the $D_s$* tends to approach zero as ω approaches unity ("ideal" behavior). This observation is consistent with the theory behind membrane behavior discussed in the literature review chapter and Section 4.2.2.

### *4.3.5 Apparent and Restrictive Tortuosity Factors*

The apparent tortuosity ($\tau_a$) results are presented in Table 4.1 and plotted as a function of membrane efficiency coefficients in Figure 4.8a. It can be observed from Figure 4.8 that the apparent tortuosity values tend to linearly decrease with increasing membrane efficiency, ω. This trend is consistent with the definition of apparent tortuosity (see Equation 4.2): provided that $D_{so}$ is constant, a decrease in $\tau_a$ must be followed by a decrease in $D_s$*, which in turn causes an increase in ω.

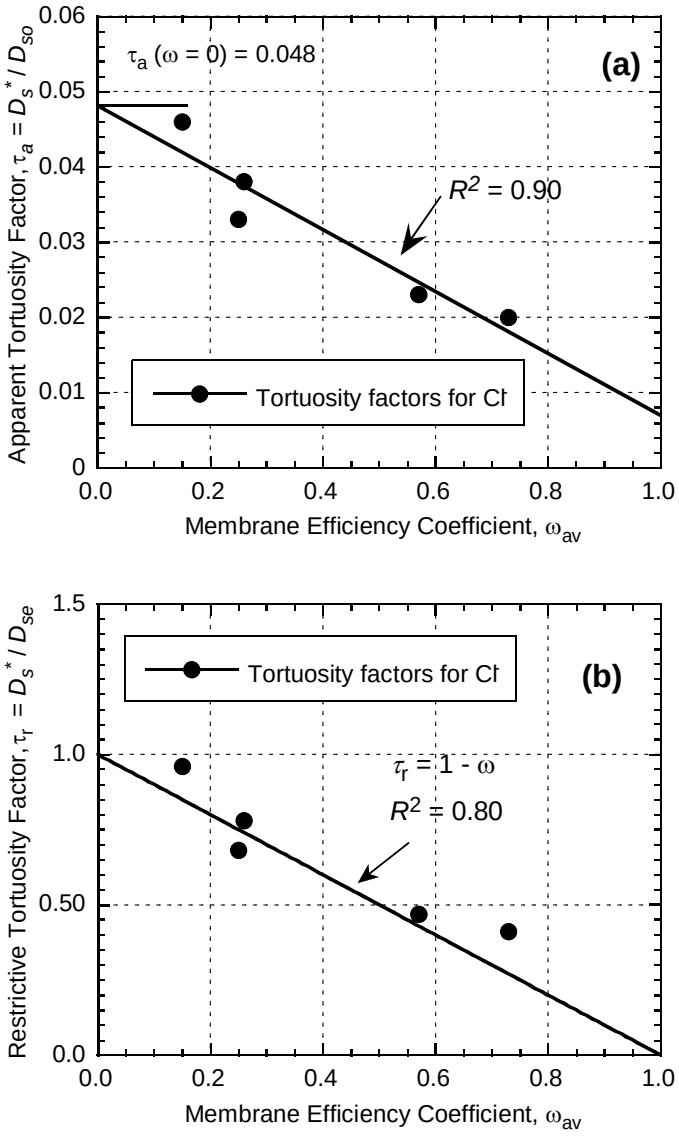


**Figure 4.8 (a) Apparent and (b) restrictive tortuosity factors based on measured $Cl^-$ concentrations as functions of membrane efficiency coefficient.**

The matrix tortuosity was determined by evaluating the regression fit for apparent tortuosity at zero efficiency ($\tau_m = \tau_a(\omega = 0) = 0.048$; see Figure 4.8a).

Equation 4.4 can also be expressed in the following way:

$$D_s^* = \tau_m \tau_r D_{so} = \tau_r D_{se} \quad (4.9)$$

where $D_{se}$ ($= \tau_m D_{so}$) is the effective salt-diffusion coefficient accounting solely for the matrix tortuosity (Malusis et al. 2013).

Finally rearranging equation 4.9 allows us to calculate the restrictive tortuosity:

$$\tau_r = D_s^*/D_{se} \quad (4.10)$$

The matrix tortuosity and $D_{so}$ are considered to be constant and independent of solute concentration, whereas $\tau_r$ values tend to decrease with increasing $\omega$ (Malusis et al. 2013). At a point when no ions pass through the membrane barrier ($\omega = 1$) $\tau_r = 0$. On the other hand, in the presence of aggressive electrolyte solutions causing the shrinkage of the diffuse-double layers (DDLs), membrane behavior does not occur ($\omega = 0$) within the clayey membranes and $\tau_r$ takes the value of unity ($\tau_r = 1$) (assuming the effects of other mechanisms restricting diffusion are insignificant). Thus, based on the equation 4.9, $D_s^* = D_{se}$, when $\omega = 0$ and $\tau_r = 1$. The values $D_{se}$ can be estimated by extrapolating the linear regression fit curves for $D_s^*$ - $\omega$ relationship. The $D_{se}$ values are presented in Table 4.1 (Table 4.2 for EC-based results) and were determined by evaluating the linear regression fits (see Figures 4.7a and 4.7b for EC-based results) at zero membrane efficiency ($\omega_{av} = 0$ and $\omega_{av.EC} = 0$) (Malusis et al. 2013).

The results for $Cl^-$ (and KCl/EC) based restrictive tortuosities are provided in Table 4.1 (Table 4.2). Figure 4.8b shows the determined restrictive tortuosities ($\tau_r$) as a function of membrane efficiency. The trend for $\tau_r$ - $\omega_{av}$ is similar to the trend observed for $\tau_a$ - $\omega_{av}$ relationship: $\tau_r$ decreases linearly with increasing membrane efficiency $\omega$. Malusis et al. 2013 showed that for conventional GCLs subjected to KCl solution with concentrations between 0 and 47 mM, relationship $\tau_r$ - $\omega_{av}$ can be very well approximated by the linear function $\tau_r = 1 - \omega$. The regression fit $\tau_r = 1 - \omega$ applied to the restrictive tortuosity data produced by this study was proven to be accurate ($R^2 = 0.80$; see Figure 4.8b).

### *4.3.6 Comparison to Conventional GCLs*

Diffusion results of this study suggest that DPH-GCL is more resilient to KCl solutions than its conventional counterpart as per given source KCl concentration, $D_s$* of DPH-GCLs is lower than that of conventional GCL (see Figure 4.9a). The decrease in $D_s$* values per given source concentration ($C_{ot}$) correlates with a decrease in porosity ($n$) values (shown in the legend of Figure 4.9).

The relationships between $D_s$* and $\omega$ for conventional and DPH-GCLs are presented in Figure 4.9b. It can be seen from the plot that all the functions follow the linear trend and are inclined to pass through the point ($\omega = 1$, $D_s* = 0$) (as discussed in section 4.3.4).

Similarly to the case of $D_s$* - $C_o$ relationship, $D_s$* values per given $\omega$ value tend to decrease with decreasing porosities ($n$).

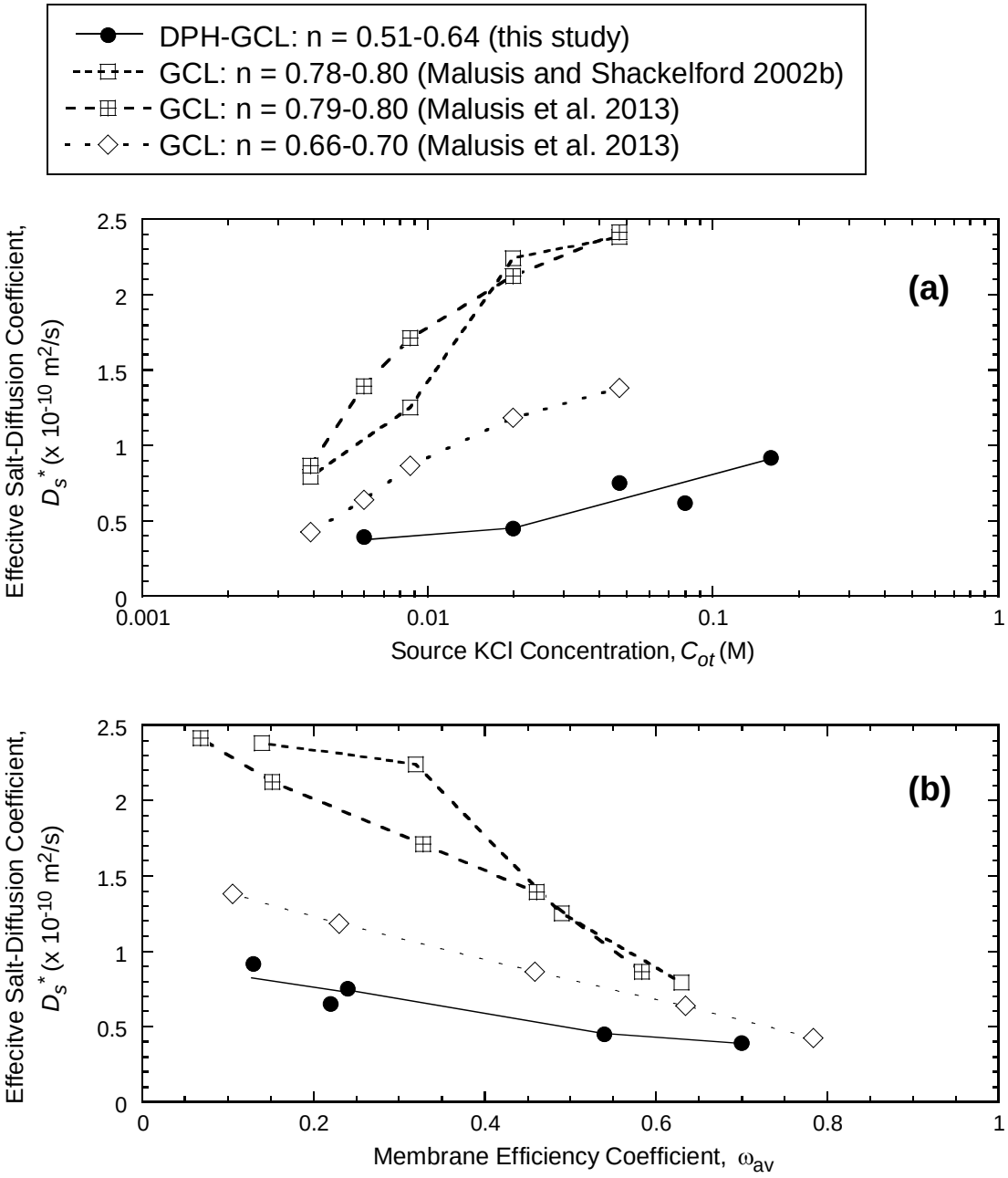


**Figure 4.9 Effective salt-diffusion coefficients as a function of (a) source KCl concentration and (b) membrane efficiency coefficient.**

When compared to conventional GCLs, DPH-GCLs exhibit lower apparent tortuosity factors per given value of ω (see Figure 4.10a). Note that $\tau_a$ - $\omega_{av}$ trends for all studies have a tendency to pass through the point ($\omega_{av}$ = 1, $\tau_a$ = 0) which is consistent with the definition of membrane efficiency (i.e., "ideal" membranes do not allow any solute passage). It can also be seen from the figure 4.10a that $\tau_a$ decreases linearly with increasing $\omega_{av}$.

Figure 4.10b shows the restrictive tortuosities for DPH-GCLs and its conventional counterparts as functions of $\omega_{av}$. The linear regression fit $\tau_r = 1 - \omega$ was applied to all the data provided in Figure 4.10b and $R^2$ value of 0.90 was achieved. This finding indicates that function $\tau_r = 1 - \omega$ is valid for relating $\tau_r$ to ω for DPH-GCLs as well as conventional GCLs (Malusis et al. 2013) subjected to KCl solutions.

## 4.4 Conclusions

The findings of this study suggest that the effective salt-diffusion coefficient $D_s$* for DPH-GCLs increases with source KCl concentration, as expected based on the previous studies conducted on conventional GCLs. That being said, DPH-GCL exhibited lower $D_s$* values per given source KCl concentration than their conventional counterparts indicating the superior performance of the DPH-GCLs. The relationship between the membrane efficiency coefficient (ω) and $D_s$* also suggests that DPH-GCLs outperformed

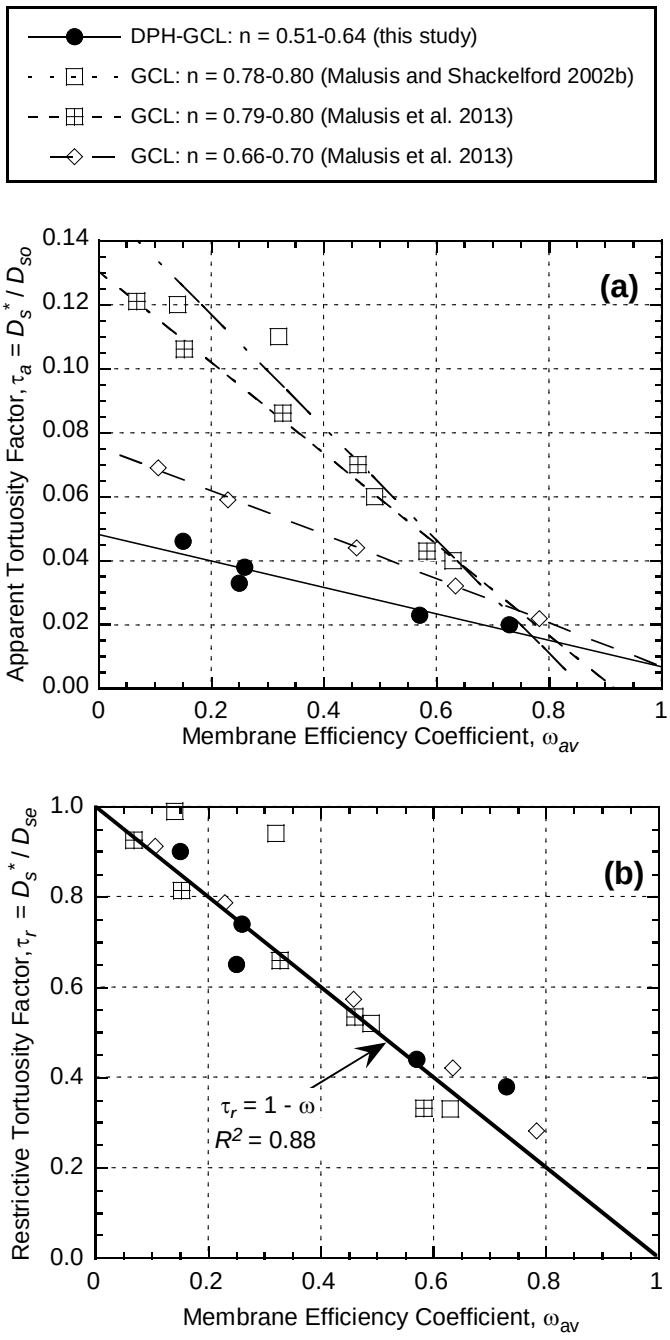


**Figure 4.10 (a) Apparent and (b) restrictive tortuosity factors based on measured $Cl^-$ concentrations.**

conventional GCLs as DPH-GCLs yielded lower $D_s$* values per given ω. The superior performance of DPH-GCLs (when compared to conventional GCLs) is attributed primarily to lower porosities measured for this material.

The $D_s$*- ω relationship for DPH-GCLs exhibits linear trend and conforms to the theory behind membrane behavior, such that at zero membrane efficiency the effective salt-diffusion coefficient ($D_s$*) takes maximum value, $D_{se}$, whereas $D_s$* takes value of zero (complete restriction of solutes) during "ideal" membrane behavior (ω = 1).

The apparent tortuosity factor, $\tau_a$, value can be expressed as the product of the restrictive tortuosity factor, $\tau_r$, (responsible for the restriction of solutes due to membrane behavior) and matrix tortuosity factor, $\tau_m$, (responsible for the restriction of solutes due to geometry of the porous media; $D_s$* = $D_{se}$ when solutes are restricted solely due to $\tau_m$). The $\tau_r$ values for DPH-GCLs were found to be linearly decreasing with increasing membrane efficiency in such way that this relationship is closely approximated by expression $\tau_r = (1 - \omega)$ similar to the results obtained for conventional GCLs subjected to KCl solutions. Though the linear trends were observed for $D_s$* - ω and $\tau_r$ - ω ($\tau_r = 1 - \omega$) in this study and the studies conducted by Malusis et al. (2013) for conventional GCLs, further research is required to determine whether such relationships hold for tests with other salts (e.g., $CaCl_2$).

Finally, this study suggests that the data from membrane/diffusion tests with source KCl concentrations above 47 mM can be accurately analyzed (e.g., used to evaluate $D_s$* -

ω relationship) using solely electrical conductivity measurements. This finding is important since the ion chromatography (method for determining ion concentrations) is a time consuming and expensive process as opposed to measuring electrical conductivity.

# 5. CONCLUSIONS

The objective of this study was to evaluate the relationship between the membrane efficiency and solute diffusion through a dense, prehydrated GCL (DPH-GCL). The testing employed membrane/diffusion apparatus and five DPH-GCL specimens subjected to KCl solutions with various concentrations. It was aimed to compare the performance of the DPH-GCLs to conventional GCLs on the basis of the membrane efficiency and effective salt-diffusion coefficients.

It was determined based on the findings of this research that the relationship between the membrane efficiency and effective salt-diffusion for DPH-GCLs can be approximated as linear. This finding is consistent with the previous studies for conventional GCLs and theoretical background for membrane behavior, as the values for effective salt-diffusion coefficients tend to decrease with increasing membrane efficiency coefficients to the point when no diffusion occurs at an “ideal” membrane behavior (unity membrane efficiency coefficient). The function for the restrictive tortuosity ($\tau_r$) for DPH-GCLs, described as the factor of the effective salt-diffusion coefficient responsible for diffusion restriction due to membrane behavior, has been found to be successfully approximated by expression $\tau_r = 1 - \omega$ (where $\omega$ is the membrane efficiency coefficient) as it was concluded by the studies conducted on conventional GCLs exposed to KCl solutions. The relationships established in this study are in agreement with the models created in previous research which supports the validity of those models. Such models (once further proven to be reliable) can be used in the design of the waste containment facilities.

The superior performance of the DPH-GCL over its conventional counterpart was evident based on the following observations: (1) ω values for the DPH-GCL specimens were shown to be greater (for a given source KCL concentration) relative to those for conventional GCL; (2) DPH-GCLs yielded lower effective salt-diffusion coefficients than conventional GCLs per given ω values. The advantages of the DPH-GCLs were primarily attributed to a higher dry density (and, therefore, lower porosity) of this material when compared to conventional GCLs. However, polymer treatment and the use of the powdered sodium bentonite (as opposed to granular) associated with DPH-GCLs could also contribute to the superior performance of the DPH-GCLs over its conventional counterpart.

Another important finding of this study was that the membrane/diffusion test data can be successfully analyzed using the electrical conductivity measurements of the outflows collected at the top and bottom specimen boundaries even in the presence of soluble salts. The results for the effective salt-diffusion coefficients suggest that the accuracy of the electrical conductivity method tends to increase with increasing source KCl concentration (at or above 47 mM) used in the test, as the effect of the background electrical conductivity associated with the soluble salts becomes negligible, in contrast to the contribution of KCl to the total electric conductivity. This finding is important as tremendous savings in time and money can be achieved, as measuring electrical conductivity is a simpler and less time consuming process, when compared to the ion chromatography (typically used to determine ion concentrations).

# 6. RECOMMENDATIONS FOR FUTURE WORK

More membrane/diffusion tests need to be conducted with DPH-GCLs subjected to source KCl solutions of higher concentrations to determine the threshold effective salt-diffusion coefficient (i.e., effective salt-diffusion at zero membrane efficiency). It is also recommended to establish the relationship between the effective salt-diffusion and source KCl concentration at points when DPH-GCLs do not exhibit any membrane behavior ($\omega = 0$). As of now there is no documented study evaluating the effective salt-diffusion of DPH-GCLs and conventional GCLs beyond the source KCl concentrations yielding zero membrane efficiency. Membrane/diffusion tests with higher source KCl concentrations are also better at approximating the field conditions where waste containment barriers are typically subjected to aggressive solutions/leachates.

Additional testing is also necessary to determine the relationship between membrane efficiency and solute diffusion for DPH-GCLs subjected to other chemical solutions (e.g., divalent salt, $CaCl_2$). The findings of such study could potentially support the linear models developed in this and previous studies (for conventional GCLs).

## REFERENCES

Crooks, V.E. and Quigley, R.M., (1984). Saline leachate migration through clay: A comparative laboratory and field investigation. *Canadian Geotechnical Journal*, 21: 349-362.

Di Emidio, G. (2010). Hydraulic and chemico-osmotic performance of polymer treated clays. *Ph.D. Dissertation*, Ghent University, Belgium.

Di Emidio, G, Mazzieri, F. and Van Impe, W. (2008). Hydraulic conductivity of a dense prehydrated GCL: impact of free swell and swelling pressure. *4th European Geosynthetics Conference.* Golder Associates.

Dominijanni A, Manassero M, and Puma S. (2013). Coupled chemical-hydraulic-mechanical behaviour of bentonites. *Géotechnique* 63(3): 191-205.

Egloffstein, T. A. (2001). Natural bentonites—influence of the ion exchange and partial desiccation on permeability and self-healing capacity of bentonites used in GCLs. *Geotextiles and Geomembranes*, 19, 7, 427-444.

EPA (2001). Geosynthetic Clay Liners Used in Municipal Waste Landfills. EPA530-F-97-002 (Revised Issue). *US Environmental Protection Agency*, Washington, D.C. http://www.epa.gov/garbage/landfill/geosyn.pdf, 8 pp.

Flynn, B. N. and Carter, G. C. (1998). *Waterproofing material and method of fabrication thereof. U.S. patent No. 6,537,676 B1*.

Freeze, R.A. and Cherry, J.A. (1979). *Groundwater*. Prentice-Hall, Englewood Cliffs, NJ, 604pp.

Fritz, S. J. (1986). Ideality of clay membranes in osmotic processes: A review. *Clays and Clay Minerals*, 34(2), 214-223.

Goodall, D. C. and Quigley, R.M. (1977). Pollutant migration from two sanitary landfill sites near Sarnia, Ontario. *Canadian Geotechnical Journal*, 14: 223-236.

Henning, J., Evans, J., and Shackelford, C. (2006). Membrane Behavior of Two Backfills from Field-Constructed Soil-Bentonite Cutoff Walls. *Journal of Geotechnical and Geoenvironmental Engineering*, 132(10), 1243–1249.

Jo, H. Y., Benson, C. H., Shackelford, C. D., Lee, J. -M. and Edil, T. B. (2005). Long-term hydraulic conductivity of a geosynthetic clay liner permeated with inorganic salt solutions., *Journal of Geotechnical and Geoenvironmental Engineering, ASCE* 131 (4), 405-417

Johnson, R.L., Cherry, J.A. and Pankow, J.F. (1989). Diffusive contaminant transport in natural clay: A field example and implications for clay-lined waste disposal sites. *Environmental Science Technology*, 23: 340-349.

Kang, J. B., and Shackelford, C. D. (2010). Membrane behavior of compacted clay liners. *Journal of Geotechnical and Geoenvironmental Engineering*, 136, 10, 1368-1382.

Kang, J. B., and Shackelford C. D. (2011) Consolidation enhanced membrane behavior of a geosynthetic clay liner. *Geotextiles and Geomembranes* 29(6): 544-556.

Katchalsky, A., and Curran, P. F. (1965). *Nonequilibrium thermodynamics in biophysics.* Cambridge: Harvard University Press.

Katsumi, T., Ishimori, H., Fukagawa, R., and Onikata, M. (2008). Long-term barrier performance of modified bentonite materials against sodium and calcium permeant solutions. *Geotextiles and Geomembranes,* 26, 1, 14-30.

Kemper, W. D., and Rollins, J. B (1966). Osmotic efficiency coefficients across compacted clays. *Soil Science Society of America, Proceedings*, 30(5), 529-534.

Kemper, W. D. and Quirk, J. P. (1972). Ion mobilities and electric charge of external clay surfaces inferred from potential differences and osmotic flow. *Soil Science Society of America, Proceedings*, 36, 426-433.

Koerner, R. M. (1998). *Designing with geosynthetics*. Upper Saddle River, NJ: Prentice Hall.

Kolstad, D. C., Benson, C. H., Edil, T. B., and Jo, H. Y. (2004). Hydraulic conductivity of a dense prehydrated GCL permeated with aggressive inorganic solutions. *Geosynthetics International*, 11, 3, 233-241.

Lee, J. M., and Shackelford, C. D. (2005). Concentration Dependency of the Prehydration Effect for a Geosynthetic Clay Liner. *Soils and Foundations*, 45, 4, 27.

Malusis, M. A., Kang, J., and Shackelford, C. (2013). Influence of membrane behavior on solute diffusion through GCLs. *Proceedings, TC 215 Symposium on Coupled Phenomena in Environmental Geotechnics*, Torino, Italy

Malusis, M. A., Kang, J. B., and Shackelford, C.D. (2014). Restricted salt diffusion in a geosynthetic clay liner. *Environmental Geotechnics*, ICE, Thomas Telford Ltd., London, in press.

Malusis, M.A., Shackelford, C.D., and Olsen, H.W. (2001). A laboratory apparatus to measure chemico-osmotic efficiency coefficients for clay soils. *Geotechnical Testing Journal*, 24(3), 229-242.

Malusis, M. A. and Shackelford, C. D. (2002a). Chemico-osmotic efficiency of a geosynthetic clay liner. *Journal of Geotechnical and Geoenvironmental Engineering*, 128(2), 97-106.

Malusis, M.A. and Shackelford, C.D. (2002b). Coupling effects during steady-state solute diffusion through a semipermeable clay membrane. *Environmental Science and Technology*, 36(6), 1312.

Malusis, M. A., Shackelford, C. D., and Olsen, H. W. (2003). Flow and transport through clay membrane barriers. *Engineering Geology*, 70(2-3), 235-248.

Manassero, M. & Dominijanni, A. (2003). Modelling the osmosis effect on solute migration through porous media. *Géotechnique* 53(5): 481-492.

Martin, R. (1960). Adsorbed water on clay: a review. *Proceedings 9th National Conference on Clays and Clay Minerals*, Clay Minerals Society, Lafayette, IN.

Mazzieri, F. (2011). Impact of Desiccation and Cation Exchange on the Hydraulic Conductivity of Factory-Prehydrated GCLs. *Geotechnical Special Publication*, 2, 211, 976-985.

Mazzieri, F., Di Emidio, G., and van Impe. W. F. (2010). Diffusion of calcium chloride in a modified bentonite: Impact on osmotic efficiency and hydraulic conductivity. *Clays and Clay Minerals*, 58, 3, 351-363.

McBride, M. (1994). *Environmental chemistry of soils*. Oxford University Press, New York, NY.

Mitchell, J. K., & Soga, K. (2005). *Fundamentals of soil behavior*. Hoboken, N.J: John Wiley & Sons.Mooney, R., Keenan, A., and Wood, L. (1952). Adsorption of water vapor by montmorillonite. II. Effect of exchangeable ions and lattice swelling as measured by X-Ray diffraction, *Journal of the American Chemical Society*, 74(6), 1371-1374.

Norrish, K. (1954). The swelling of montmorillonite, *Transactions Farady Society* 18: 120-134.

Norrish, K. and Quirk, J. (1954). Crystalline swelling of montmorillonite, use of electrolytes to control swelling, *Nature*, 173, 255-257.

Olsen, H. W., Yearsley, E. N., and Nelson, K. R. (1990). Chemico-osmosis versus diffusion-osmosis. *Transportation Research Record No. 1288, Transportation Research Board, Washington D.C.,* 15-22.

Petrov, R.J. and Rowe, R.K. (1997). Geosynthetic clay liner compatibility by hydraulic conductivity testing: Factors impacting performance. *Canadian Geotechnical Journal Vol*. 34, No. 6, pp 863-885.

Rowe R. K. (2007). Advances and Remaining Challenges for Geosynthetics in Geoenvironmental Engineering Applications, 23rd Annual Rocha Lecture, *Soils and Rocks*, 30(1) (3-30).

Lake, C.B. and Rowe, R.K. (2000). Diffusion of Sodium and Chloride Through Geosynthetic Clay Liners. *Geotextiles and Geomembranes,* 18(2):102-132.

Robinson, R. A., and Stokes, R. H. (1959). *Electrolyte solutions,* 2nd Ed., Butterworths Scientific Publications, London, England.

Scalia, J. and Benson, C. (2011), Hydraulic Conductivity of Geosynthetic Clay Liners Exhumed from Landfill Final Covers with Composite Barriers, *Journal of Geotechnical and Geoenvironmental Engineering*, 137(1), 1-13.

Shackelford, C. D. (1991). Laboratory diffusion testing for waste disposal — A review. *Journal of Contaminant Hydrology*, 7, 3, 177-217.

Shackelford, C. D., (1994) Waste-Soil interactions that Alter Hydraulic Conductivity, *Hydraulic Conductivity and Waste Contaminant Transport in Soil. ASTM STP 1142.* David E. Daniel and Stephen J. Trautwein, Eds., American Society for Testing and Materials. Philadelphia.

Shackelford, C.D. (2013). Membrane behavior of bentonite-based barriers: state of the art. *Proceedings of the International Symposium, ISSMGE TC 215, Coupled Phenomena in Environmental Geotechnics: From Theoretical and Experimental Research to Practical Applications*. Torino, Italy, M. Manassero, A. Dominijanni, S. Foti, and G. Musso, Eds., Taylor and Francis Group, London, UK, 45-60.

Shackelford, C. D. and Daniel, D. E. (1991). Diffusion in saturated soil: I. Background., *Journal of Geotechnical Engineering* 117: 467-484

Shackelford, C. D. and Lee, J.-M. (2003). The destructive role of diffusion on clay membrane behavior. *Clays and Clay Minerals*, 51(2), 187-197.

Shackelford, C. D., Malusis, M. A., Majeski, M. J., and Stern, R. T. (1999). Electrical conductivity breakthrough curves. *Journal of Environmental and Geotechnical Engineering.*, 125(4), 260–270.

Shackelford, C. D., Malusis, M. A., and Olsen, H. W. (2003). Clay membrane behavior for geoenvironmental containment, *Soil and Rock America Conference* 2003, P. J. Culligan, H.H.

Sharma, H. D., and Reddy, K. R. (2004). *Geoenvironmental engineering: Site remediation, waste containment, and emerging waste management technologies*. Hoboken, N.J: Wiley.

van Olphen, H. . (1963). *An introduction to clay colloid chemistry: For clay technologists, geologists, and soil scientists*. New York: Interscience Publishers.

Whitworth, T. M. and Fritz, S. J. (1994). Electrolyte-induced solute permeability effects in compacted smectite membranes. *Applied Geochemistry*, 9(5), 533-546.

Yeo, S.-S., Shackelford, C. D., and Evans, J. C. (2005). Membrane behavior of model soil-bentonite backfill mixtures. *Journal of Geotechnical and Geoenvironmental Engineering*, 131(4), 418-429.

# APPENDIX A: MEMBRANE/DIFFUSION TESTING DATA

## TEST 1

| | | | | | |
|---|---|---|---|---|---|
| *Co* = | 0.0087 | M KCl | Syringe Displacement Rate = | 41.76 | ml/day |
| *n* = | 0.53 | | Specimen Area, A = | 39.48 | sq.cm |
| *L* = | 5.2 | mm | | | |
| *T* = | 21.5 | °C | | | |
| *R* = | 8.314 | J/mole-K | | | |

| | Bottom | | | | | Top | | | | |
|---|---|---|---|---|---|---|---|---|---|---|
| | | Concentration (mM) | | | | | Concentration (mM) | | | |
| Time (days) | EC (μS/cm) | Cl- | K+ | Na+ | KCl* | EC (μS/cm) | Cl- | K+ | Na+ | KCl* |
| -5.70 | 1410 | | | | | 1090 | | | | |
| -4.68 | 339 | | | | | 356 | | | | |
| -3.73 | 196.1 | | | | | 188.6 | | | | |
| -2.98 | 113.2 | | | | | 113.6 | | | | |
| -1.99 | 88.6 | | | | | 80.1 | | | | |
| -1.00 | 74.7 | | | | | 65.2 | | | | |
| 0.00 | 67.4 | 0 | 0 | 0.817 | 0.00 | 57.2 | 0.006 | 0.01 | 0.6 | 0.00 |
| 1.11 | 65.2 | 0.020 | 0.010 | 0.801 | 0.44 | 600 | 3.217 | 2.628 | 1.396 | 4.09 |
| 2.17 | | | | | | | | | | |
| 3.19 | 70.4 | 0.168 | 0.011 | 0.820 | 0.48 | 1171 | 7.846 | 5.389 | 2.941 | 7.98 |
| 4.19 | 72 | | | | 0.49 | 1167 | | | | 7.96 |
| 5.22 | 73.9 | 0.215 | 0.016 | 0.835 | 0.50 | 1172 | 0.000 | 0.000 | 0.000 | 7.99 |
| 6.24 | 72.5 | | | | 0.49 | 1170 | | | | 7.98 |
| 7.33 | 77.3 | 0.233 | 0.025 | 0.848 | 0.53 | 1158 | 7.920 | 5.390 | 3.048 | 7.90 |
| 8.34 | 74.5 | | | | 0.51 | 1045 | | | | 7.13 |
| 9.35 | 71.7 | 0.229 | 0.032 | 0.769 | 0.49 | 1161 | 0.000 | 0.000 | 0.000 | 7.92 |
| 10.34 | 67.4 | | | | 0.46 | 1168 | | | | 7.96 |
| 11.29 | 63.2 | 0.216 | 0.053 | 0.662 | 0.43 | 1162 | 7.968 | 5.612 | 2.799 | 7.92 |
| 12.27 | 60.8 | | | | 0.41 | 1171 | | | | 7.98 |
| 13.38 | 62.3 | 0.223 | 0.064 | 0.629 | 0.42 | 1170 | 0.000 | 0.000 | 0.000 | 7.98 |
| 14.41 | 63 | | | | 0.43 | 1170 | | | | 7.98 |
| 15.28 | 62.4 | 0.227 | 0.074 | 0.607 | 0.43 | 1168 | 7.923 | 5.675 | 2.710 | 7.96 |
| 16.35 | 61.7 | | | | 0.42 | 1167 | | | | 7.96 |
| 17.28 | 61 | 0.230 | 0.083 | 0.571 | 0.42 | 1164 | | 0.000 | 0.000 | 7.94 |
| 18.28 | 59.7 | | | | 0.41 | 1172 | | | | 7.99 |
| 19.29 | 59.1 | 0.234 | 0.085 | 0.538 | 0.40 | 1166 | 7.978 | 5.812 | 2.567 | 7.95 |
| 19.80 | 58.9 | | | | 0.40 | 1177 | | | | 8.03 |
| 21.28 | 58.9 | 0.237 | 0.096 | 0.517 | 0.40 | 1164 | | | | 7.94 |
| 22.30 | 53.4 | | | | 0.36 | 1185 | | | | 8.08 |
| 23.27 | 57.3 | 0.236 | 0.104 | 0.479 | 0.39 | 1165 | 7.935 | 6.126 | 2.336 | 7.94 |
| 24.26 | 58.3 | | | | 0.40 | 1177 | | | | 8.03 |
| 25.24 | 58 | 0.246 | 0.113 | 0.462 | 0.40 | 1185 | | | | 8.08 |

*Based on EC measurements

# TEST 1 (CONTINUED)

| | Bottom | | | | | Top | | | | |
|---|---|---|---|---|---|---|---|---|---|---|
| | | Concentration (mM) | | | | | Concentration (mM) | | | |
| Time (days) | EC (μS/cm) | Cl- | K+ | Na+ | KCl* | EC (μS/cm) | Cl- | K+ | Na+ | KCl* |
| 26.24 | 57.6 | | | | 0.39 | 1191 | | | | 8.12 |
| 27.22 | 57 | 0.251 | 0.114 | 0.425 | 0.39 | 1216 | 7.955 | 6.216 | 2.227 | 8.29 |
| 28.22 | 56.4 | | | | 0.38 | 1208 | | | | 8.24 |
| 29.22 | 56.8 | 0.256 | 0.117 | 0.388 | 0.39 | 1214 | | | | 8.28 |
| 30.23 | 56.5 | | | | 0.39 | 1220 | | | | 8.32 |
| 31.28 | 57.1 | 0.259 | 0.125 | 0.368 | 0.39 | 1212 | 8.025 | 6.430 | 2.086 | 8.26 |
| 32.24 | 56.9 | | | | 0.39 | 1232 | | | | 8.40 |
| 33.24 | 57.2 | 0.263 | 0.136 | 0.357 | 0.39 | 1236 | | | | 8.43 |
| 34.26 | 58.7 | | | | 0.40 | 1235 | | | | 8.42 |
| 35.29 | 58.4 | 0.268 | 0.152 | 0.350 | 0.40 | 1212 | 7.956 | 6.540 | 1.941 | 8.26 |
| 36.22 | 60 | | | | 0.41 | 1214 | | | | 8.28 |
| 37.24 | 57.4 | 0.263 | 0.163 | 0.333 | 0.39 | 1200 | | | | 8.18 |
| 38.29 | 57.4 | | | | 0.39 | 1207 | | | | 8.23 |
| 39.16 | 57.5 | 0.262 | 0.174 | 0.315 | 0.39 | 1206 | 7.854 | 6.672 | 1.744 | 8.22 |
| 40.28 | 57.4 | | | | 0.39 | 1218 | | | | 8.30 |
| 41.24 | 57.5 | 0.263 | 0.185 | 0.302 | 0.39 | 1216 | | | | 8.29 |
| 42.25 | 57.8 | | | | 0.39 | 1215 | | | | 8.28 |
| 43.27 | 58.1 | 0.267 | 0.199 | 0.290 | 0.40 | 1209 | 7.864 | 6.838 | 1.601 | 8.24 |
| 44.29 | 57.5 | | | | 0.39 | 1208 | | | | 8.24 |
| 45.29 | 57.5 | 0.263 | 0.205 | 0.274 | 0.39 | 1213 | | | | 8.27 |
| 46.31 | | | | | | | | | | |
| 47.31 | 58.3 | 0.265 | 0.215 | 0.269 | 0.40 | 1225 | 7.859 | 6.970 | 1.472 | 8.35 |
| 48.11 | 84.4 | | | | 0.58 | 1203 | | | | 8.20 |
| 49.19 | 61.1 | 0.278 | 0.248 | 0.269 | 0.42 | 1222 | | | | 8.33 |
| 50.22 | 58 | | | | 0.40 | 1224 | | | | 8.35 |
| 51.30 | 56.9 | 0.264 | 0.208 | 0.216 | 0.39 | 1230 | 8.102 | 6.772 | 1.342 | 8.39 |
| 52.29 | 56.6 | | | | 0.39 | 1235 | | | | 8.42 |
| 53.28 | 56.3 | 0.267 | 0.214 | 0.206 | 0.38 | 1239 | | | | 8.45 |
| 54.27 | 57.1 | | | | 0.39 | 1239 | | | | 8.45 |
| 55.27 | 58 | 0.270 | 0.227 | 0.197 | 0.40 | 1239 | 8.116 | 6.922 | 1.207 | 8.45 |
| 56.23 | 57.8 | | | | 0.39 | 1243 | | | | 8.48 |
| 57.24 | 57.5 | | | | 0.39 | 1244 | | | | 8.48 |
| 58.25 | 57.5 | | | | 0.39 | 1252 | | | | 8.54 |
| 59.25 | 58.3 | 0.279 | 0.246 | 0.180 | 0.40 | 1246 | 8.133 | 7.054 | 1.108 | 8.50 |
| 60.23 | 58.1 | | | | 0.40 | 1257 | | | | 8.57 |
| 61.25 | 57.4 | 0.280 | 0.252 | 0.167 | 0.39 | 1254 | | | | 8.55 |
| 62.31 | 59.3 | | | | 0.40 | 1258 | | | | 8.58 |
| 63.31 | 58.2 | 0.287 | 0.266 | 0.162 | 0.40 | 1250 | 8.172 | 7.192 | 0.984 | 8.52 |

*Based on EC measurements

# TEST 1 (CONTINUED)

| | Bottom | | | | | Top | | | | |
|---|---|---|---|---|---|---|---|---|---|---|
| | | Concentration (mM) | | | | | Concentration (mM) | | | |
| Time (days) | EC (μS/cm) | Cl- | K+ | Na+ | KCl* | EC (μS/cm) | Cl- | K+ | Na+ | KCl* |
| 64.28 | 59.1 | | | | 0.40 | 1259 | | | | 8.58 |
| 65.29 | 60.2 | 0.29 | 0.28 | 0.154 | 0.41 | 1262 | | | | 8.60 |
| 66.27 | 60.7 | | | | 0.41 | 1269 | | | | 8.65 |
| 67.22 | 61.1 | 0.29 | 0.29 | 0.147 | 0.42 | 1259 | 8.217 | 7.325 | 0.871 | 8.58 |
| 68.26 | 59.3 | | | | 0.40 | 1275 | | | | 8.69 |
| 69.27 | 60 | 0.3 | 0.29 | 0.136 | 0.41 | 1267 | | | | 8.64 |
| 70.25 | 59.9 | | | | 0.41 | 1278 | | | | 8.71 |
| 71.26 | 60.4 | 0.3 | 0.3 | 0.128 | 0.41 | 1271 | 8.298 | 7.451 | 0.775 | 8.67 |
| 72.26 | 61.4 | | | | | 1266 | | | | |

*Based on EC measurements

# TEST 2

| | | | | | |
|---|---|---|---|---|---|
| *Co* = | 0.02 | M KCl | | | |
| *n* = | 0.64 | | | | |
| *L* = | 5.6 | mm | | | |
| *T* = | 21.5 | °C | Syringe Displacement Rate = | 41.76 | ml/day |
| *R* = | 8.314 | J/mole-K | Specimen Area, A = | 39.48 | sq.cm |

| | Bottom | | | | | Top | | | | |
|---|---|---|---|---|---|---|---|---|---|---|
| | | Concentration (mM) | | | | | Concentration (mM) | | | |
| Time (days) | EC (μS/cm) | Cl- | K+ | Na+ | KCl* | EC (μS/cm) | Cl- | K+ | Na+ | KCl* |
| -1.07 | 81.4 | | | | | 79.6 | | | | |
| 0 | 79.3 | 0.001 | 0.01 | 0.52 | 0.00 | 79.5 | 0 | 0 | 0.58 | 0.00 |
| 1.0968 | 75.4 | 0.05243 | 0.01 | 0.54 | 0.20 | 1261 | 7.5 | 5.45 | 3.36 | 9.92 |
| 1.9886 | 115.8 | 0.41216 | 0.02 | 0.94 | 0.48 | 2347 | 16.19 | 10.2 | 7.11 | 18.79 |
| 2.977 | 152.4 | 0.64896 | 0.03 | 1.16 | 0.73 | 2562 | 18.12 | 11.4 | 7.68 | 20.54 |
| 3.9902 | 162.4 | 0.71149 | 0.07 | 1.2 | 0.79 | 2582 | 18.32 | 11.9 | 7.38 | 20.71 |
| 5.0089 | 164 | 0.73458 | 0.1 | 1.17 | 0.80 | 2610 | 18.39 | 12.3 | 7.06 | 20.93 |
| 6.0568 | 166.7 | 0.75314 | 0.11 | 1.1 | 0.82 | 2633 | | | | 21.12 |
| 6.5763 | | | | | 0.00 | | | | | 0.00 |
| 8.033 | 169.8 | 0.7708 | 0.17 | 1.01 | 0.84 | 2663 | 18.47 | 13.5 | 5.85 | 21.37 |
| 8.9413 | 170.9 | | | | | 2673 | | | | |
| 9.9258 | 172 | 0.78492 | 0.24 | 0.94 | 0.86 | 2667 | | | | 21.40 |
| 10.939 | 172.4 | | | | 0.86 | 2680 | | | | 21.51 |
| 12.021 | 172.7 | 0.78941 | 0.31 | 0.84 | 0.86 | 2668 | 18.52 | 14.4 | 4.8 | 21.41 |
| 12.985 | 174.4 | | | | 0.88 | 2671 | | | | 21.43 |
| 14.069 | 175.3 | 0.82199 | 0.4 | 0.8 | 0.88 | 2679 | | | | 21.50 |
| 15.006 | 175 | | | | 0.88 | 2706 | | | | 21.72 |
| 16.064 | 176.2 | 0.83596 | 0.46 | 0.73 | 0.89 | 2702 | 18.29 | 14.8 | 4.2 | 21.68 |
| 17.043 | 178 | | | | 0.90 | 2694 | | | | 21.62 |
| 18.033 | 181.8 | 0.85189 | 0.53 | 0.66 | 0.93 | 2709 | | | | 21.74 |
| 18.982 | 180.9 | | | | 0.92 | 2710 | | | | 21.75 |
| 19.877 | 182.1 | 0.85669 | 0.58 | 0.53 | 0.93 | 2701 | 18.48 | 15.6 | 3.32 | 21.68 |
| 20.669 | 182.7 | | | | 0.93 | 2703 | | | | 21.69 |
| 21.613 | 184.6 | 0.86172 | 0.62 | 0.48 | 0.95 | 2721 | | | | 21.84 |
| 22.533 | 182.5 | | | | 0.93 | 2724 | | | | 21.86 |
| 23.531 | 183.2 | 0.85492 | 0.65 | 0.43 | 0.94 | 2719 | 18.43 | 16.1 | 2.69 | 21.82 |
| 24.556 | 186.3 | | | | 0.96 | 2715 | | | | 21.79 |

*Based on EC measurements

# TEST 2 (CONTINUED)

| | Bottom | | | | | Top | | | | |
|---|---|---|---|---|---|---|---|---|---|---|
| | | Concentration (mM) | | | | | Concentration (mM) | | | |
| Time (days) | EC (μS/cm) | Cl- | K+ | Na+ | KCl* | EC (μS/cm) | Cl- | K+ | Na+ | KCl* |
| 25.594 | 187.7 | 0.875 | 0.707 | 0.387 | 0.97 | 2718 | | | | 21.82 |
| 26.633 | 186 | | | | 0.95 | 2733 | | | | 21.94 |
| 27.64 | 190.8 | 0.880 | 0.750 | 0.344 | 0.99 | 2733 | 18.37 | 16.54 | 2.13 | 21.94 |
| 28.64 | 185 | | | | 0.95 | 2732 | | | | 21.93 |
| 29.653 | 175 | 0.771 | 0.692 | 0.267 | 0.88 | 2761 | | | | 22.17 |
| 30.741 | 179.7 | | | | 0.91 | 2763 | | | | 22.18 |
| 31.823 | 185 | 0.823 | 0.749 | 0.245 | 0.95 | 2760 | 18.39 | 17.11 | 1.45 | 22.16 |
| 32.878 | 175.1 | | | | 0.88 | 2770 | | | | 22.24 |
| 33.905 | 187.1 | 0.859 | 0.831 | 0.228 | 0.96 | 2770 | | | | 22.24 |
| 34.946 | 194.4 | | | | 1.01 | 2770 | | | | 22.24 |
| 35.933 | 196.4 | 0.917 | 0.929 | 0.230 | 1.03 | 1760 | 18.72 | 17.55 | 1.16 | 13.99 |
| 36.878 | 194.4 | | | | 1.01 | 2760 | | | | 22.16 |
| 37.929 | 188.6 | 0.843 | 0.907 | 0.196 | 0.97 | 2770 | | | | 22.24 |
| 38.929 | 187.9 | | | | 0.97 | 2770 | | | | 22.24 |
| 39.992 | 187.2 | 0.829 | 0.904 | 0.172 | 0.96 | 2770 | 18.65 | 17.76 | 0.94 | 22.24 |
| 40.94 | 187.4 | | | | 0.96 | 2770 | | | | 22.24 |
| 41.941 | 186.2 | 0.828 | 0.932 | 0.137 | 0.96 | 2790 | | | | 22.40 |
| 42.92 | 187.3 | | | | 0.96 | 2780 | | | | 22.32 |
| 43.882 | 188.9 | 0.833 | 0.937 | 0.123 | 0.97 | 2780 | 18.71 | 17.90 | 0.78 | 22.32 |
| 44.935 | 180.8 | | | | 0.92 | 2760 | | | | 22.16 |
| 45.968 | 199.2 | 0.880 | 0.982 | 0.116 | 1.04 | 2780 | | | | 22.32 |
| 46.944 | 197.8 | | | | 1.04 | 2790 | | | | 22.40 |
| 47.887 | 191.3 | 0.856 | 0.973 | 0.099 | 0.99 | 2780 | 18.14 | 17.63 | 0.64 | 22.32 |
| 48.954 | 189.9 | | | | 0.98 | 2790 | | | | 22.40 |
| 49.884 | 191.4 | 0.852 | 0.972 | 0.091 | 0.99 | 2780 | | | | 22.32 |

*Based on EC measurements

# TEST 3

| | | | | | |
|---|---|---|---|---|---|
| *Co* = | 0.047 | M KCl | Syringe Displacement Rate = | 41.76 | ml/day |
| *n* = | 0.60 | | Specimen Area, A = | 39.48 | sq.cm |
| *L* = | 5.0 | mm | | | |
| *T* = | 21.5 | °C | | | |
| *R* = | 8.314 | J/mole-K | | | |

| | Bottom | | | | | Top | | | | |
|---|---|---|---|---|---|---|---|---|---|---|
| | | Concentration (mM) | | | | | Concentration (mM) | | | |
| Time (days) | EC (µS/cm) | Cl- | K+ | Na+ | KCl* | EC (µS/cm) | Cl- | K+ | Na+ | KCl* |
| -2.12 | | | | | | | | | | |
| -1.08 | 70.6 | | | | | 68.9 | | | | |
| 0.0 | 63.418 | | 0.01 | 0.53 | 0.00 | 71.482 | | 0.01 | 0.51 | 0.15 |
| 1.1 | 64.5 | 0.16234 | 0.01 | 0.74 | 0.09 | 64.3 | 14.33 | 11.2 | 4.76 | 20.22 |
| 2.1 | 77.2 | 0 | 0 | 0 | 1.53 | 2540 | 0 | 0 | 0 | 39.40 |
| 3.0 | 288 | 2.5566 | 0.16 | 3.11 | 2.53 | 4890 | 39.93 | 27.4 | 12.1 | 43.32 |
| 3.9 | 435 | 3.0187 | 0.32 | 3.32 | 2.88 | 5370 | 41.04 | 29 | 11.4 | 43.16 |
| 4.9 | 487 | 3.1486 | 0.49 | 3.29 | 3.03 | 5350 | 41.16 | 29.8 | 10.9 | 43.57 |
| 6.0 | 509 | 3.1053 | 0.67 | 2.99 | 3.03 | 5400 | 41.15 | 31.1 | 9.81 | 43.89 |
| 7.0 | 508 | | | | 3.12 | 5440 | | | | 43.97 |
| 7.9 | 522 | 3.2062 | 1.1 | 2.6 | 3.18 | 5450 | 41.25 | 32.3 | 8.63 | 43.81 |
| 9.0 | 530 | | | | 3.20 | 5430 | | | | 43.81 |
| 10.0 | 533 | 3.2192 | 1.5 | 2.18 | 3.24 | 5430 | 41.22 | 33.6 | 7.3 | 43.81 |
| 11.0 | 539 | | | | 3.27 | 5430 | | | | 43.83 |
| 12.0 | 543 | 3.2096 | 1.82 | 1.78 | 3.25 | 5432 | 41.38 | 35 | 5.98 | 44.06 |
| 13.1 | 541 | | | | 3.35 | 5461 | | | | 43.93 |
| 14.0 | 556 | | | | 3.51 | 5444 | | | | 46.47 |
| 14.8 | 579 | | | | 3.57 | 5756 | | | | 46.10 |
| 15.8 | 588 | 3.5748 | 2.81 | 1.13 | 3.65 | 5710 | 42.5 | 39.2 | 4.03 | 46.39 |
| 16.8 | 599 | | | | 4.24 | 5746 | | | | 46.04 |
| 17.8 | 686 | | | | 3.69 | 5703 | | | | 46.43 |
| 18.8 | 605 | | | | 3.48 | 5751 | | | | 46.17 |
| 19.8 | 574 | 3.4523 | 3.19 | 0.72 | 3.46 | 5719 | 42.91 | 41.4 | 2.59 | 46.77 |

*Based on EC measurements

# TEST 4

| | | | | | |
|---|---|---|---|---|---|
| *Co* = | 0.08 | M KCl | Syringe Displacement Rate = | 37.96 | ml/day |
| *n* = | 0.63 | | Specimen Area, A = | 39.48 | sq.cm |
| *L* = | 5.1 | mm | | | |
| *T* = | 21.5 | °C | | | |
| *R* = | 8.314 | J/mole-K | | | |

| | Bottom | | | | | Top | | | | |
|---|---|---|---|---|---|---|---|---|---|---|
| | | Concentration (mM) | | | | | Concentration (mM) | | | |
| Time (days) | EC (μS/cm) | Cl- | K+ | Na+ | KCl* | EC (μS/cm) | Cl- | K+ | Na+ | KCl* |
| -5.15 | 80.8 | | | | | 79.3 | | | | |
| -4.11 | 79.1 | | | | | 73.4 | | | | |
| -3.10 | 76.7 | | | | | 71.8 | | | | |
| -2.10 | 74.6 | | | | | 70.5 | | | | |
| -1.09 | 71.1 | | | | | | | | | |
| 0.00 | 72.4 | | | 2.45 | 0 | 68.4 | | | 0.87 | 0 |
| 1.08 | 100.8 | 2.5585 | 0.17 | 3.16 | 0.374 | 4510 | 26.798 | 23.5 | 8.41 | 36.45 |
| 2.14 | 435 | 4.3842 | 0.74 | 4.35 | 2.652 | 8250 | 60.314 | 48.2 | 15.2 | 66.98 |
| 3.16 | 666 | 4.6663 | 1.3 | 4.01 | 4.227 | 8970 | 67.788 | 55.7 | 14.4 | 72.86 |
| 4.20 | 738 | 5.1888 | 2 | 3.73 | 4.596 | 9080 | 69.126 | 58.5 | 12.6 | 73.61 |
| 5.19 | 822 | | | | 5.168 | 9140 | 69.703 | 60.7 | 10.7 | 74.10 |
| 6.14 | 875 | 5.3954 | 3.27 | 2.8 | 5.530 | 9160 | | | | 74.26 |
| 7.19 | 862 | | | | 5.441 | 9280 | | | | 75.24 |
| 8.19 | 835 | 5.1717 | 3.93 | 1.84 | 5.257 | 9270 | | | | 75.16 |
| 9.25 | 850 | | | | 5.359 | 9260 | 70.144 | 66.5 | 5.78 | 75.08 |
| 10.20 | 868 | 5.2406 | 4.52 | 1.27 | 5.482 | 9290 | | | | 75.33 |
| 11.20 | 868 | | | | 5.482 | 9400 | | | | 76.22 |
| 12.18 | 881 | 5.2899 | 4.95 | 0.85 | 5.571 | 9350 | | | | 75.82 |
| 13.14 | 882 | | | | 5.578 | 9460 | 68.348 | 67.5 | 3.23 | 76.71 |
| 14.19 | 857 | 5.1536 | 5.14 | 0.55 | 5.407 | 9600 | | | | 77.86 |
| 15.23 | 876 | | | | 5.537 | 9540 | | | | 77.37 |
| 16.20 | 878 | 5.1482 | 5.31 | 0.4 | 5.550 | 9480 | | | | 76.88 |
| 17.15 | 894 | | | | 5.659 | 9470 | 67.934 | 68.3 | 1.59 | 76.80 |
| 18.21 | 897 | 5.2239 | 5.49 | 0.31 | 5.680 | 9470 | | | | 76.80 |
| 19.14 | 904 | | | | 5.728 | 9380 | | | | 76.06 |
| 20.18 | 890 | 5.0439 | 5.42 | 0.21 | 5.632 | 9410 | | | | 76.31 |
| 21.17 | 860 | | | | 5.428 | 9660 | 69.026 | 69.9 | 1.15 | 78.35 |
| 22.08 | 861 | 5.0347 | 5.47 | 0.17 | 5.434 | 9670 | | | | 78.43 |
| 23.14 | 866 | | | | 5.468 | 9670 | | | | 78.43 |
| 24.13 | 878 | 5.0798 | 5.55 | 0.14 | 5.550 | 9640 | | | | 78.18 |
| 25.11 | 881 | | | | 5.571 | 9600 | 69.443 | 70.7 | 0.96 | 77.86 |

*Based on EC measurements

# TEST 4 (CONTINUED)

| | Bottom | | | | | Top | | | | |
|---|---|---|---|---|---|---|---|---|---|---|
| | | Concentration (mM) | | | | | Concentration (mM) | | | |
| Time (days) | EC (μS/cm) | Cl- | K+ | Na+ | KCl* | EC (μS/cm) | Cl- | K+ | Na+ | KCl* |
| 26.19 | 878 | 4.970 | 5.486 | 0.118 | 5.550 | 9600 | | | | 77.86 |
| 27.11 | 865 | | | | 5.462 | 9640 | | | | 78.18 |
| 27.99 | 874 | 4.928 | 5.475 | 0.099 | 5.523 | 9570 | | | | 77.61 |
| 29.04 | 868 | 4.923 | 5.470 | 0.092 | 5.482 | 9560 | 69.4 | 70.8 | 0.85 | 77.53 |
| 30.09 | 861 | | | | 5.434 | 9650 | | | | 78.26 |

*Based on EC measurements

# TEST 5

| | | | | | |
|---|---|---|---|---|---|
| *Co* = | 0.16 | M KCl | Syringe Displacement Rate = | 37.96 | ml/day |
| *n* = | 0.62 | | Specimen Area, A = | 39.48 | sq.cm |
| *L* = | 4.9 | mm | | | |
| *T* = | 22.0 | °C | | | |
| *R* = | 8.314 | J/mole-K | | | |

| | Bottom | | | | | Top | | | | |
|---|---|---|---|---|---|---|---|---|---|---|
| | | Concentration (mM) | | | | | Concentration (mM) | | | |
| Time (days) | EC (μS/cm) | Cl- | K+ | Na+ | KCl* | EC (μS/cm) | Cl- | K+ | Na+ | KCl* |
| -4.95 | 100.9 | | | | | 98.7 | | | | |
| -3.93 | 93.6 | | | | | 91.8 | | | | |
| -2.98 | 87.9 | | | | | 89.1 | | | | |
| -1.93 | 84.4 | | | | | 82.4 | | | | |
| -1.06 | 82.1 | | | | | 80 | | | | |
| 0.00 | 79.6 | | | 0.53 | 0.00 | 77.7 | | | 0.52 | 0.00 |
| 1.00 | 138.5 | 0.65409 | 0.08 | 1.05 | 0.62 | 9520 | 69.19 | 65.8 | 11 | 77.33 |
| 1.88 | 1026 | 6.1898 | 0.6 | 6.53 | 6.67 | 15550 | 118.3 | 99.3 | 20 | 126.57 |
| 2.89 | 1671 | 11.58 | 2.72 | 8.97 | 11.07 | 16780 | 132.4 | 113 | 18.4 | 136.61 |
| 3.95 | 1951 | 13.495 | 5.5 | 7.64 | 12.98 | 17200 | 132.6 | 117 | 14.2 | 140.04 |
| 4.99 | 2008 | 13.807 | 7.76 | 5.62 | 13.36 | 17330 | 137 | 124 | 11 | 141.10 |
| 5.98 | 2058 | 13.751 | 9.15 | 4.18 | 13.71 | 17410 | 138.2 | 128 | 8.77 | 141.75 |
| 7.10 | 2088 | 13.915 | 10.3 | 3.24 | 13.91 | 17530 | 138.7 | 131 | 6.71 | 142.73 |
| 8.03 | 2132 | 14.038 | 11.3 | 2.57 | 14.21 | 17630 | 138.3 | 132 | 5.86 | 143.55 |
| 9.03 | 2230 | 14.585 | 12.4 | 1.99 | 14.88 | 17710 | 137.4 | 132 | 4.87 | 144.20 |
| 9.88 | 2250 | 14.687 | 12.9 | 1.53 | 15.01 | 17690 | 138.3 | 133 | 4.15 | 144.04 |
| 10.92 | 2260 | | | | 15.08 | 17880 | | | | 145.59 |
| 11.92 | 2280 | 14.637 | 13.6 | 0.84 | 15.22 | 17960 | | | | 146.24 |
| 12.94 | 2230 | | | | 14.88 | 18150 | | | | 147.79 |
| 13.95 | 2250 | 14.632 | 14 | 0.55 | 15.01 | 18140 | 137.7 | 135 | 2.55 | 147.71 |
| 14.94 | 2260 | | | | 15.08 | 18110 | | | | 147.47 |
| 15.79 | 2290 | 13.475 | 13.2 | 0.37 | 15.29 | 17820 | | | | 145.10 |
| 16.69 | 2193 | | | | 14.63 | 17830 | | | | 145.18 |
| 17.69 | 2168 | 13.881 | 13.7 | 0.3 | 14.46 | 17910 | 138.1 | 137 | 1.96 | 145.83 |
| 18.68 | 2220 | | | | 14.81 | 18200 | | | | 148.20 |
| 19.70 | 2200 | 14.189 | 14 | 0.25 | 14.67 | 17960 | | | | 146.24 |
| 20.65 | 2210 | | | | 14.74 | 17800 | | | | 144.94 |
| 21.66 | 2200 | 14.487 | 14.3 | 0.23 | 14.67 | 17910 | 139.5 | 139 | 1.85 | 145.83 |
| 22.67 | 2240 | | | | 14.95 | 18140 | | | | 147.71 |
| 23.67 | 2260 | 14.679 | 14.6 | 0.19 | 15.08 | 17990 | | | | 146.49 |
| 24.69 | 2278 | | | | 15.21 | 18060 | | | | 147.06 |

*Based on EC measurements

# TEST 5 (CONTINUED)

| | Bottom | | | | | Top | | | | |
|---|---|---|---|---|---|---|---|---|---|---|
| | | Concentration (mM) | | | | | Concentration (mM) | | | |
| Time (days) | EC (μS/cm) | Cl- | K+ | Na+ | KCl* | EC (μS/cm) | Cl- | K+ | Na+ | KCl* |
| 25.74 | 2270 | 14.6 | 14.6 | 0.2 | 15.15 | 18280 | 135 | 136 | 1.75 | 148.86 |
| 26.65 | 2300 | | | | 15.36 | 18120 | | | | 147.55 |
| 27.68 | 2280 | 14.8 | 14.8 | 0.2 | 15.22 | 18210 | | | | 148.28 |
| 28.69 | 2290 | 14.8 | 14.9 | 0.19 | 15.29 | 18120 | 141 | 141 | 1.79 | 147.55 |
| 29.68 | 2280 | 14.7 | 14.8 | 0.18 | 15.22 | 18060 | 139 | | 1.77 | 147.06 |

*Based on EC measurements

# APPENDIX B: SPECIFIC GRAVITY TEST DATA

| test # | m_empty flask (g) | m_flask and deaired DIW (g) | m_flask water and soil (g) | m_pan (g) | m_pan and dry mass (g) | m_dry dph-gcl (g) | Gs | Gs AVERAGE between tests 1 and 2 |
|---|---|---|---|---|---|---|---|---|
| 1 | 104.35 | 353.78 | 362.29 | 390.39 | 403.89 | 13.50 | 2.71 | **2.69** |
| 2 | 105.52 | 354.93 | 364.15 | 302.97 | 317.70 | 14.73 | 2.67 | |